UNIVERSITY OF MISKOLC
FACULTY OF MECHANICAL ENGINEERING AND INFORMATICS

FATIGUE STRENGTH AND FATIGUE CRACK PROPAGATION DESIGN CURVES FOR HIGH STRENGTH STEEL STRUCTURAL ELEMENTS

PHD THESES

Prepared by

Haidar Faisal Helal Mobark
Agriculture and Machinery Equipments Engineering Techniques (BSc),
Machine Design (MSc)

ISTVÁN SÁLYI DOCTORAL SCHOOL OF MECHANICAL ENGINEERING SCIENCES
TOPIC FIELD OF ENGINEERING MATERIALS SCIENCE, PRODUCTION SYSTEMS AND PROCESSES
TOPIC GROUP OF MATERIALS ENGINEERING AND MECHANICAL TECHNOLOGY

Head of Doctoral School

Dr. Gabriella Bognár
DSc, Full Professor

Head of Topic Group

Dr. Miklós Tisza
DSc, Professor Emeritus

Scientific Supervisor

Dr. János Lukács
CSc, PhD, Full Professor

Miskolc
2020

CONTENTS

SUPERVISOR'S RECOMMENDATIONS

Haidar Faisal Helal Mobark was born in Babylon city (Iraq) on 27th April 1980; his nationality is Iraqi. He is married since 2006 with three children, two girls and one boy.

He was a bachelor student between October 1998 and July 2002, studied at Agriculture and Machinery Equipment Engineering Techniques Department at Technical College of Al-Mussaib (T.C.M) in Babylon city. He got his BSc degree "First with Honor's" on average (74.09%) level.

After the graduation, from July 2002 to March 2004 he was worked together with his father in their small market. He started a first governmental job in Babylon Directorate of Water Resources. He was a member at Department of Water Regulators between March 2004 and January 2006 deals with setup, maintenance, repairing of barriers, gates and dams work on water i.e. canals, streams and rivers.

He was earned a new government job (and left the previous) under the Iraqi Ministry of Higher Education and Scientific Research. He worked at the Department of Mechanical Engineering / College of Engineering / University of Babylon between January 2006 and August 2010. He performed administration, practical and teaching activities at the department and college as well. He did practical teaching activity for Bachelor Engineering Students form different departments belong to the College of Engineering in workshops: welding place on different welding machines, grinding machines place, and in turning place. He has made practical teaching activities in computer laboratory also for training different class of Bachelor Mechanical Engineering Students on Auto-CAD program for using in the design of machine tools and engineering drawing.

He has been abroad in India between August 2010 and June 2012 for doing a Master of Technology (M-Tech) during Indian Council for Cultural Relations (ICCR) scholarship. He completed his master study in Machine Design, at Department of Mechanical Engineering, Faculty of Engineering and Technology in JAMIA MILLIA ISLAMIA in New Delhi. He has studied many subjects: Optimization Methods, Theoretical and Experimental Stress Analysis, Advanced Mechanisms, Advanced Mechanical Engineering Design (Theoretical & Practical), Advanced Mathematical (1st semester); Finite Element Methods (FEM) (Theoretical & Practical), Mechatronics, Mechanical Vibration, Tribological System Design, Concurrent Engineering (2nd semester); Robotics, Design of Experiment, Minor Project (3rd semester); Dissertation (4th semester). However, he got "First with Honor's" in average (8.78 out of 10 CGPA) level and completed his study under several respected professors and doctors i.e. Prof. Zahid Akhtar Khan, Prof. I. A. Khan, Prof. Rasheed Ahmed Khan, Prof. Mohammed Suhaib, Dr. Sabah Khan, and Prof. Aas Mohammed how was his supervisor during his master study.

He has come back to his home and joined a new administration job at the same College of Engineering / University of Babylon in between June 2012 and August 2013. On August 2013 he converted his work location to another new governmental university also in Babylon city, right

now his job concerning with Department of Soil and Water Resource at College of Agriculture at Al-Qasim Green University till August 2016.

He was a Lecturer Assistant at his younger and renewing university, and he thought the BSc students theoretically and practically in the subjects as follows: Tractors and Agriculture Equipments, Computer Applications i.e. Auto-CAD application. Even with teaching activities, he carried out different administration activities regarding their teaching staff, college employees and students i.e. member and head in different groups: students' examination committee, computer maintenance committee, inspection and receipt committee, procurement committee.

During his governmental work (2004-2016) he earned (3) letters of thanks from Iraqi Minister of Higher Education and Scientific Research, as well as (25) extra letters of thanks from university presidents and deans i.e. "President of Babylon University", "President of Al-Qasim Green University" and "Dean of College of Engineering", "Dean of College of Agriculture".

He shared developing courses to improve his academic abilities and practical knowledge: course of developing teaching skills, computer maintenance course, learning Ansys-5 course at University of Babylon and course of education communication skills, the terminal seminar for department teaching staff at Al-Qasim Green University.

From September 2016 till now he is a full-time PhD student in the framework of "Stipendium Hungaricum Scholarship Programme" at István Sályi Doctoral School of Mechanical Engineering Sciences; his affiliated organisation is Institute of Materials Science and Technology / Faculty of Mechanical Engineering and Informatics.

Through his previous studies and industrial practice, he has had a wide knowledge in different specializations, but he had not adequate and sufficient knowledge in the field of welding, fatigue and fracture. Therefore, in the first period, he started to study the relevant literature focusing on his research topic. He has selected systematically the subjects, hold presentations on research seminars, and taken part in institutional research work.

We have planned his research work collectively, and built-up a research and investigation plan (investigation matrix). He prepared and investigated welded joints through the academic and assistant staff of the Institute, with different technological and testing parameters. Both high cycle fatigue and fatigue crack growth tests were performed and evaluated, applying statistical methods. As an evident consequence of cyclic loading conditions, the long testing period has been predicted. He was active and persistent during that two and half years long work.

After the successful complex exam and reaching the first investigation results, his publication activity has increased. The results of the research work have presented in doctoral seminars, doctoral forums, and international conferences; scientific papers have prepared for journals and conference proceedings. His self-dependence has developed in this field continuously.

During his PhD studies his knowledge, his affinity to research work, his ability and suitability for the holding of presentations have developed significantly. He has acquired new knowledge and competences, which can be utilised and individually developed his future work, his future academic and scientific life.

I am sure that his Stipendium Hungaricum scholarship period will initiate new possibilities for Haidar Faisal Helal Mobark in the near future.

Miskolc, 15th April 2020

Prof. Dr. János Lukács
Supervisor

LIST OF SYMBOLS AND ABBREVIATIONS

GREEK LETTERS

α	Ferrite (solid solution of iron alloy)	N/A
α	Shape parameter in Weibull-distribution function (Equation 7.1)	–
β	Scale parameter in Weibull-distribution function (Equation 7.1)	–
γ	Austenite (solid solution of iron alloy)	N/A
ε	Level of significance	–
η	Thermal efficiency	–
σ	(Normal) stress	MPa
$\Delta\sigma$	(Normal) stress range	Mpa
$\Delta\sigma_D$	(Constant amplitude) fatigue limit	Mpa
$\Delta\sigma_{1E07}$	Stress range belonging to 1×10^7 cycles	Mpa
ΔF	Load range	N
ΔJ	Cyclic J-integral	kJ/m^2
ΔK	Stress intensity factor range	Mpa $m^{1/2}$
ΔK_{fc}	Fatigue fracture toughness	Mpa $m^{1/2}$
ΔK_{th}	Threshold stress intensity factor range	Mpa $m^{1/2}$
ΔW	Strain energy range	J

LATIN LETTERS

a	Crack size or crack length	mm
a	Material constant of the Basquin equation (Equations 1.1 and 6.1)	–
a_0	Initial crack length (FCG specimens)	mm
a_0	Specimen width (HCF specimens)	mm
A	Elongation	%
AC	Air cooling	mm
AcC	Accelerated cooling	N/A
AHSS	Advance high strength steel	N/A
b	Material constant (Equation 1.1)	–
b_0	Specimen thickness (HCF specimens)	mm
B	Specimen thickness (FCG specimens)	mm
BM	Base material	N/A

BWJ	Butt welded joint	N/A
BL	Buffer layer	N/A
C	Constant of Paris-Erdogan equation	–
C_i, C_j	Constants of fatigue crack propagation equations (i = m, p; j = 1, 2)	–
CE, C_{eq}	Carbon equivalent	%
CCT	Centre cracked tension specimen (subchapter 3.4.)	N/A
CCT	Continuous Cooling Transformation (subchapter 2.4.)	N/A
CR	Controlled rolling	N/A
CVN	Charpy impact energy (V notched specimen)	J
da/dN	Fatigue crack propagation rate	mm/cycle
E_v	Linear energy	J/mm
f	Testing frequency	Hz
FCG	Fatigue crack growth	N/A
FM	Filler metal	N/A
FCAW	Flux cored arc welding	N/A
F_3	Shape factor of welded joint	–
GMAW	Gas metal arc welding	N/A
h	Specimen direction (HCF specimens)	N/A
hhi	High heat input	N/A
HAZ	Heat affected zone	N/A
HCF	High cycle fatigue	N/A
HFMI	High frequency mechanical impact	N/A
HOP	Heat treatment on-line process	N/A
HS	High strength	N/A
HSLA	High strength low alloyed	N/A
HSS	High strength steel	N/A
HSSS	High strength structural steel	N/A
HTT	High temperature tempering	N/A
HV	Vickers hardness	–
I	Welding current	A
IIW	International Institute of Welding	N/A
JSME	Japan Society of Mechanical Engineers	N/A
k	Specimen direction (HCF specimens)	N/A
K	Stress intensity factor	MPa $m^{1/2}$
K_i	Stress intensity factor (i = I, II, III)	MPa $m^{1/2}$
K_c	Critical stress intensity factor (Equation 3.3)	MPa $m^{1/2}$
lhi	Low heat input	N/A
LEFM	Linear elastic fracture mechanics	N/A
L-S, L-T	Specimen orientations (FCG specimens)	N/A

LTT	Low temperature tempering (subchapter 2.4)	N/A
LTT	Low transformation temperature (Fig. 3.11)	N/A
m	Exponent of fatigue crack propagation equation (Equation 3.1)	–
m	Material constant of Basquin equation (Equation 6.1)	–
mhi	Medium heat input	N/A
M-A	Martensite - Austenite (island)	N/A
MAG	Metal active gas	N/A
MMM	Metal magnetic memory	N/A
MMR	Mismatch ratio	N/A
M	Matching	N/A
n	Exponent of Paris-Erdogan equation	–
n_i	Exponents of fatigue crack propagation equations (i = 1, 2)	–
N	Number of cycles (FCG)	cycle
N, $N_{fracture}$	Number of cycles to failure (HCF)	cycle
NGLW	Narrow gap laser welding	N/A
N_k	Number of cycles for the break point of the S-N curve	cycle
N_0	Threshold parameter in Weibull-distribution function (Equation 7.1)	–
OLAC	On-line accelerated cooling	N/A
OM	Overmatching	N/A
p	Exponent of fatigue crack propagation equation (Equation 3.3)	–
PWHT	Post weld heat treatment	N/A
P-GMAW	Pulsed gas metal arc welding	N/A
Q+T	Quenched and tempered	N/A
R, R_σ	Stress ratio	–
RD	Rolling direction	N/A
RPC	Relaxation precipitation control	N/A
R_i	Yield strength (i = y, p0.2)	MPa
R_m	Tensile strength	MPa
SAW	Submerged arc welding	N/A
SD	Standard deviation	N/A
SP	Specimen	N/A
S-N	Stress vs. number of cycles to failure curve	N/A
S_0	Cross section of the specimen (HCF specimens)	mm^2
t	Plate or specimen thickness	mm
$t_{8/5.}$ $t_{8.5/5}$	Cooling time from 800°C to 500°C and 850°C to 500°C	s
TM	Thermomechanical(ly treated)	N/A
TMCP	Thermomechanical control process	N/A
TMR	Thermo-mechanical rolling	N/A
TPB	Three point bending test specimen	N/A
TTT	Time-temperature-transformation	N/A

T-L, T-S	Specimen orientations (FCG specimens)	N/A
U	Welding voltage	V
UHS	Ultra-high strength	N/A
UHSS	Ultra-high strength steel	N/A
UIT	Ultrasonic impact treatment	N/A
UM	Undermatching	N/A
v	Specimen direction (HCF specimens)	N/A
v_w	Welding speed	cm/min
W	Specimen width (FCG specimens)	mm
WJ	Welded joint	N/A
WM	Weld metal	N/A
Y/T	Ratio of the yield strength and tensile strength	MPa/MPa
1W, 21W 3W, 23W	Notch and crack path orientations (FCG specimens cut from welded joints)	N/A

SUBSCRIPTS

eff	effective	N/A
ip	interpass	N/A
max	maximum	N/A
min	minimum	N/A
pre	preheating	N/A

1. INTRODUCTION, GLOBAL AIMS OF THE RESEARCH WORK

The term fatigue was mentioned for the first time by Braithwaite in 1854; he described many service fatigue failures of water pumps, propeller shafts, crankshafts, railway axles, levers, cranes, etc.. In 1870 Wöhler presented his law (Wöhler law), based on investigations of railway axles. He composed as follows: "*Material can be induced to fail by many repetitions of stresses, all of which are lower than the static strength. The stress amplitudes are decisive for the destruction of the cohesion of the material. The maximum stress is of influence only in so far as the higher it is, the lower are the stress amplitudes which lead to failure*". In 1936 Wöhler's successor presented the S-N curve, it is called Wöhler curve, and Basquin represented the finite life region of the Wöhler curve and described it by a simple formula [1]:

$$\sigma = aN^b. \tag{1.1}$$

After that Bauschinger mentioned for fatigue by his sentence "*the change of the elastic limit by often repeated stress cycles*". The first experiments to improve the fatigue strength of components probably were carried out in the U.K. during the First World War [1].

From 1960 onwards the number of fatigue experts increased still further. This must also be attributed to the rapid development of fracture mechanics, i.e. of fatigue-crack propagation. Paris established that fatigue-crack propagation could be described by the following equation [2]:

$$\frac{da}{dN} = C\Delta K^n, \tag{1.2}$$

which equation soon set out on a veritable triumphant advance around the world [1]. The complex process of crack propagation is undoubtedly described much too simply by this equation; this fact however, did not prevent its – either undiscriminating or adding further characteristics – use all over the world to this very day.

The most commonly used structural material for the construction of engineering structures is steel, and the most widely used manufacturing technology is welding. Nowadays, steel providers create a modern version of a high-strength base materials and filler metals with yield strength start from 690 MPa and up. However, high strength lightweight structures with low cost of steel weldments lead to apply in many manufacturing aspects (e.g. mobile cranes, hydropower plants, offshores, trucks, earthmoving machines, and drums), because of an extensive reduction in weight [3].

As in (Fig. 1.1 a) can be seen, the interaction of load, material, and design represents reliability of welded components. A superposition of local and global welding stresses may lead to high residual stress levels which are able to reduce the components safety (see Fig.1.1 b) [3].

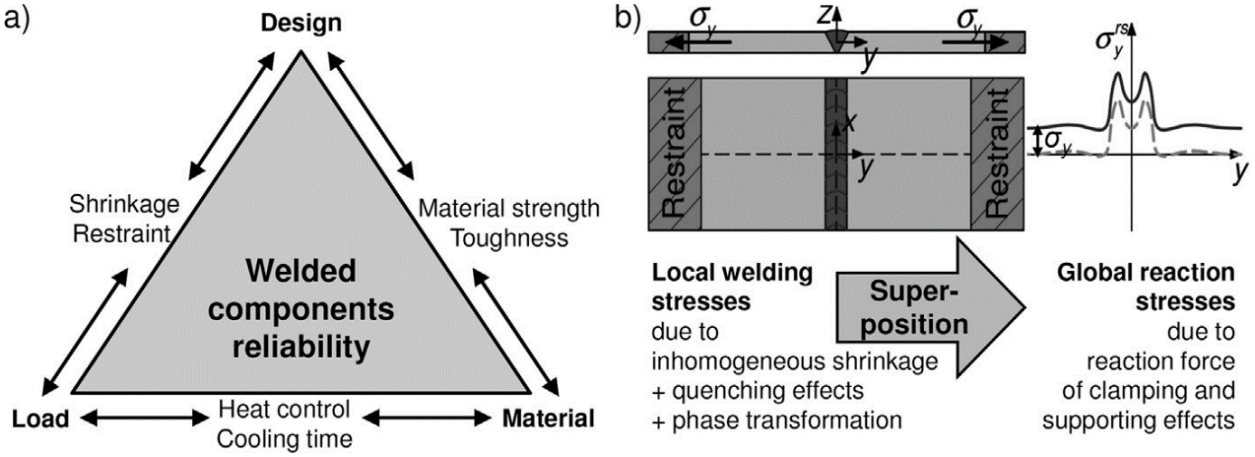

Fig. 1.1. Interaction of design, material and load during component production and service a) [4]; welding stresses as a result of local and global restraint b) [5].

Welded joints are very sensitive parts of structures, because the welded regions are in complex metallurgical and stress conditions. Before the Second World War, the design of all engineering structures was based on yield/tensile strength and ductility. Mild steel was used as the structural material and the minimum yield strength of the weld metal was found to be around 340 MPa. The yield strength to tensile strength ratio of the weld metals that were used for welding the mild steel in early designs was very high and the designers did not pay much attention to the yield strength of the weld metals. It has been reported that the maximum yield strength of the filler metal that has been used for joining the mild steel plates was about 59% higher than the base material [6].

High strength structural steels (HSSS) with yield strengths from 690 MPa upwards are applied in growing amount industrial applications. Specific design solutions and economic aspects of modern steel constructions lead to an increasing trend in light-weight design. Steel producers currently provide a diversified spectrum of high-strength base materials and filler metals. Thus an extensive reduction in weight and production costs can be achieved with increasing material strength [3]. During the welding process the joining parts are affected by heat and force, which cause inhomogeneous microstructure and mechanical properties, and furthermore stress concentrator places can form. Both the inhomogeneity of the welded joints and the weld defects play important role in case of cyclic loading conditions. High cycle fatigue (HCF) and fatigue crack growth (FCG) phenomena are a very common problem in welded structures; however, there are a limited knowledge about the fatigue behaviour of HSSS base materials and welded joints up to now. In accordance with the welding challenges nowadays, the mismatch effect should be examined too [7].

The research work is a significant continuation of previous researches, builds upon their experience [7] and uses their measurement results [8][9]. The global aims of the research work are to study the influence of mismatch characteristics on cyclic loaded high strength steel welded joints and to determine high cycle fatigue strength and fatigue crack propagation design curves for different high strength steel base materials and their diversely mismatched welded joints, such as structural elements [10].

2. HIGH STRENGTH STEELS

2.1. Classification and trends of development

For years, metallurgists have been searching ways of producing structural steels which would have the highest (possible) mechanical properties and maintain satisfactory plastic properties at the same time. Due to an increase in yield point, it is now possible to manufacture structures consisting of smaller wall thickness elements, thus lighter and less expensive to transport. A smaller wall thickness requires a smaller amount of filler metals and a shorter welding time, simultaneously. An increase in the mechanical properties of steels may be obtained by an appropriate selection of chemical composition through a classic process of toughening (hardening and tempering) or by means of thermomechanical treatment. However, no matter how high its mechanical properties might be, structural steel will only have practical application if it can be welded by means of commonly used methods; toughened steels offer such a possibility. Due to the appropriate selection of chemical composition and proper heat treatment, these steels are characterised by very good mechanical properties as well as good weldability.

The modern development of structural steels has involved on the one hand toughened steels such as S690Q, S890Q and S960Q, while on the other hand thermomechanically rolled steels of lower mechanical properties but of a higher impact strength (S355M, S460M and S500M) [11].

Steels of 690 MPa yield have become commercial about three decades ago. In the last years thermomechanical rolling followed by accelerated cooling becomes alternative production route. Different techniques to increase high tensile properties of steel to yield point 690 MPa occurs by martensitic hardening, precipitation hardening, work hardening, and grain refinement [11][12].

Due to very high mechanical properties, steels of a yield point in excess of 1100 MPa have found application in the production of high-loaded elements of car lifts, travelling cranes and special bridge structures. The advantages of using steels with high mechanical properties are visible as regards the costs of transport, plastic working, cutting, and welding [11].

New methods have been developed since the seventies, when quenched and tempered (Q+T) group appeared. With this heat treatment process, combined with alloying components, the maximal yield strength can reach 1300 MPa. However, it should not be ignored that filler metals are not available, up to now, for this extreme strength, only if undermatching (approximately 15-20%) is allowed. It is important to note that applying undermatching during the selection of the filler metal may have some additional positive effects (residual stress, fatigue properties, etc.). Due to the above mentioned causes, instead of S1100Q and S1300Q, the S960Q is more widespread, which can be welded by matched filler metals, as well. By the recent development of the thermomechanical (TM) process, the yield strength of TM steels have approached Q+T steels, thus it is worth examining this group by the upcoming welding researches [13]. Fig. 2.1 summarizes the chronology of structural steel developments [8][14].

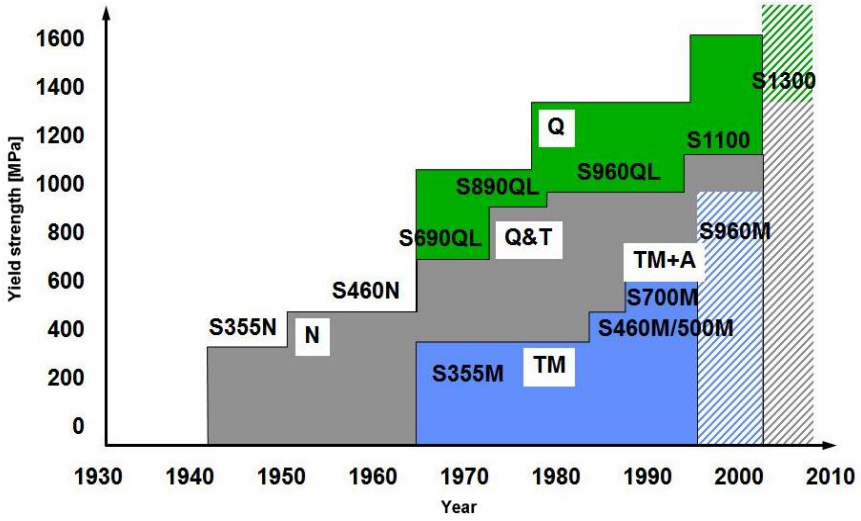

Fig. 2.1. Chronology of structural steels developments [8][13][14].

According to steel manufacturing companies' data the minimum yield strengths of (extra) high strength steel plates stated for Q+T steels 1300 MPa [107][108] and for TM steels 1100 MPa [109]. These mean that hatched areas in Fig. 2.1 are nowadays available for users and development trends have shifted for higher strengths.

For better mechanical properties and weldability of structural steels these occur during proper chemical composition and by apply classical methods (Q+T, TMCP) improving microstructure of steels. The competition between steelmakers to produce a thinner steel wall with higher mechanical and plastic properties; lighter and low cost during transportation of components and also low cost of welding technology by a decrease in filler metal and short time during welding aspect [12]. Fig. 2.2 contains the investigated materials in abbreviated form, too: RUUKKI Optim 700QL, SSAB Weldox 700E, SSAB Weldox 960E and VOESTALPINE Alform 960M.

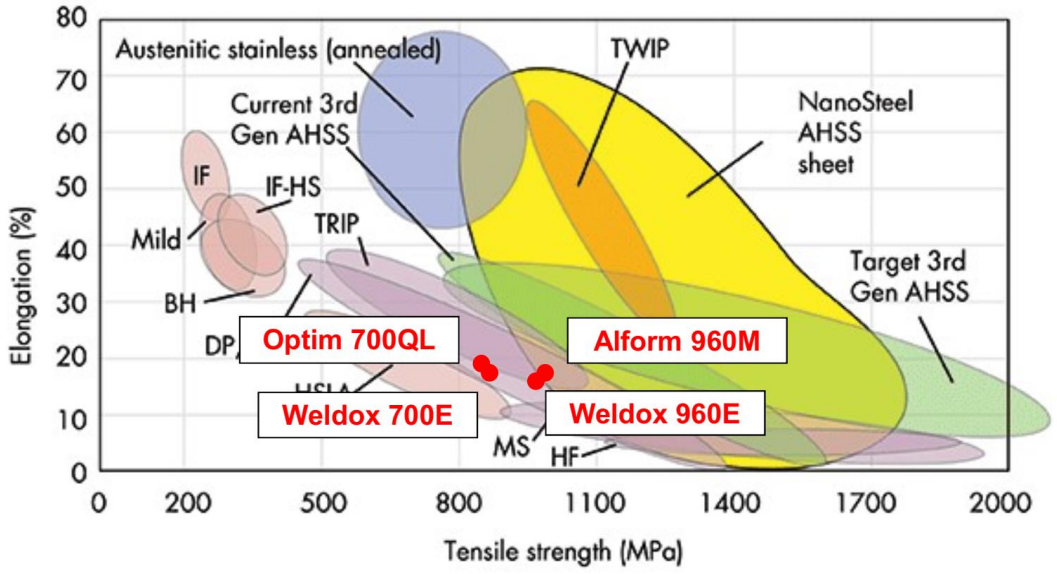

BH: Bake hard, CP: Complex phase, DP: Dual phase, HF: Hot forming, HSLA: High strength low alloy, IF: Interstitial free, IF-HS: Interstitial free-hard steel, Mild: Mild steel, MS: Martensitic, TRIP: Transformation induced plasticity, TWIP: Twinning induced plasticity.

Fig. 2.2. The banana curve [15], included investigated materials with red colour.

The development of the metallurgical process obtained by decrease both production cost and disadvantages impurities in structural steel to protect it from lamellar tearing or hot cracking [16]. For example, yield point increased 130 MPa, carbon equivalent decrease by 0.05%, and better weldability obtained by applying new production technology than conventional one. The comparison between conventional and new technologies of production of structural steel belong Q+T type occur by apply heat treatment and conditions of rolling and kept same chemical composition. The range of structural steel thicknesses will grow along with the development of metallurgical processes. In the case of these steels, one of the most important features of the successfulness of the weldability is the heat input which can be described with the linear energy. If the value of this is too low, the cooling rate of the welded joint may be too fast, and then cold cracks can be developed. In the opposite case, strong coarse grain microstructure can be evolved in the HAZ, which can be caused by the decreasing of the strength and toughness features [110]. The advantages of using steels with high mechanical properties are regards to the costs of transport, plastic working, cutting, and welding [11].

There are different elements effects on chemical composition during metallurgical process of Q+T steel [8][11][110] as follows.

- Cr and Mo: decrease critical cooling rate and increase hardenability.
- Nb: fine grains of austenite during rolling and thus very tiny lamellas of supersaturated ferrite (martensite) after cooling. Tempering 600ºC, precipitation hardening of NbC or V_4C_3 develop strength and impact resistance i.e. obtained a fine-grained structure with dispersive carbides.
- Ni: improve impact strength.
- Micro-addition of B below 0.005%: improve hardenability.
- Sufficient amount of Ti: to bind nitride in TiN and avoid worsening the ductility of steel.
- V: addition V levels 0%, 0.047%, 0.097% and 0.151% gives a strengthening to the steels, tensile and yield strengths increase. The simulated HAZs of steels containing 0%, 0.047%V exhibited good combination of strength and impact toughness. The simulated HAZs of steels containing 0.097%, 0.15l%V showed higher strength and lower impact toughness. Size of Martensite-Austenite (M-A) particle in HAZ increased with increasing V content. The largest M-A constituent in HAZ of 0.151%V steel caused lowest impact toughness.

  The essential advantages of TM steel developing are as follows [8][17][18][19][20].
- Weight / volume reduction: light weight and smaller volume, which is cost-saving advantage.
- Best cuttability: the low carbon content and homogeneous surface make HS, UHS steel grades suitable for cutting methods.
- Very good cold formability: improved forming behavior with more than twice the minimum yield strength than conventional structural steels.
- Outstanding weldability: combination of thermomechanical rolling and micro-alloying makes very low carbon content. However lower maximum hardness in HAZ, reduced tendency to temper softening in HAZ, and reduced susceptibility to cold cracking.
- Excellent toughness: thermomechanical rolling and accelerated cooling lend steel grades a fine-grained structure and excellent toughness.
- Perfect flatness: excellent flatness is achieved through precisely controlled rolling processes in combination with modern leveling units and production-route-based temper softening.
- Clean surface: during a uniform layer of scale forms on the sheet surface following hot rolling process.

2.2. Production processes and their influences on welding

One of the famous technology that absolutely used to development microstructural control technology and has an essential role during welding process technology is thermomechanical control process (TMCP). The production of TMCP steels occurs by two ways: non-accelerated cooling (Non-AcC) and accelerated cooling (AcC) processes (see Fig. 2.3) [21].

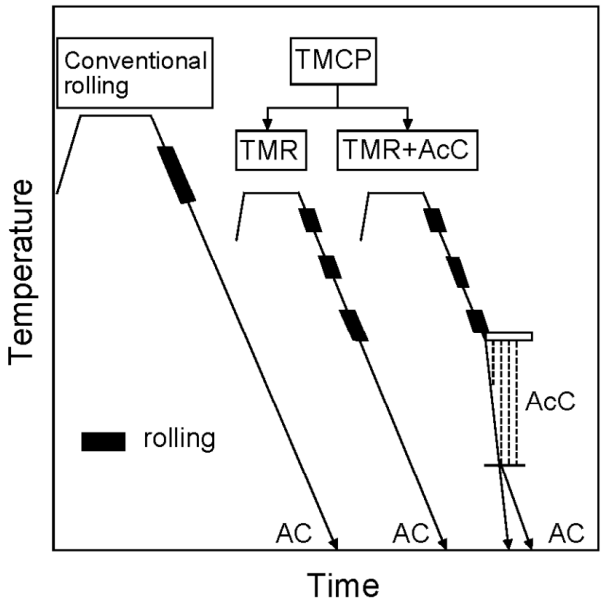

Fig.2.3. Schematic illustration of thermo-mechanical control process (TMCP) (TMR: thermo-mechanical rolling, AcC: accelerated cooling, AC: air cooling) [21].

Non-AcC process consists of low slab reheating temperature and intensification of rolling reduction in the austenite unrecrystallized region. The controlled rolling is finished either in the region of austenite or in the intercritical region, austenite + ferrite. The purposes of lowering the slab reheating temperature are: refining the initial austenite grain size before rolling, promotion of recrystallization and expansion of the recrystallized region to a lower temperature, and grain refinement of recrystallized austenite grains by rolling in the recrystallized region. Non-AcC type TMCP steel plates, especially the plate manufactured by TMCP which the controlled rolling is finished in the region in the intercritical region, have excellent brittle fracture arrestability through the refinement of grains [21].

In AcC process, accelerated cooling is carried out after controlled rolling. Cooling rate and finishing-cooling temperature in the process are controlled depending on required properties. By the way accelerated cooling after controlled rolling plays a role of clogging the growth of grain size. AcC type TMCP, in particularly, brings about further improvement in toughness and makes possible to be applied for very high heat input welding. It is natural that the improvement of HAZ toughness leads to increase fracture toughness. Through manufacturing process of AcC type TMCP steel plate to prevent larger scatter of distortion after thermal processes such as flame cutting and welding of steel plates (due to releases residual stress, leading to distortion). Cold leveler with high press are developed for removing residual stress in TMCP plates after compressive yielding in almost half zone of a plate in thickness direction [21].

During welding aspect many different microstructures generate in HAZ depending on thermal cycles due to welding and chemical composition of steel. The maximum hardness decreases as C_{eq} is lowered and bead length becomes large. Since it has the possibility of generation of micro-cracking in the HAZ if the maximum hardness becomes larger than 400HV or more [21].

Japanese researchers revealed that TMCP (applied on 320, 360, 400 MPa yield strength) steel plates tend to decrease their welded joints because of lowering C_{eq} due to controlled rolling and because of softening of HAZ caused by welding with heat input greater than about 70 kJ/cm. When high heat input i.e. 300 kJ/cm applied through welding, the decreased HAZ strength about 10% or less of that of the base plate and the width of the softened HAZ is less than about 70% of the plate thickness. The results belong those shows using very high heat input welding then results of fatigue crack propagation rate in the softened HAZ for AcC type TMCP is almost the same as that in the HAZ for conventional steel (see Fig. 2.4) [21].

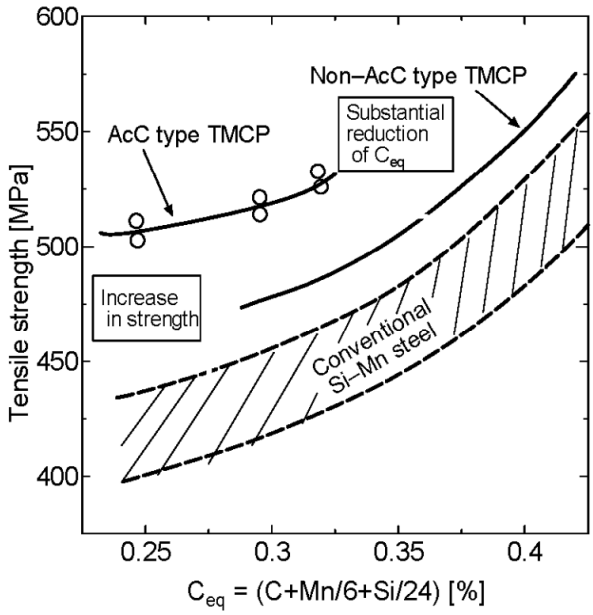

Fig. 2.4. Relationship between carbon equivalent (C_{eq}) and tensile strength [21].

Because of the enhanced strength of TMCP steel by controlled rolling, so-called separation or splitting is often observed in the fractured specimens taken from the longitudinal or the transverse direction of steel plates, especially in steel plate controlled rolled in the intercritical temperature region. Cracks called separation propagate in planes perpendicular to the main fractured surface and parallel to the plate surface during the final fracture process due to restriction force exposed in the thickness direction. Separation starts from an origin such as micro-orientation texture boundary or an elongated non-metallic inclusion such as MnS, which would be formed or elongated during TMCP rolling. Separation is particularly observed in the fracture surface of V-notch Charpy impact specimens [21].

Conjunction TMCP with another processes was employed by Japanese company JFE Steel to develop high-performance steel plates [22]. Another process adopted by other searchers to produce high strength low alloy steel plates (HSLA) by combination of thermomechanical control process and relaxation precipitation control (TMCP+RPC) used to produce high performance steels with strength of 960 MPa [21]. Based on different sources [21][22][23], the applied technologies are as follows (see Fig.2.5 and Fig. 2.6 too).

Thermomechanical Control Process (TMCP): see before.

OLAC® (On-Line Accelerated Cooling): manufacturing high-performance steel plate via accelerated cooling facility (unachievable alone). *Super-OLAC*: Producing high-performance steel plate. An advanced accelerated cooling system capable of cooling plates homogeneously at high cooling rates close to the theoretical limits (unachievable alone).

HOP®(Heat treatment On-line Process): an on-line induction heating facility. Improves the strength and toughness for steel plates over 600 MPa produced by the direct Q+T process by refining carbides. The smaller number of coarse cementite particles is thought to contribute to the excellent toughness in plates tempered by HOP. The heating rates in tempering by HOP are one to two orders of magnitude higher than those by conventional furnaces (unachievable alone).

Super-OLAC+HOP process online without any off-line heat treatment: appling heat treatment process occur by accurately controlling the stop cooling temperature then immediately tempered after the direct quenching, at very rapid heating rates of 2 to 20°C/s this improves the toughness of the HS steels by refining carbides. Usually used for over 600 MPa tensile strength steel manufactured by quenching and tempering Q+T to achieve HSS (610 MPa & 780 MPa) and UHSS (960 MPa & 1100 MPa).

M-A (martensite-austenite constituent): to achieve extremely hard martensite-austenite constituent (M-A) that compromises toughness tends to be formed in the upper-bainite structure at the HAZ of welds, especially in large-heat input welding it's unachievable with conventional (Q+T/TMCP)

Microstructural control technology with HOP using martensite-austenite constituent (M-A): using martensite-austenite constituent (M-A) as a hard phase through the Super-OLAC+HOP process and by controlling of (C, Si, Al) in order to suppress the formation of M-A as in Fig. 2.6 to obtain HS steel plates with low yield ratios. Employed on 780 MPa steel plate to produce tensile strength of over 900 MPa, a low yield ratio of under 80% and high absorbed energy of 216 J in Charpy impact tests at 0 °C.

TMCP+RPC: to improve the mechanical properties of 960 MPa steel plates produced by employed process TMCP+RPC than by a unique process TMCP; because steel microstructure from first process has more acicular ferrite and more precipitation and the bainite laths and their packets finer. The RPC means that the plate would be air-cooled for a moment between certain temperatures after controlled rolling.

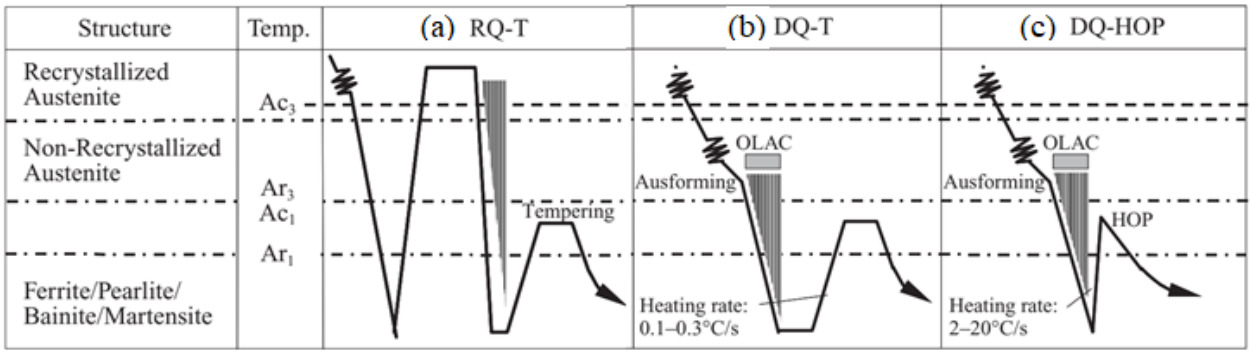

Fig. 2.5. Schematic diagrams of (a) RQ-T, (b) DQ-T, and (c) DQ-HOP [22].

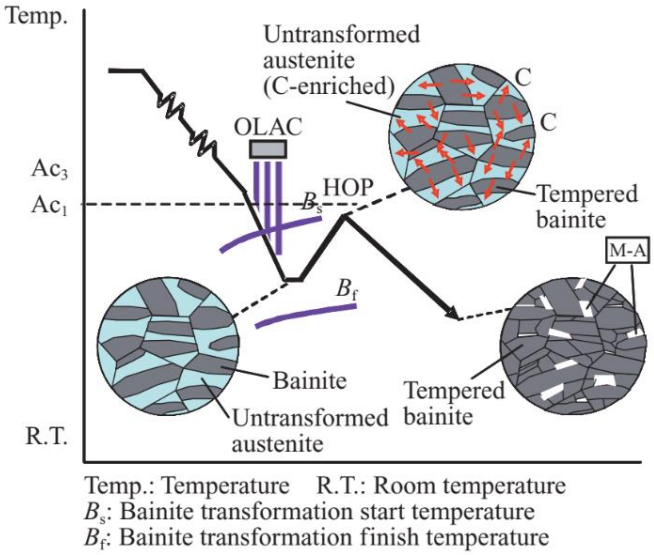

Fig. 2.6. Schematic illustrations; temperature profile and microstructural changes in the new processing with HOP [22].(The source does not contain the name of the horizontal axis, which is Time.)

Another type of structural steels are toughened steels a fine-grained alloy steels. By selecting a proper chemical composition as well as the conditions of rolling and heat treatment, one obtains steels having different levels of yield point ranging from 460 to 1300 MPa. Most high strength Q+T steels are produced with a carbon content between 0.12 % and 0.18% generally this is the most useful range. Where increasing of carbon content then hardness of martensite increase also in a linear relationship. The necessary hardenability can be achieved by different combinations of alloying elements, of course the ones that also raise carbon equivalents [11][12].

The steels are usually melted in a continuous way. After the typical process of rolling, the sheets/plates are heated up to the temperature of austenitizing and cooled by means of high-pressure spraying devices. Quenching of high strength steels is performed after austenizing at temperatures of some 900°C. In order to suppress during cooling, the formation of softer microstructure such as ferrite, an accelerated cooling is necessary [11][12].

Tempering martensite means essentially reducing the super-saturation of the matrix by the formation of carbides leading to a relaxation and a reduction of the high dislocation density associated with martensite formation. A suitable tempering of the martensitic microstructure is necessary in order to get a satisfactory combination of tensile and toughness properties [11].

The development of steel metallurgical processes aims on one hand at the growth of efficiency, and on the other hand at decreasing disadvantageous impurities in steel leads lamellar or hot cracking. There were cases when toughened steels developed cold cracks after 3-4 weeks. In some cases it is possible to use post-weld heat treatment in order to prevent cold cracks (stress relief annealing in the range 530 - 580°C). The study revealed that an increase in the yield point (R_y) or hardness (HV) of a parent metal or weld deposit is accompanied by a decrease in the allowed hydrogen content in a metal observe a growing susceptibility to cold cracking [11].

There is another manufacturing method to produce toughened steels using direct hardening of plates/sheets at the temperature of rolling, i.e. in the process of thermomechanical treatment. Such a method allows one to obtain, with the same chemical composition, a yield point higher by approximately 130 MPa than the one obtained in a conventional toughening process. By

applying this methods one can produce steels which have a carbon equivalent lower than approximately 0.05%. Such steels are characterised by better weldability in comparison with steels produced in a conventional way. Schematic diagrams of the production processes of toughened steels can be seen in Fig. 2.7 and Fig. 2.8 shows the relation between yield strength and transition temperature for different type of steels [11].

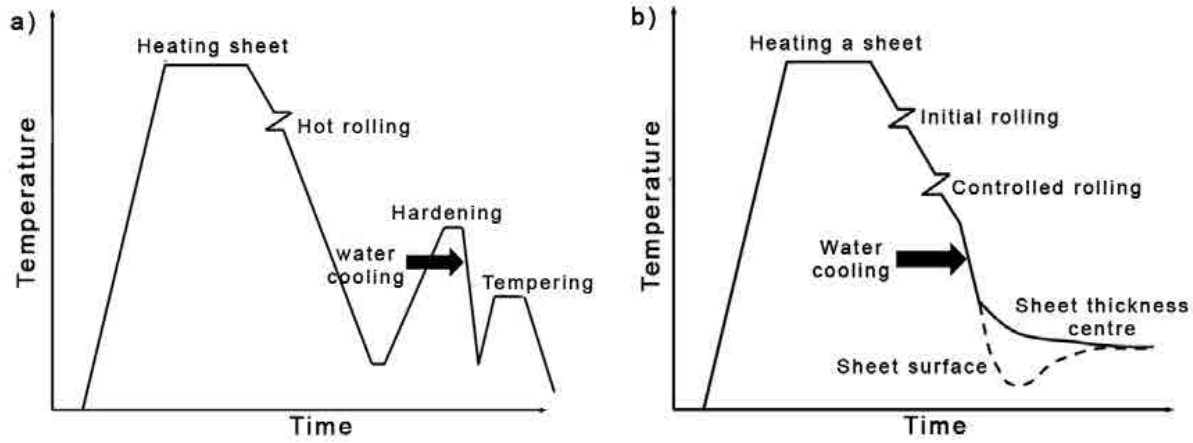

Fig. 2.7. Diagrams of production processes of toughened steels a) hardening and tempering processes, b) direct hardening process [11].

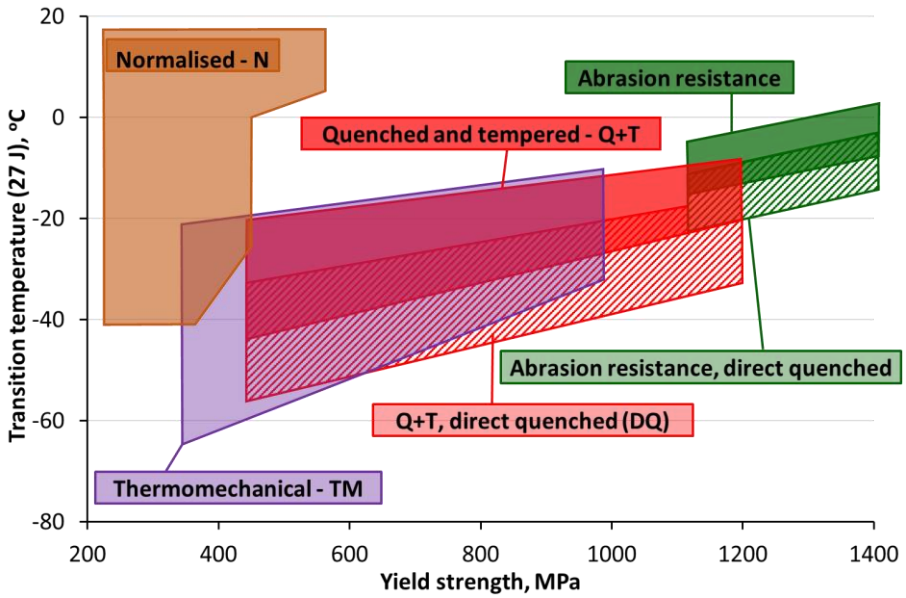

Fig. 2.8. Yield strength - transition temperature relation for different type of steels [11][12][23][24].

While developing a technology for welding of toughened steels characterised by high mechanical properties, one should also have focused on apart from cold crack formation, such phenomena as follows: welding-induced HAZ softening (“soft layer issue”); failure to obtain a required toughness level in the weld and HAZ (brittleness caused by ageing and precipitation hardening). “Soft layer issue” during welding of toughened steels develops in their HAZ a softened microstructural area with worse mechanical properties [11].

This phenomenon is particularly visible in steels after rolling and intensified cooling. Fig. 2.9 presents hardness changes in the cross-section of the welded joint made of toughened steel (Q+T). In the HAZ of toughened steel a hardness decrease is to a small extent caused by phase transitions; much greater in this case is the impact of tempering. Welding with limited linear energy makes the layer narrow. In this case, although the hardness of this layer is lower, this fact, due to a narrow softening zone, does not have to result in the deterioration of the mechanical properties of the joint, because of the "contact strengthening" phenomenon generated by plain strains induced in the soft layer [11].

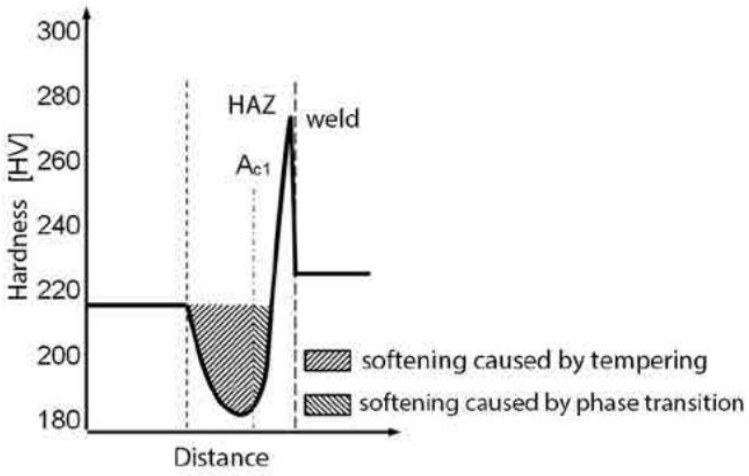

Fig. 2.9. Hardness distribution in welded joint made of toughened steel (Q+T) where R_y > 500 MPa and $t_{8/5}$ = 30 s [11].

Regarding weldability of toughened steels it is required to select a proper welding parameters i.e. appropriate filler material higher or lower than that of parent metal. Welding conditions used with toughened steels is significantly narrower allowed variability limits comparing with conditions used thermomechanically rolled steels [11].

There are an increase in HAZ hardenability occur due to the dissolution of micro-additions causes a shift of transformation curves in the continuous time-temperature-transformation (TTT) diagram towards a longer self-cooling time, resulting in an increase in a martensite and bainite content. These structures, combined with a grain size increase may lead to toughness decrease, especially if the linear energy of an arc is high [11]. Features of toughened steels are as follows [8][11].

- Very good mechanical properties, good weldability, via appropriate selection of chemical composition and proper heat treatment, i.e. hardening and tempering.
- Additions Cr and Mo decrease critical cooling rate and increase hardenability. The hardenability of such steels improved by introducing a micro-addition of B below 0.005%.
- The most effective alloying elements to enhance hardenability are C, Mn, Mo, and Cr.
- Tempering by 600ºC results a high level of mechanical properties and good plasticity. After the tempering the steel is characterised by a fine-grained structure with dispersive carbides and a favourable combination of strength and impact resistance.
- Adding Ni can replace C, Mn and other alloying elements that are less favourable for HAZ.
- The strength of the simulated HAZs increased with increasing V content in the HSLA steels.

- Precipitation hardening of NbC or V_4C_3 leads to increase in mechanical properties. Impact strength improving by adding Ni, and reduce impurities (S, P) the metallurgical processes of toughened steels improved.
- The aim of quenching and tempering (Q+T) is to produce a microstructure consisting mainly in tempered martensite. Some amounts of lower bainite are also acceptable.
- A homogenous hardness is achieved with a CE of 0.70% whereas a CE of 0.55% results in a marked gradient in hardness.

From other side the limitations of toughened steels are as follows [8][11].

- Worse plastic properties, thus cannot be used in pressure equipment. The high yield point of these steels have susceptible to cold cracking.
- Presence of Nb or V in these steels guarantees obtaining fine grains of austenite during rolling and thus occur very tiny lamellas of supersaturated ferrite (martensite) after cooling.
- Increasing temper parameter reason for lowered tensile properties are and raise of impact toughness.
- Steel of too low carbon content would tolerate ineffective tempering temperatures or soften.
- Impact toughness of the simulated HAZs decreased with increasing V levels. Especially, when V greater than 0.05% the impact toughness dropped remarkably.

Table 2.1. Development impact of metallurgical processes on the level of impurities in steels [11]

Element (ppm)	**Metallurgical processes in the years**		
	1950/1960	**1980/1990**	**1990/2010[2)]**
Sulphur	100-300	50-80	60
Phosphorus	150-300	80-140	6
Hydrogen	4-6	3-5	–
Nitrogen	80-150	<60	–
Oxygen	60-80	<12[1)]	–

[1)] Technology made it possible to obtain the oxygen content at the amount <12 ppm however in practice, the oxygen content in steel was higher.
[2)] The manufacturers do not indicate the content of hydrogen, nitrogen and oxygen.

2.2.1. Precipitation hardening

Occurs by the formation of carbides and nitrides. Precipitation of microalloying elements (Nb, V and Ti) can be used. As these precipitates are lowering the toughness in parent material and in the HAZ the concentration of such microalloys is kept at low levels. Alloying elements Mo, Cr are also forming carbides. The nature of these carbides (M_3C, M_2C, $M_{23}C_6$, and M_7C_3) and their effect on secondary hardening depends on their volume and distribution. In some steels the precipitation hardening of Cu is used (Cu ageing steels). Before the quenching equipment was installed in the plate mills such NiCu-age steels were produced to reach high tensile properties in the normalized+aged condition. For an optimized heat treatment 100 MPa can be gained by 1% Cu [12].

2.2.2. Grain refinement and work hardening

Steels of 690 MPa yield strength can also be produced by thermomechanical rolling followed by direct quenching or accelerated cooling. In this case rolling at low temperatures improves the grain refinement and dislocation density. When considering the Hall-Petch correlation one could gain 200 MPa "simply" by ferrite grain refinement from 20 μm to 2 μm grain diameter. With normal TMCP process a grain diameter of 10μm can readily be produced, yet, other strengthening mechanisms have to be added. The strengthening effect of work hardening and grain refinement is lost in parts of the HAZ so that there in a risk of insufficient strength to occur next to the weld. In particular, the welding of thin plates requires stickly limited heat input in order not to affect the load bearing capacity by excessive softening [12].

The procedure of combination between base materials and filler metals take into consideration to avoid risk customer of selection to a proper combination for base materials and filler metals; i.e. may not meet the specified and required properties for the application and results often in suboptimum weld properties. Under marketed series alform® welding system (Fig. 2.10), a new way was carried out by the base material producer and the filler metal producer. Within a project, the companies have developed an entire series of base material /filler metal combination for HS and UHS weld joints with yield strengths ranging between 700 and 1100 MPa. The essential advantages of this fine-tuned solution are the extended welding range for HS and UHS weld joints as well as lower cold cracking sensitivity in welds and optimized properties [18].

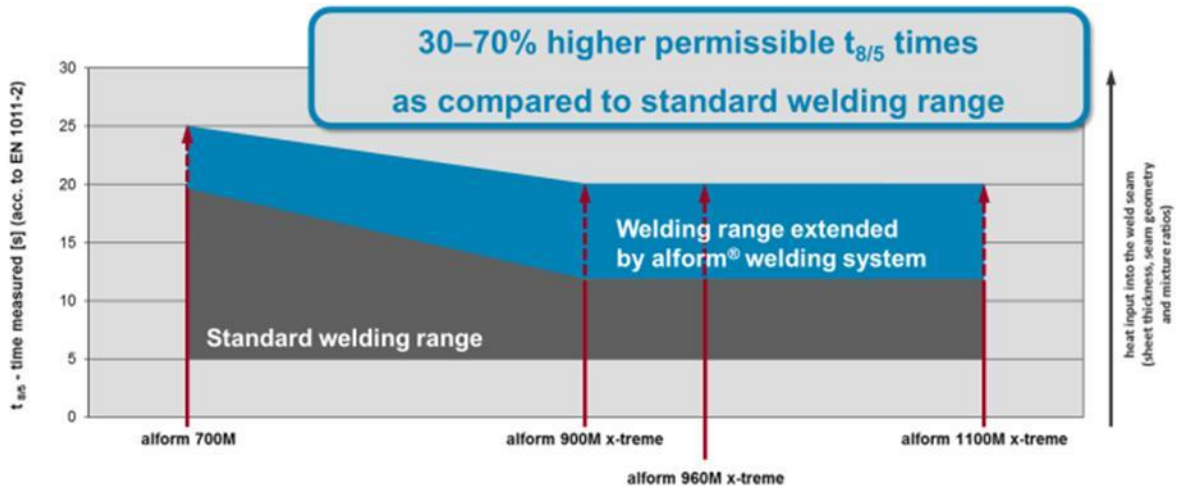

Fig. 2.10. Possible welding range expansion through the use of alform® welding-systems [18].

Welding effected by carbon content however, conventional Q+T steels is generally much higher carbon content than TM controlled rolling steels, according to that there are three different areas distributed on Graville diagram (see later) have a direct related to increase carbon content and then cold cracking sensitivity be visible as defects of welding, where these regions are: low, medium, and high [18].

Determination of a suitable welding procedure along with the respective combination of welding current source, base material and filler metal is always challenging process. However, there are some welding parameters that have an effects on properties like heat input, layer buildup, interpass temperature, and dilution between the filler metal and the base material [18].

The extent of dilution depends heavily on the shape of the bead and buildup sequence of the seam. These in turn are determined by the selected welding parameters. The investigations revealed that an increase in the interpass temperature from 20°C to 100°C would lead to an inadmissible prolongation of the $t_{8/5}$ cooling time by 50% (from 20 seconds to 30 seconds). The prescribed $t_{8/5}$ cooling times can be regarded only as reference values for heat input and can be achieved with a variety of different parameter combinations. In designing weld seams, the bead shape and layer sequence must be taken into account along with the $t_{8/5}$ cooling time because all of these factors determine welding properties [18].

2.3. Application fields, requirements, loads and processing technologies

Welded parts have been used in the majority of engineering applications such as engineering structures, power generation, offshore structures, and in vehicle industry (thick plates) and auto industry (thin plates). Welded joints are very sensitive parts of the structures, because the welded regions are in complex metallurgical and stress conditions. Steel producers currently provide a diversified spectrum of high strength base materials and filler metals. Specific design solutions and economic aspects of modern steel constructions can be found in the practice; extensive reduction in weight and production costs can be achieved with increasing material strength. High strength structural steels with nominal yield strengths from 690 MPa upwards are applied in growing amount of applications [25][26]

During the welding process the joining parts are affected by heat and mechanical loads, which cause inhomogeneous characteristics (microstructure, mechanical properties, and stress distribution). These particularities appear in deflections (basically acceptable), or rather in failures (basically unacceptable), and influence both the behaviour and the loadability of welded joints [27][28][29]. Discontinuities in base materials and their welded joints have especially high danger in case of cyclic loading conditions, which are typical for different structures and structural elements (e.g. bridges, vehicles) [30].

There are many different applications (Fig. 2.11) in our world rely on HSS steel as a raw material in the manufacturing. Steel grades are applied in railcars, knuckle-boom cranes, spreaders, concrete pumps, agricultural and forestry machinery, mobile cranes, long-wall mining systems, trailers, push-off trailers, power generation plants rely on coal, nuclear, and oil/gas as energy supplies and much more [17][31][32].

Fig. 2.11. Multi-grades steel applications [17].

2.3.1. First case study: H-shape beam

JFE Steel developed and manufactures large-section constant-outer-size H-shape beams (Fig. 2.12) with a web height of 1000 mm (Super HISLEND H-Shape), which is widely used in buildings, factories, and various types of plants to protect from giant earthquakes which caused widespread damage in structures [20].

A schematic diagram of an advanced TMCP process which considers a manufacturing technology specifically for H-shape beams in comparison with conventional controlled rolling (CR) can be seen in Fig. 2.13.

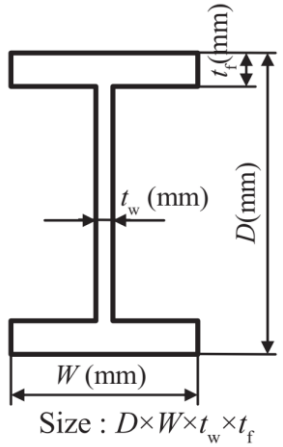

Fig. 2.12. H-shape made by JFE Steel [20].

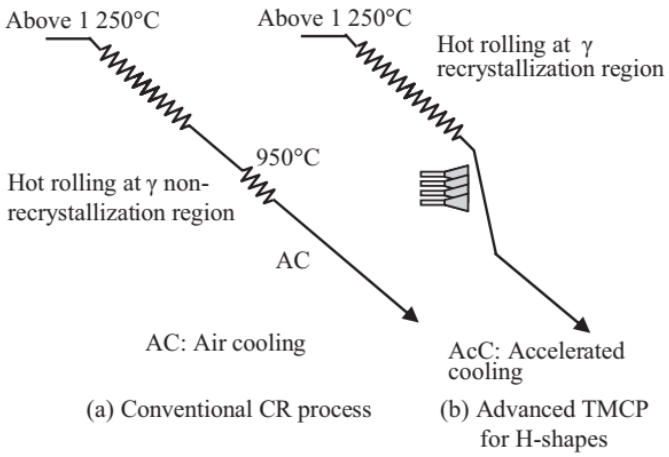

Fig. 2.13. Schematic illustration of conventional CR process and TMCP for H-shape beams [20].

It is necessary to perform composition design properly in order to promote refinement of the initial γ grain size and recrystallization of γ during hot rolling. In hot rolling, H-shape beams with HS and excellent ductility and toughness can be manufactured by securing the amount of reduction in the high temperature region necessary to ensure adequate recrystallization of the

coarse initial γ grain size, followed by accelerated cooling. Although the strengths of the CR steel and TMCP steel are on the same level, the TMCP steel possess superior toughness [20].

The conventional CR steel is a 0.15%C-1.45%Mn steel with microalloying of Nb and V. The TMCP steel is a 0.13%C-1.55%Mn steel without addition of Nb and V microalloys. With the TMCP steel, accelerated cooling by water cooling from the γ region was performed after hot rolling. The CR steel has a ferrite + pearlite structure, whereas the TMCP steel has a fine bainite structure [20].

2.3.2. Second case study: boggi beam and dipper arm

The outdated components today a boggi beam in an articulated hauler and a dipper arm in an excavator have plate thicknesses from 10-25 mm with a yield around 350 MPa and are in as welded condition (Figs. 2.14). The structural weight could be reduced from 18-24% using plates thicknesses 8-12 mm in material yield 700 MPa with approximately twice as high yield limit (700 MPa) and applying HFMI treatment on highest stressed weld toes to treat weld toe transitions to develop allowed stress levels in the beam to fulfill life requirements [33].

Fig. 2.14. Boggi beam (left) and excavator arm (right) [33].

Fig. 2.15 shows the new design of boggi beam and dipper arm, furthermore the comparison between the former and new design for both structural elements are clarified in Table 2.2.

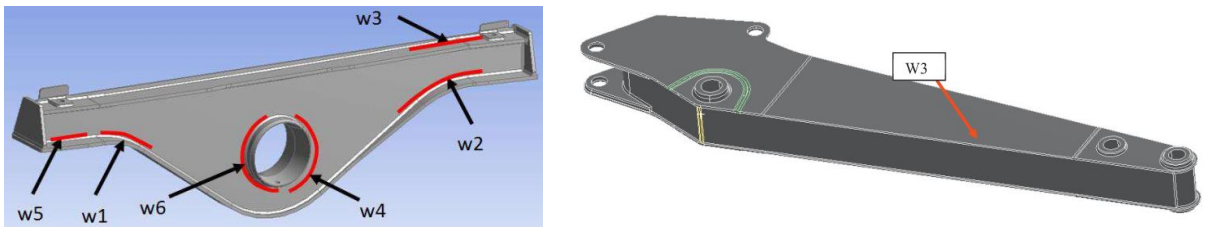

Fig. 2.15. New design of both boggi beam (left) and excavator arm (right) [33].

Table 2.2. Characteristics of boggi beam and dipper arm [33]

Properties / Types	**Previous design**		**New design**
Boggi beam			
Plate thickness (mm)	12 and 15		6, 8 and 12
Yield stress (MPa)	355		690 and 700
Stress range (MPa)	W4,W6: 530	W1,W2: 440	W4,W6: 370
Fatigue life (hour)	W4,W6: 270	W1,W2: 670	10000
Dipper arm			
Plate thickness (mm)	10, 12, 20, and 25		
Yield/Computed stress (MPa)	355/688		700/1100
Critical weld position	Right end (W3) and back connection of casting		Non
Fatigue life			Increased and other points will be critical

Advantages of applied TMCP plates, based ont he first two case studies [17][18][20][33]:

- weight and volume reduction (reduced material thicknesses);
- best cuttability (low carbon content and homogeneous surface);
- very good cold formability (homogeneous and fine-grained microstructure);
- outstanding weldability (TR and micro-alloying, achieved very low carbon content);
- excellent toughness (TR and AcC, achieved fine-grained structure);
- perfect flatness (precisely controlled manufacturing processes);
- clean surface (hot rolling);
- short processing times (flatness and surface, achieved increased cutting speeds and optimized work processes);
- reduction of revision work (homogeneous properties of the materials);
- reduction of transport and logistics costs (reduced material thicknesses);
- perfect welded joints (lower cold cracking sensitivity, optimized properties, see Fig. 2.10);
- exceptional strength (high design strength due to low yield/tensile ratio);
- operational reliability (excellent value);
- best product quality (aggregation of the individual details).

2.3.3. Third case study: butt and fillet welds HSS of yield strength 350 – 960 MPa

Butt welds: S700 and S960 grades, with three mismatch cases (undermatched, matched and over matched), X and V shape, and fully partially penetration [31]. For S700 grade: partially penetrated joints, the maximum load carrying capacity is 70% of the fully penetrated joints. No significant difference in load capacity of different mismatch cases. Failure started in weld root and propagated along the HAZ. For S960 grade: the loss in load carrying capacity in matched joints 30% and in under-matched joints 57% of the base plate strength. Hardness is higher in matching than undermatching in comparision with base material. Failure for matching joints occurred in base plate while undermatching joints occurred in between the weld metal and the HAZ.

Fillet welds: joints are made from S600MC while the flange is S690QL, penetration are full (100%) and partial (50% and 75%), two mismatch cases, overmatching and undermatching [31].

In an overmatched case and (full penetration ratio) ultimate strength capacity is increased 16% while in (partial penetration ratio) the capacity decrease by 20%. In an undermatched case when increase penetration ratio (from 75% to 100%), the ultimate strength capacity of the joint increased by 63% while decrerase penetration ratio (from 75% to 50%) decreased the ultimate strength capacity by 28%. Failure for the full penetration welds occurred in the web plates of the steel grade S600 MC while for the partial penetrated fillet welds failure occurred on the welds.

2.3.4. Fourth case study: welding of advanced alloyed

Different cases were studied to describe research needs and recent results in areas [32]:

- *Metal Arc Welding Under Oil (MAW-UO) of Steels for In-Situ Repairs:* repairing flaws and corrosion damage, for in situ internal repairs of in-service pipelines, tanks, and vessels;
- *Underwater Welding of Steels*: used in operation and maintenance of offshore structures for oil and gas exploration, production, processing, and transport;
- *Low Hydrogen Consumables for HS Steels:* two concepts, duplex weld microstructural design and hydrogen management strategies;
- *Computational Welding Consumable Design:* HS pipelines need for welding consumables with matching mechanical properties;
- *Consumables for Residual Stress Management and Improved Fatigue Strength:* decreasing of develop high tensile residual stresses and methods to develop compressive stresses;
- *Minimization of HAZ Degradation in Advanced High-Strength Steels:* employing laser or hybrid laser welding processes.

2.4. Weldability questions, mismatching, cracking phenomena

There are several possible ways to increase the strength of steels (e. g. grain size reduction; formation of a complex phases, like DP, TP and TWIP; precipitation hardening of the maraging steels (see Fig. 2.2)). In case of the examined heavy plate thickness range, the higher strength can be effectively reached by grain refinement and the change of the second phase quality, size and distribution [27][34][35]

Among the fine grained HS steels, the highest strength can be achieved by the quenched and tempered (Q+T) group, where the minimal yield strength is 1300 MPa already reached nowadays. Other type of fine grained HS steel is the thermomechanical (TM) group which is already above 960 MPa level. Both type steels have a non-equilibrium microstructure that can be irreversible changed due to the welding heat input [27][34][35]

During Q+T process (see subchapter 2.2.), after a hot rolling above A_3 temperature, the slow cooling rate is generated until the plate cools down to room temperature. Then, the hot rolled plate is reheated above A_3 temperature, and held there for a short period, while the micro-structure in the whole cross section transforms to austenite. After that, a quenching process takes place, when an extremely high cooling rate is applied, which can be achieved by water quenching [111]. In order to realize the quenched condition in the whole cross section, alloying components (Cr, Mo) are added to the steel, which moves the CCT curves to the right. Microalloying elements (Ti, Nb, V) are also used in order to ensure and preserve the fine grain microstructure. Then, in the tempering cycle (HTT: high temperature tempering) of the heat

treatment process, the plate is heated under A_1 temperature, which is followed by a slow cooling process.

Direct quenched high strength steels (see subchapter 2.2.), marked with QC by the producer, have been recently developed by RUUKKI [112]. During the production process, an intensive cooling is applied directly after the hot rolling, resulting in a quenched microstructure. This is the first heating cycle, which is followed by a low temperature tempering (LTT), with a much lower temperature than A_1. Therefore, the microstructure of QC steels builds up from martensite and bainite, and rarely contains precipitates. During their production the lower energy consumption (two heat cycles instead of three, and LTT instead of HTT) and the reduced number and extent of alloying elements have a cost-saving effect. Since the considerable part of the microstructure is martensite, the part of HAZ, heated between 450 °C and A_3, significantly loses its strength due to the tempering of martensite. Therefore, the $t_{8.5/5}$ cooling time should be maximized [112], and it can only be extended if the design requirements allow undermatching [13][113][114].

Graville diagram (Fig. 2.16) characterised cold cracking sensitivity (which can be avoided by the application of preheating temperature (T_{pre})) of the structural steels, different kinds of structural steels are situated in the diagram on the basis of their chemical composition. The investigated S960M (Alform 960M) steel falls into the area I., which indicates low sensitivity to cold cracking similar to the conventional S235JR steel. However, the different grades of Q+T steels (S690Q (Optim 700QL and Weldox 700E) and S960Q (Weldox 960E)) are located in the area III., which means that they have high carbon content and high hardenability [37].

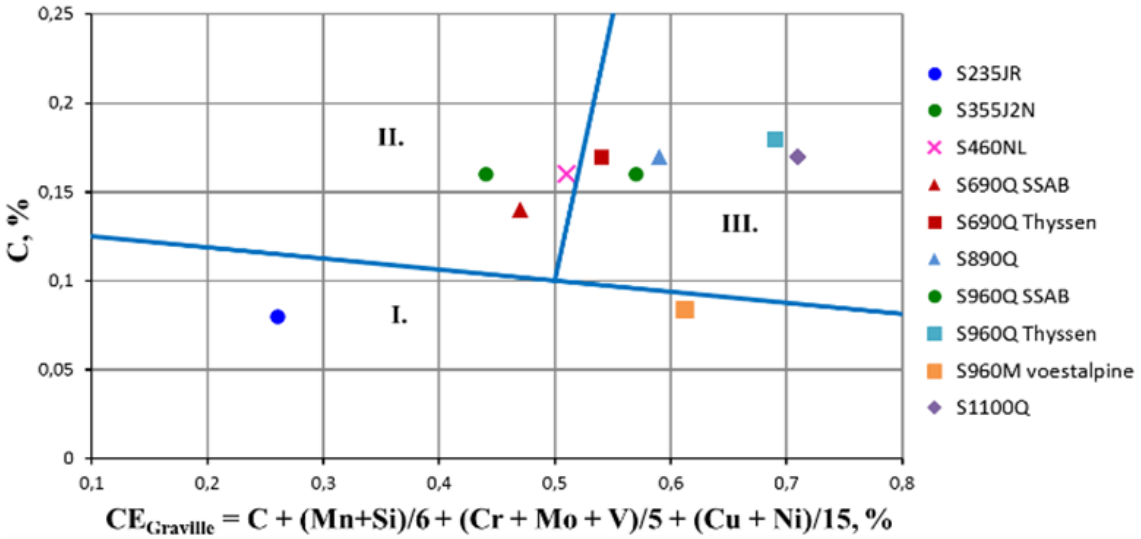

Fig. 2.16. The Graville diagram [37].

In case of high HSS, the control of the linear energy (E_v) is a key to their successful welding and to avoid cold cracks. If the value of the linear energy is too low, the cooling rate of the welded joint may be too fast (cold cracks may occur in the steel grade), In the opposite case, when high heat input is applied, a wide HAZ can form with softened areas, furthermore the toughness properties can drastically decrease [37].

More factors influencing on the linear energy, the cooling time ($t_{8.5/5}$) was implemented for welding conditions and parameters, including linear heat input and preheating (T_{pre})/interpass (T_{ip}) temperature. The $t_{8.5/5}$ value shows the cooling time of the welded joint from 850 °C to 500 °C, which is a relevant interval in terms of the microstructural changes in the weld metal (WM)

and the HAZ. Steel producers recommend $t_{8.5/5}$ range for their products, very narrow interval in HSSS; furthermore, a narrow welding lobe is recommended for welding of HSSS, too. Also, the different types of filler metals, in mismatch cases influence these phenomena [37].

2.4.1. Solidification cracking (hot cracking)

Hot cracks are solidification cracks that occur in the fusion zone near the end of solidification. Simplistically, they result from the inability of the semisolid material to accommodate the thermal shrinkage strains associated with weld solidification and cooling. Cracks then form at susceptible sites (susceptible sites are interfaces, such as solidification grain boundaries and interdendritic regions that are at least partially wetted) to relieve the accumulating strain [37].

Solidification cracking requires both a sufficient amount of mechanical restraint (strain) and a susceptible microstructure. Under conditions of rapid solidification and cooling, the rate of strain accumulation is rapid, leading to an increased cracking susceptibility. Inherently, then, requisite strains for solidification cracking are more likely to be experienced with welding processes that promote rapid solidification and cooling [36].

Previous investigations show that Weldox 700E (S690QL) steel is not prone to hot cracking [106].

2.4.2. Hydrogen-induced cracking (cold cracking)

Cold cracks are defects that form as the result of the contamination of the weld microstructure by hydrogen. Whereas solidification cracking and HAZ cracking occur during or soon after the actual welding process, hydrogen-induced cracking is usually a delayed phenomenon, occurring possibly weeks or even months after the welding operation. The temperature at which these defects tend to form ranges from -50 °C to 150 °C in steels. The fracture is either intergranular or transgranular cleavage. As with other forms of cracking, hydrogen-induced cracking involves both a requisite microstructure and a threshold level of stress. It also involves a critical level of hydrogen, which is alloy and microstructure dependent. The primary source of hydrogen in weld metal is disassociation of water vapor in the arc and absorption of gaseous or ionized hydrogen into the liquid, and all organic compounds [37].

2.4.3. Lamellar tearing

It is cracking that occurs beneath welds and found in rolled steel plate weldments. The tearing always lies within the base material, generally outside the HAZ and parallel to the weld fusion boundary. Lamellar tearing occurs when three conditions are simultaneously present [37]: firstly, strains caused by weld metal shrinkage in the joint and increased by residual stresses and loading; secondly, the weld orientation is such that the stress acts through the joint across the plate thickness (z direction); thirdly, the material has poor ductility in the z direction.

Butt joints rarely exhibit lamellar tearing, because weld shrinkage does not set up a tensile stress in thickness direction of the plates. Arc welding processes with high heat input are less likely to create lamellar tearing, because of the fewer number of applications of heat and the lesser number of shrinkage cycles involved in making a weld [37].

2.4.4. Case studies of different mismatches investigated

First group of case studies: comparison of experimental works of nominally 700 MPa HSSS.

TM subgroup

- J. Górka [38]: S700MC, R_y = 768 MPa, matching, butt joint, Metal Active Gas (MAG) process – too much heat applied cause loss of the properties gained during TMCP.
- S. Ravi [39]: HSLA-80, R_y = 700 MPa, undermatching and overmatching, butt joint, Shielded Metal Arc Welding – the total fatigue life of the overmatched joints is greater than the undermatched joints irrespective of post eeld heat treatment. The better fatigue performance of overmatched joint is may be due to the following three reasons: superior mechanical properties of the weld metal; ideal microstructure of the weld region; favorable residual stress pattern in the weld metal region.

Q+T subgroup

- A. J. R. Loureiro [40]: RQT 701 = S690QL, undermatching, butt joint, Submerged Arc Welding (SAW) process – increase heat input coarsened microstructure and loss hardness, strength and ductility of the weld.
- M. Mirzaei et al. [41]: HSLA-100, t = 7 mm, ER100S-1 alloy welding wire, Pulsed Gas Metal Arc Welded (P-GMAW) and Conventional Gas Metal Arc Welding (GMAW) – acicular ferrite and lath martensite, small amounts of allotriomorphic and Widmanstatten ferrite; good mechanical properties; decreasing impact energy by decreasing welding velocity and increasing pulse frequency.
- K. Devakumaran et al. [42]: HSLA steel of SAILMA 410HI / SA543, t = 25 mm, thoriated tungsten electrode, Multi-Pass Conventional Metal Arc Welding Deposition and Pulsed Metal Arc Welding Deposition – significant variation of weld metal chemistry when using narrow groove GMA compared to conventional V-groove GMA; high rate of metal transfer in P-GMAW enhances the dilution of weld deposit; minimizes the effect of dissolution by fusion and solid state diffusion.
- P. Collin [43]: S500QT (WELDOX 500) and S690QT (WELDOX 700), undermatching and undermatching / overmatching, butt joint and fillet joint, Manual Metal Arc, Submerged Arc and Flux Core Welding processes – achieved plastic deformation in the base material with undermatched electrodes; no detrimental effects of the softened zone in the HAZ, the strength of the welds is at the same level as the base material for S500; for S690 the strength is slightly lower than that of the base material and with one exception it is higher the strength of the filler metal; it seems reasonable to accept undermatched butt welds in situations there the stress level is low or moderate.
- E. Harati [44]: DOMEX 650, WELDOX 700, R_y = 650 and 700 MPa, metal cored wires, OK Aristorod 89 high strength solid wire and OK Autrod 12.51 medium strength solid wire, butt joint and fillet joint, GMAW – very good fatigue testing results for all combinations of low transformation temperature consumables and HSS with varying strength levels.

Second group of case studies: comparison of experimental works of nominally 960 MPa HSSS.

TM subgroup

- M. Stoschka [45] and [46]: S960TM, thin walled structure, R_y = 960 MPa, G89 solid and metal cored wire, R_y = 915 MPa, undermatching, fillet weld and butt weld, GMAW – highest

fatigue strength condition using a high-strength metal cored wire filler in combination with a three-component mixed gas.

Q+T subgroup

- W. Guo et al. [47]: S960, t = 8 mm, Union X96 (ER120S-G), matching, butt joint with a parallel groove configuration, Narrow Gap Laser Welding (NGLW) and GMAW – the strength of the ultra-NGLW specimens was comparable to base material, with all welded specimens failed in the base material in the tensile tests.
- W. Guo et al. [48]: S960, t = 8 mm, without fillar metal, matching, butt joint, laser welding process – the tensile properties of laser welded joint matched base material, with failure occurring in base material away of weld, impact toughness reduced compared by base mataerial.
- M. Gáspár and A. Balogh [13]: S960QL, t = 15 mm,: UNION X96, matching, single side butt welds (V type prepared), GMAW process – generally, the upper limit of linear energy, which gives acceptable mechanical properties, is 900-1000 J/mm. When larger linear energy is set, the tensile strength and Charpy-V energy reduce under the required minimum values. By increasing the strength of structural steels, the welding lobe becomes narrow.

TM and Q+T subgroup:

- M. Gáspár and R. P. S. Sisodia [49]: S960QL and S960M, UNION X96, matching, single side butt welds (V type prepared), GMAW process – on the basis of the simulation results S960M can be welded without preheating, which has a positive effect on the production time and energy saving. Regarding the Charpy V-notch impact tests the welding heat input significantly affected the HAZ toughness in both steels, however the absorbed energy was always higher in S960M compared to S960QL.
- P. Collin [29]: S1100QL (WELDOX 1100) and S960QL (WELDOX 960), undermatching, butt joint, Flux Cored Arc Welding (FCAW) – the weld width and volume has a strong influence on the strength of the joint
- E. Harati [44]: WELDOX 900 and XABO 890, R_y = 890-900 MPa, OK Tubrod 14.03, OK Tubrod 15.30 metal cored wires, OK Aristorod 89 high strength solid wire and OK Autrod 12.51 medium strength solid wire, butt joint and fillet joint, GMAW process – very good fatigue testing results for all combinations of low transformation temperature consumables and HSS with varying strength levels.

2.5. Recommendations to the aims

- Q+T and TM type base materials with different strength categories should be investigated;
- the directions, in other words, the possible crack paths are important, longitudinal, transversal and thickness directions should be investigated, if possible;
- the welding characteristics have great influence on the joint quality, therefore the narrow welding lobe should be applied which has industrial relevance;
- mismatch phenomenon should be investigated and by reason of the different strength categories beside matching conditions both undermatching and overmatching variants should be accomplished, too.

3. CYCLIC LOADS

3.1. Failure statistics

The previous works were revealed many fatigue failures for example: on 27th July 1934 a Curtis "Condor" accident killed 11 people by fatigue failure of a wing strut in Germany; on 5th October 1842, a locomotive axle broke at Versailles, claiming the lives of 60 people about the same number as were lost in the two crashes of 1954; the United States Air Force in particular suffered many accidents due to fatigue, on 13th March 1958, two Boeing B-47 nuclear bombers crashed due to fatigue failure of the wing, within two months two more aircraft also failed in the same manner; in 1958 two large steam turbine rotors burst during test runs, as well as several "Polaris" rockets during pressure tests. In all cases, the cause was crack-like material defects, which in the Polaris rocket were very small because UHS steel was used. In 1969 the fatigue fracture of an F-111 wing led to a complete change of the structural specifications of the US Air Force, combined with an immense fracture mechanics programme that is continuing to this day. As late as 1987 Swift of the FAA showed, however, that in reality, a design fault had been the cause of the accidents: the fuselage frames were in one piece, whereas in more modern aircraft types they are built up of two independent frames. A Boeing 707 crashed in Lusaka, Africa, by fatigue failure of the empennage. Other accidents in Chicago by a failure of an engine mount and on 10 September 1989 in Sioux city by the uncontained burst of an engine disc [1].

3.2. Generalities, importance, classification

3.2.1. Fundamentals of assessment procedures

The local approaches to be reviewed aim at covering the dominating parameters of an extremely complex physical reality in order to make it controllable by the engineer. This reality comprises primarily microstructural phenomena (moving dislocations, microcrack initiation on slip bands, further crack growth by local slip mechanisms at the crack tip), but can be approximately described by a macroscopic elastic-plastic stress and strain analysis according to continuum mechanics which refers to cyclic crack initiation, stable cyclic crack propagation and unstable final fracture, as can be seen in Fig. 3.1 [50][51][52].

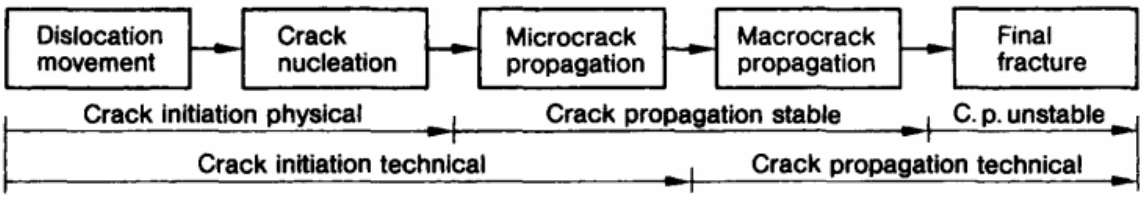

Fig. 3.1. Micro and macro phenomena of material fatigue [51][52].

The cyclic initiation of the technical incipient crack is primarily determined by the amplitudes of the cyclic stress and strain components at the notch root, the volume of the highly stressed material being also important. The influence parameters controlling the limit values of the stress and strain parameters which refers to the local approach insofar as local stresses and strains are introduced instead of external loading. The number of the influence parameters is large, but can be handled within the procedure of strength assessment. A problem arises from the lacking possibility to decouple the effects of the influence parameters in case of engineering tasks [50][53].

The cyclic crack propagation is primarily determined by the amplitudes of the cyclic stress intensity factor or of the cyclic J-integral at the crack tip. The influence parameters controlling the limit values of the stress and strain parameters at the crack tip, which once more refers to the local approach by introducing the local parameters. Considering crack initiation in comparison, some influence parameters have been dropped and others added. The influence of surface is omitted, the influence of crack shape and crack size added [50][52].

Strength assessments comprise the explicit or implicit comparison of load, stress and strain parameters including their limit values, which cause a definite damage, a definite deformation, an incipient crack or total fracture. The loads comprise forces and moments, the stresses and strains are of the nominal, structural and notch type, stress intensity factors and the J-integral are derived therefrom. The appertaining limit values are designated as strength values. The assessment of fatigue strength is also performed in such a way that the specimen or component life is determined at a given load value instead of the strength at a preset number of cycles [50].

Strength assessments are termed global approaches if they proceed directly from the acting forces and moments or from the nominal stresses derived therefrom under the assumption of a constant or linearized stress distribution (therefore nominal stress approach). The global approaches originally use limit values of load or nominal stress which are related to global phenomena such as fully plastic yielding or final fracture of the specimen. Strength assessments are termed local approaches if they proceed from local stress and strain parameters. The local processes of damaging by fatigue of material are considered, cyclic crack initiation, cyclic crack propagation and final fracture [50][54].

The most important basic variants of the global and local approaches are shown in Fig. 3.2 (El. = elastic, El.-pl. = eastic-plastic), each variant characterized by the typical load, stress or strain parameters and the appertaining strength diagram. The local quantities result from the global quantities proceeding from the left hand side to the right hand side of the figure by increasingly taking local conditions into account. The following strength diagrams are presented: load *S-N* curve, nominal stress S-N curves for standardized notch cases, structural stress *S-N* curve, notch strain *S-N* curve, Kitagawa diagram (cyclic limit stress over the length of short cracks) and crack propagation rate over the cyclic stress intensity factor of longer cracks [50].

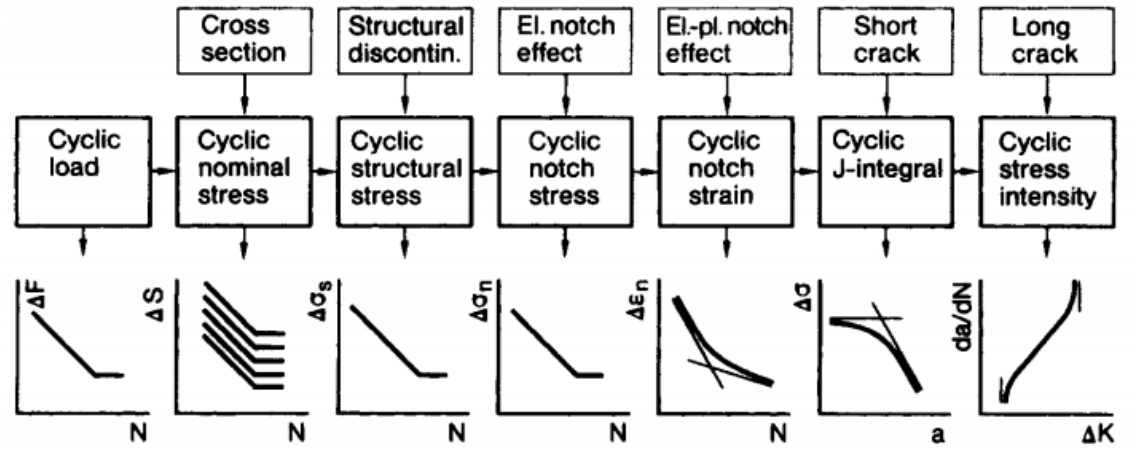

Fig. 3.2. Global and local approaches for describing the fatigue strength [50] (El.=Elastic, El.- pl.=Eastic plastic).

3.2.2. Types of assessment procedures

The nominal stress approach [50][54] for assessing the fatigue strength and service life proceeds from the nominal stress amplitudes in the structural component and compares them with the nominal stress S-N curve, which is contain the influence of material, shape (inclusive of notch effect and size effect) and surface (inclusive of residual stresses), as can be seen in Fig. 3.3 [50].

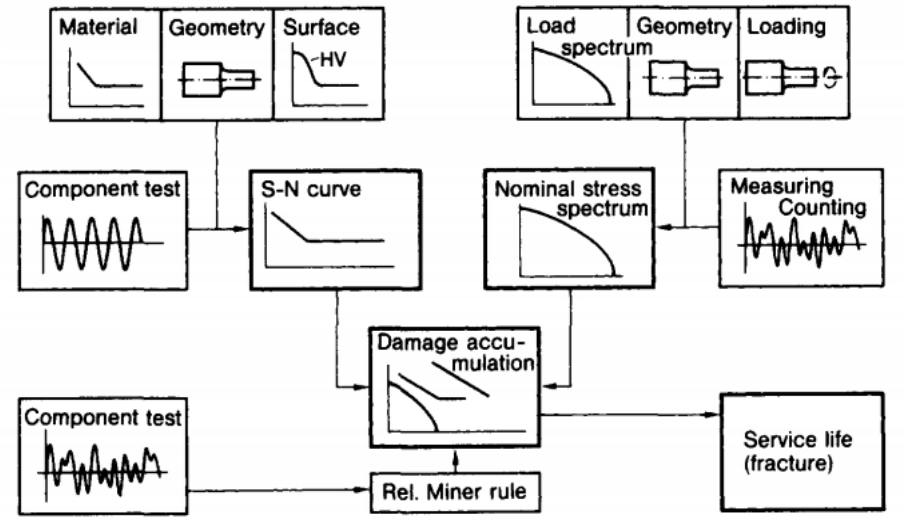

Fig. 3.3. Nominal stress approach for assessing the fatigue strength and service life of non-welded structural components [50].

The nominal stress S-N curve and the nominal stress spectrum according to a simple hypothesis of damage accumulation are resulting service life, mostly according to the relative Miner rule. The service life calculation is generally performed in respect of final fracture, but it can also be made in respect of crack initiation [50].

The structural stress approach for assessing the fatigue strength and service life proceeds from the structural stress amplitudes in the component and compares them with a structural stress curve. The approach is sufficiently developed in this form for welded structures only. It aims at

optimizing especially macrogeometrical influence parameters. The structural stress approach for welded joints gives an indication of how quantitative statements may be achieved for notched areas also, without resorting to the notch root approach which requires higher expenditure [50].

The notch root approach for assessing the fatigue strength and service life up to crack initiation proceeds from the elastic-plastic strain amplitudes at the notch root and compares them with the strain S-N curve of the material in the unnotched comparison specimen. The idea behind this approach is that the mechanical behaviour of the material at the notch root in respect of local deformation, local damage and crack initiation is similar to the behaviour of a miniaturized, axially loaded, unnotched or mildly notched specimen in respect of global deformation, global damage and complete fracture [50][53].

The comparison specimen is either imagined as positioned at the notch root, or really cut out from this area. It should have the same microstructure, the same surface condition (inclusive of residual stresses) and about the same volume as the material at the notch root. At least, well founded corrections of the test results with the specimen should be possible for the purpose of comparison [50].

The strength assessment consists of determining the stresses and strains at the notch root in the elastic-plastic condition and comparing them with the strain curve of the material in the miniaturized specimen up to complete fracture or in a larger specimen up to the technical crack initiation (crack depth about 0.5 mm, crack width at the surface about 2 mm), as shown in Fig. 3.4 [50].

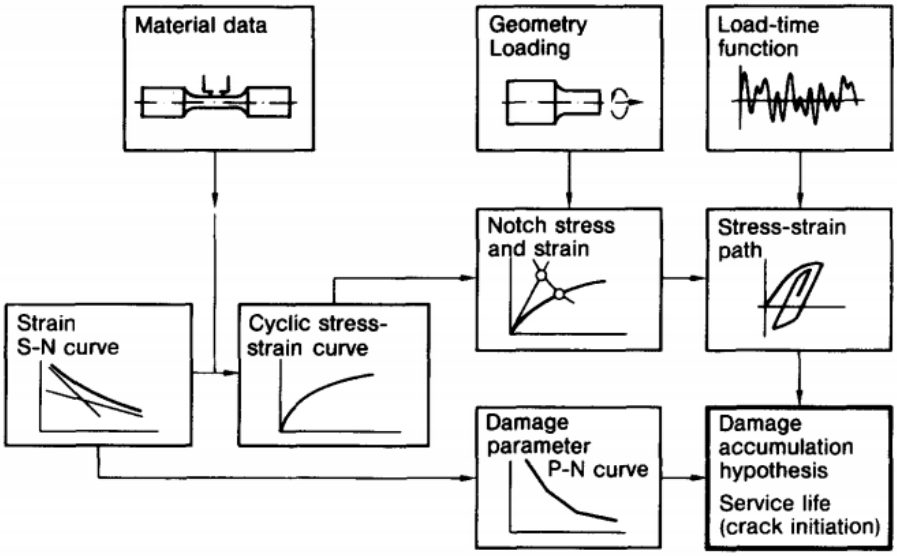

Fig. 3.4. Notch root approach for assessing the fatigue strength and service life of nonwelded structural components [50].

The stresses and strains at the notch root of the structural component are calculated proceeding from the cyclic stress-strain curve and the macrostructural support formula. Considering the case of a sharp notch, the microstructural support effect has additionally to be taken into account according to one of the well-known hypotheses. The mean values and the principal directions of the stresses and strains are introduced besides their amplitudes. Finally, a sequence of hysteresis loops in the stress-strain diagram (i.e. the stress-strain path) results on the basis of the load time function [50][54][55].

Uniaxial conditions are the basis of Fig. 3.4 in order to simplify the representation. Biaxial conditions (on the surface) and triaxial conditions (under the surface) on the other hand prevail at the notch root of structural components [50].

The assumption is well founded in this case that no appreciable plastic deformation occurs at the notch root, i.e. the notch effect of the structural component can be described as linear elastic and set against the endurance limit of the material, see Fig. 3.5. The elastic stress concentration factor is dependent on shape, dimensions and loading of the structural component [50].

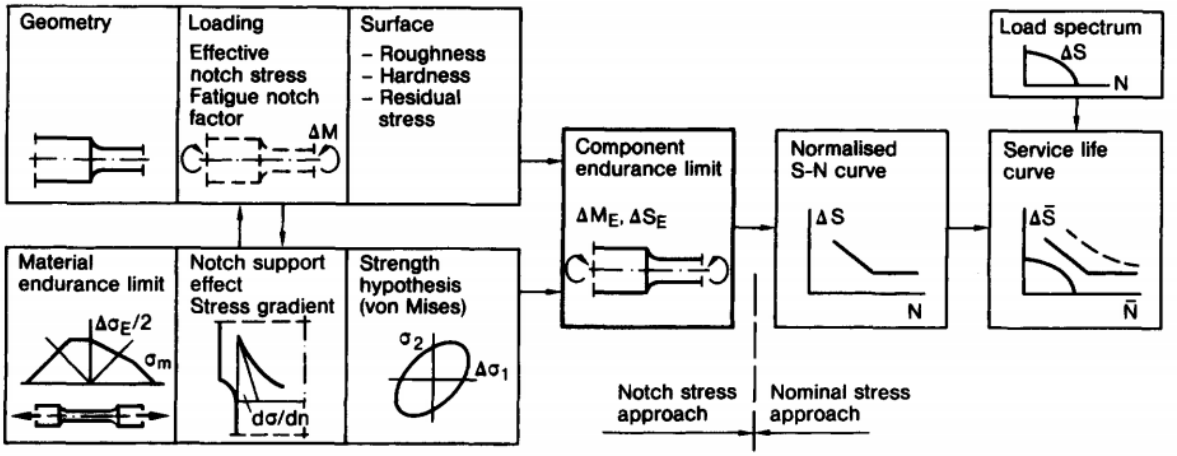

Fig. 3.5. Notch root approach for assessing the endurance limit of nonwelded structural components [50].

The fatigue crack growth theory, which is fracture mechanical theory, can be seen in Fig. 3.6 [54]. From the loading side the stress-time history should be recorded and analysed, from the structural element side the geometry, the surface and the fatigue crack propagation resistance of the applied material should be taken into consideration. Using the different stress intensity factors (K_I and/or K_{II} and/or K_{III}) different modes of loading conditions can be approached.

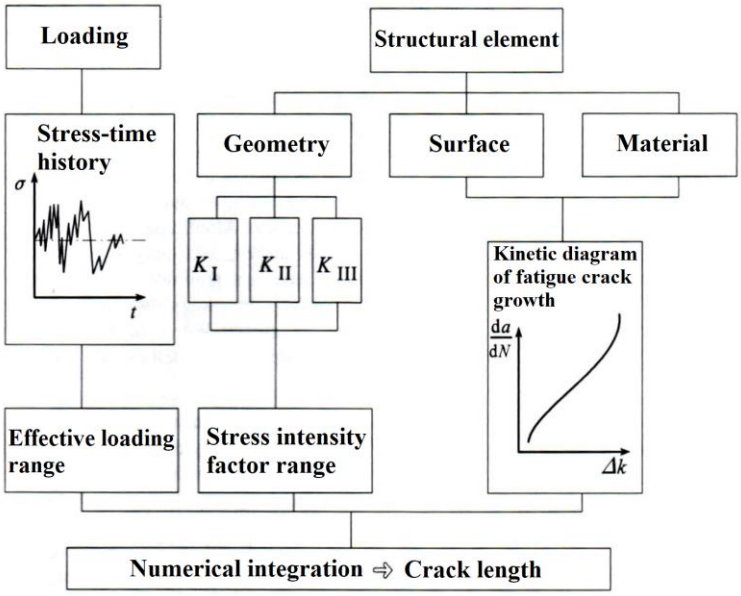

Fig. 3.6. Fatigue crack growth approach for assessing a structural element containing crack or crack like defects under cyclic loading condition [54].

3.3. High cycle fatigue (HCF) characteristics and fatigue strength curves

When studying the old works some interesting points attract attention, as follows.

- Wöhler, for example, as early as 1860 suggested design for finite fatigue life. In other respects, however, their opinions were astonishingly primitive and erroneous.
- Knowledge about certain methods was highly developed in one location.
- Decades after final clarification of certain problems, they continue being discussed over and over again in the literature.
- It takes a long time, sometimes decades, until parameters known for ages are treated scientifically.
- Many well-known old publications treat additional important problems besides the subjects for which they are still remembered today.
- Some well-known fatigue scientists and engineers wrote only a few papers on the subject.
- Fatigue failures of machines, plants and vehicles in service always led to significant efforts and advancements of the state of the art (see Fig. 3.7) [1].

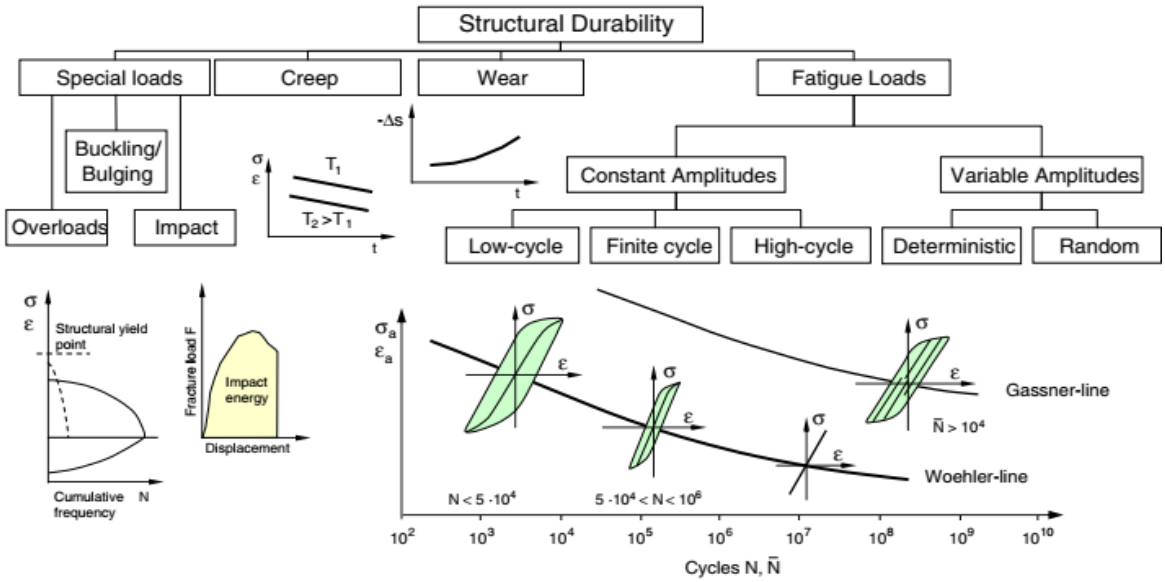

Fig. 3.7. Partition of structural durability [56].

3.3.1. Details of welding charachteristics, base materials (BM) and filler metals (FM)

A short overview of different base material-filler metal pairing and mismatch cases for butt welded joints are as follows.

- M. Toyosada [21]: AH400, MAG process, 20 specimens, t = 25 mm / 30 mm.
- R. J. M. Pijpers et al. [25]: Naxtra M 70 (S690) and Weldox S1100 E (S1100), Megafill 742M Tenacito 75 filler metal, overmatching and undermatching, FCAW and SMAW processes, 6 and 7 specimens, 750×120×12 and 1000×100×10 mm specimen dimensions.
- B. Jonsson et al. [32]: S355 and S700, t = 12-15 mm and t = 8-12 mm specimen thicknesses.
- M. Stoschka et al. [46]: S960TM, G89 metal cored wire, undermatching, SMAW process, 165 specimens, 325×50×5 mm specimen dimensions.
- M. J. Ottersböck et al. [57]: S1100, G89MC filler metal, undermatching, GMAW process, 78 specimens, t = 6 mm.

– T. Nykänen and T. Björk [58]: S235 and S1100, GMAW process, 775 specimens, t =3-40 mm.
– T. Teng, C. Fung and P. Chang [59]: ASTM A36 carbon steel, GMAW process, 16 specimens, t = 10 mm.

3.3.2. Fatigue resistance curves – as welded cases

HCF tests were performed on different strength categories (355 to 1300 MPa) including quenched and tempered (Q+T) and thermomechanical (TM) types. During the HCF tests base materials in different strength categories and their gas metal arc welded joints were investigated at different mismatch conditions (matching, undermatching, overmatching). Filler metal type, filler metal transition temperature, stress ratio were studied, too (see selected cases in Figs. 3.8 – 3.12).

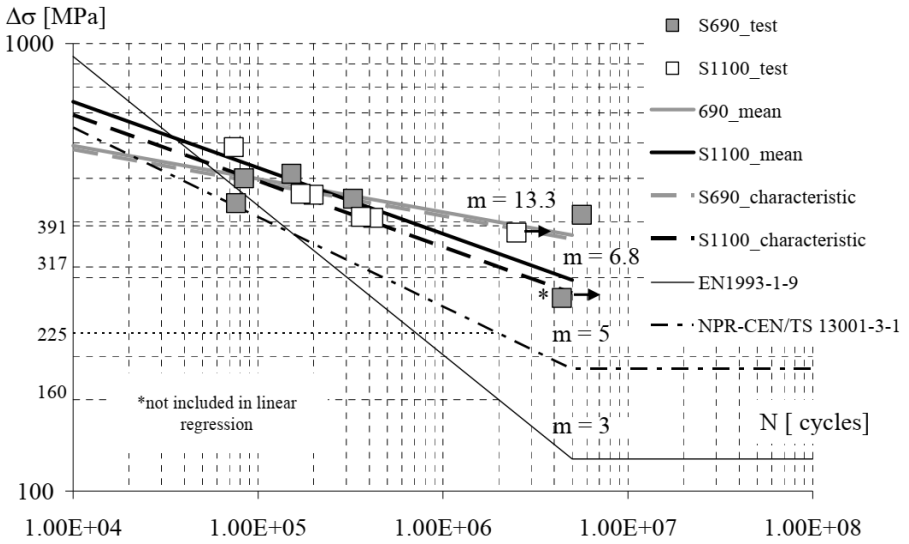

Fig. 3.8. S-N curve of S690 and S1100 base material specimens [25].

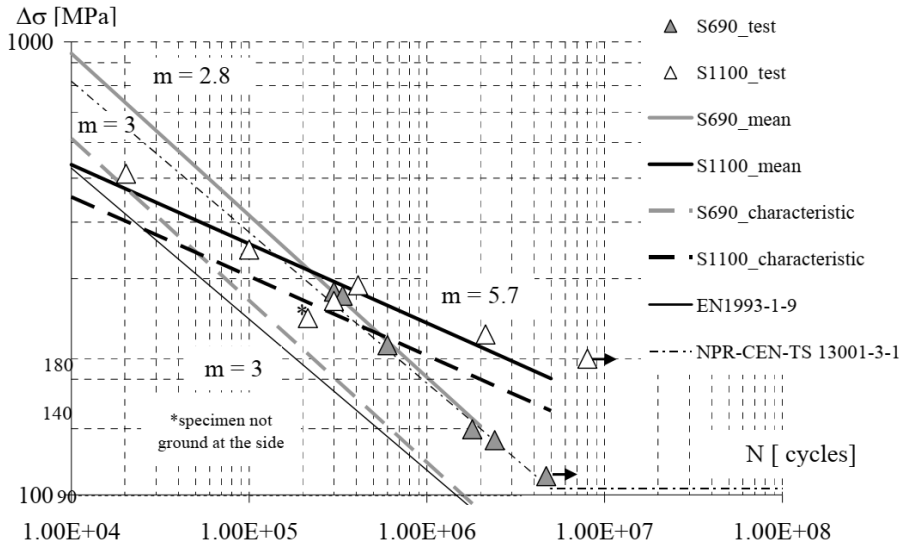

Fig. 3.9. S-N curve of S690 and S1100 transverse butt weld specimens [25].

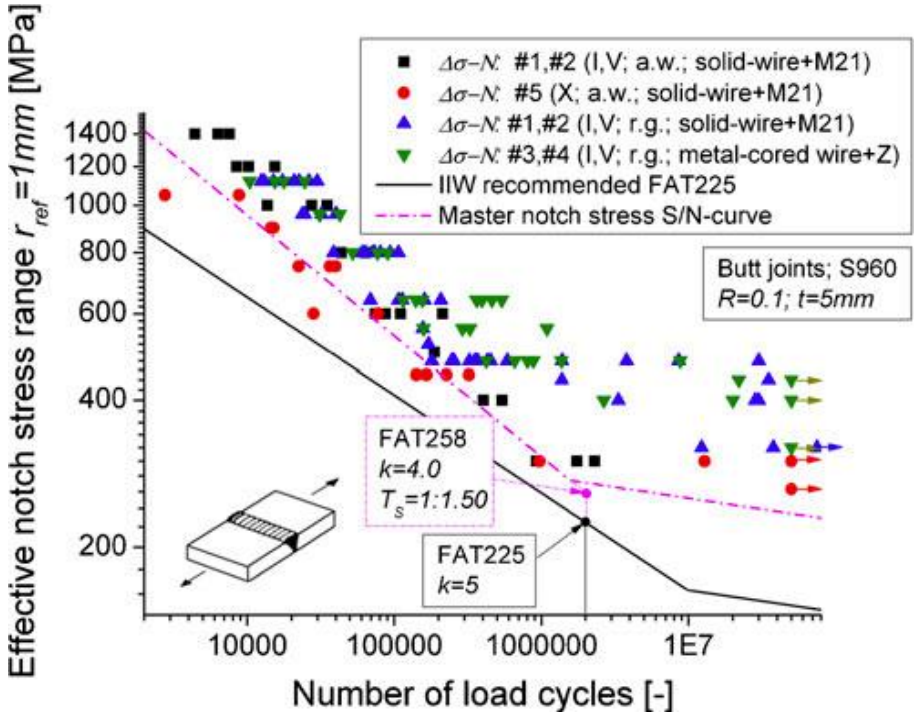

Fig. 3.10. Notch stress master S/N curve for thin-walled butt joints made of S690 steel [46].

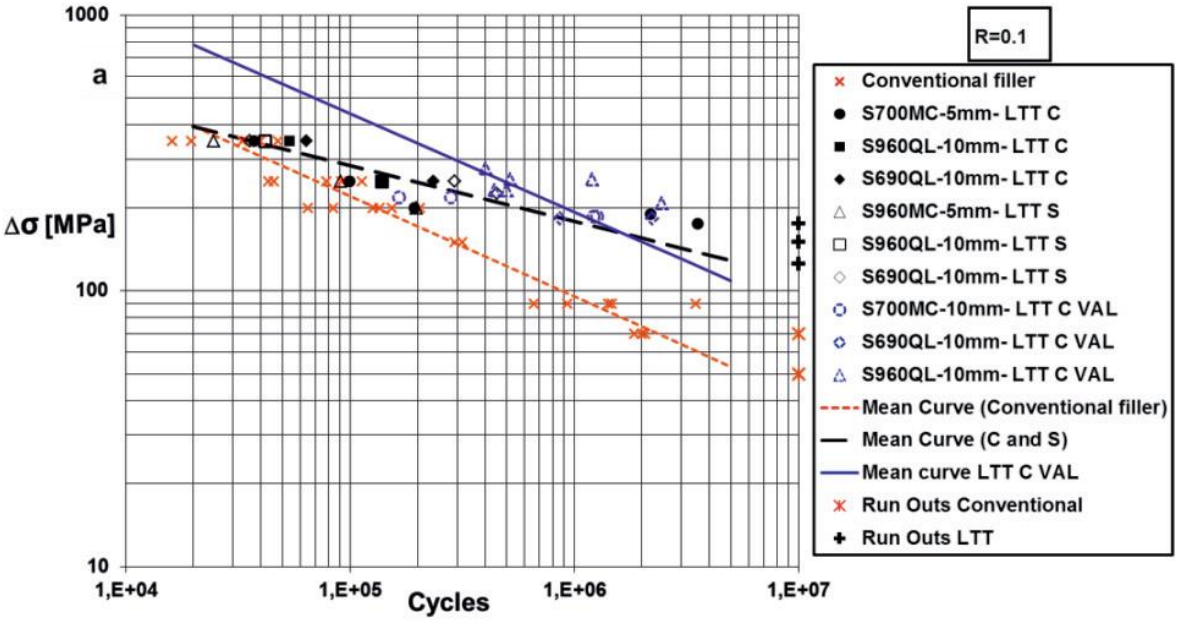

Fig. 3.11. Comparison of specimen tested under constant amplitude loading (CAL)and variable amplitude loading (VAL) at R=0.1 stress ratio, „C" identifies Cr-Ni based and „S" Cr-Mn based filler vires [60].

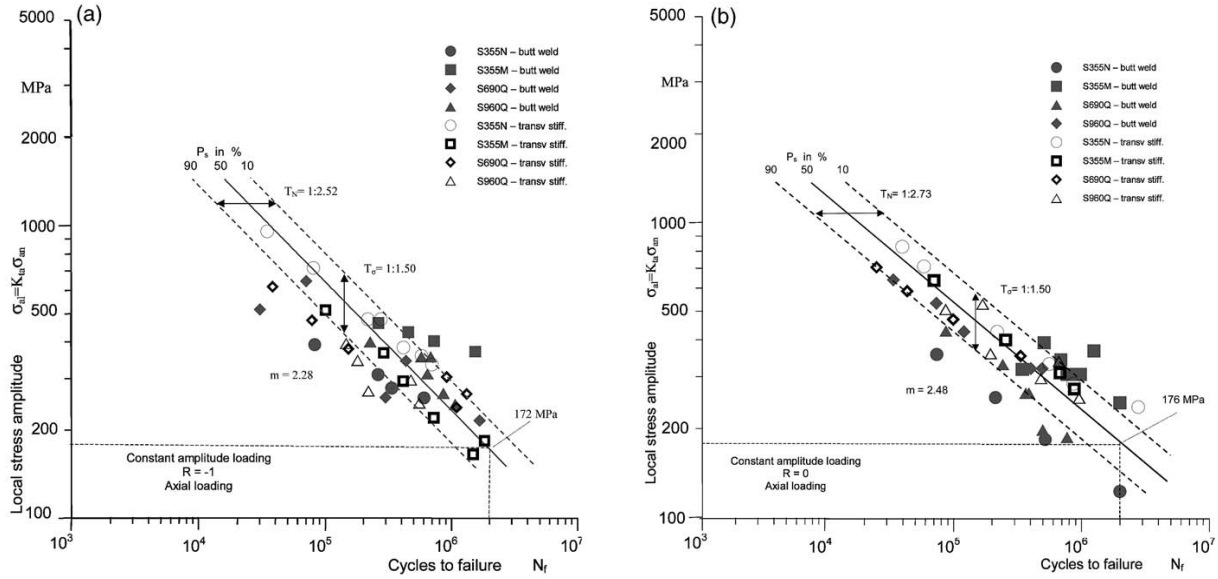

Fig. 3.12. Wöhler curves for axial constant amplitude loading of different materials and specimen types[61].

3.3.3. Fatigue resistance curves – weld improvement cases

There are varios techniques that improve the fatigue strength of the weld itself and these techniques can be devided into two main groups: weld geometry improvement methods and residual stress methods (see Fig. 3.13 [60]). As the figure shows, there are further subgroups too, and another way of the classification may be the consideration of the heat effect, there are methods with and without heat effect.

For the techniques, burr grinding, TIG dressing and hummer peening appear to hold the most potential for e.g. ship structure applications. Each of these techniques provides a significant and repeatable improvement in fatigue strength and involve equipment and procedures that are familiar to shipyards. Stress relief techniques including thermal stress relief, vibratory stress relief, Gunnert's method and exposive treatments not practical for ship application. For these techniques, the fatigue strength improvement benefit is minimal and/or the procedures involved are simply not possible in a shipyard environment. Other techniques, including spot heating and local compression may hold some potential as treatments for specific repair applications [60].

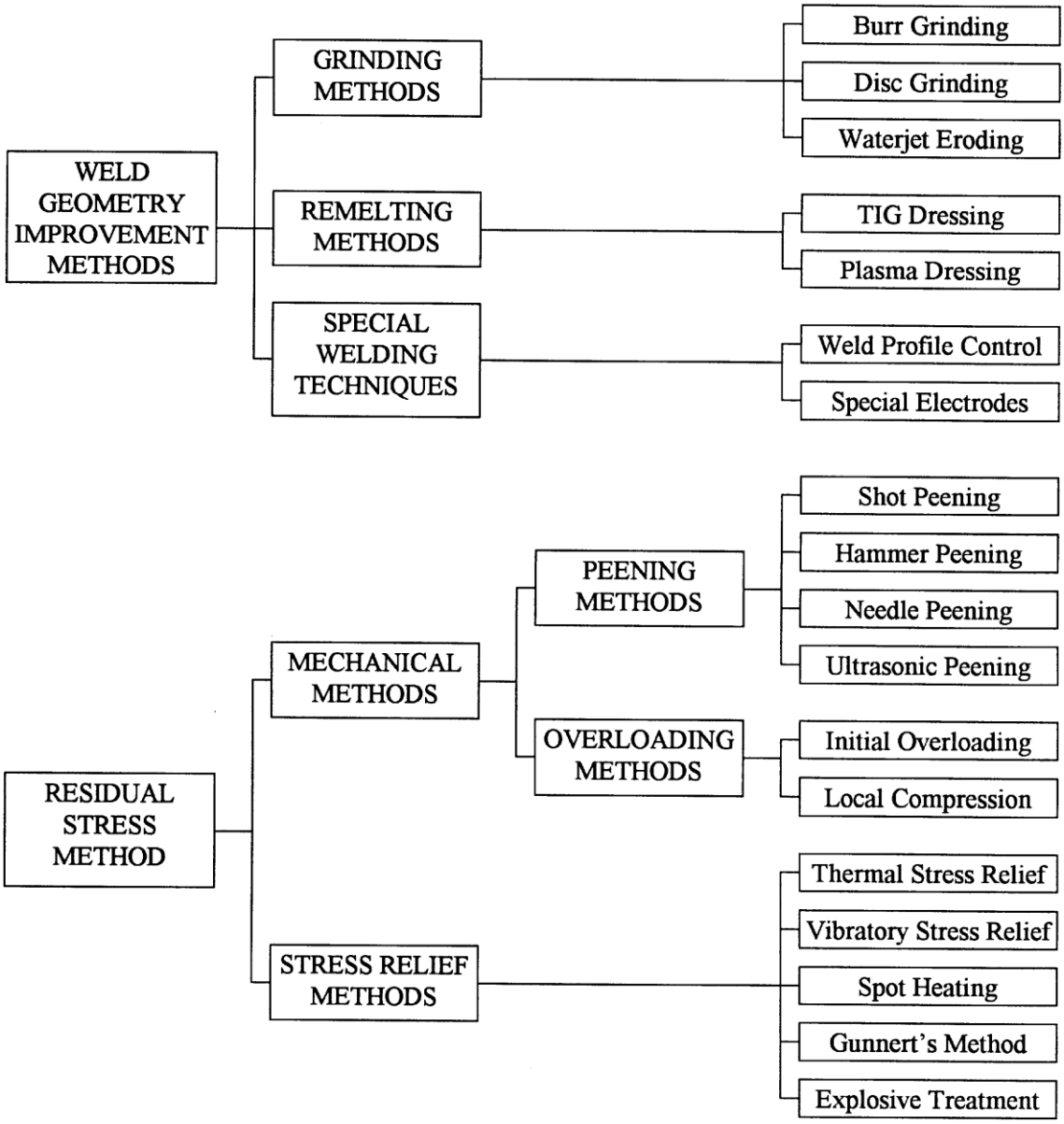

Fig. 3.13. Classification of some weld-improvement methods [62].

Fig. 3.14 and Fig. 3.15 demonstrate two characteristic applications of different weld improvement techniques, for both S690 and S960 strength categories welded joints [63][64]. Based ont he sources it is statable that on the one hand the post weld treatment improves the high cycle fatigue resistance of the welded joints, on the other hand there is an effectiveness order among the different techniques and methods.

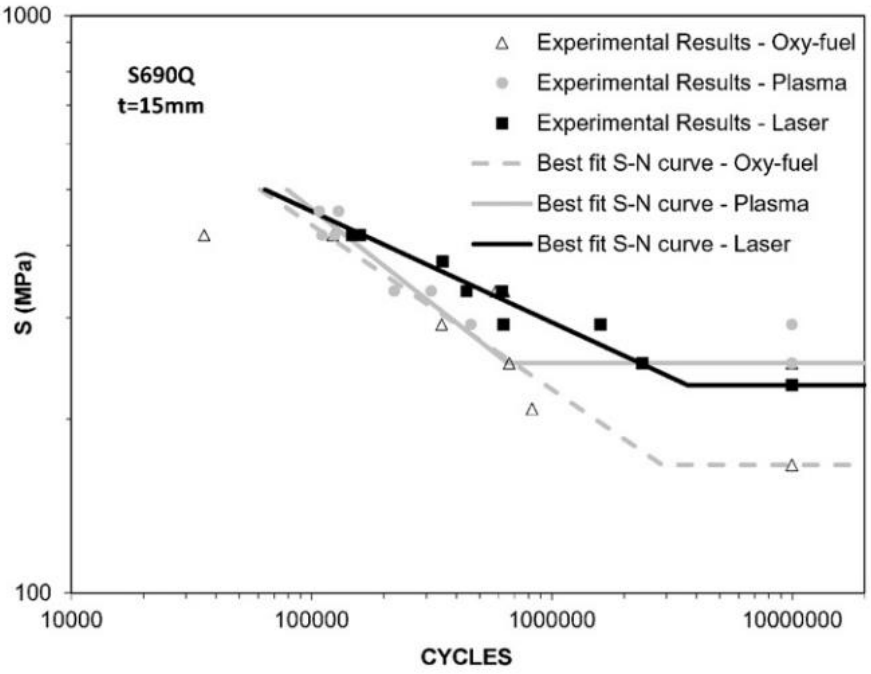

Fig. 3.14. Fatigue results of treated S690Q welded joints with different improvement techniques: a comparison [63].

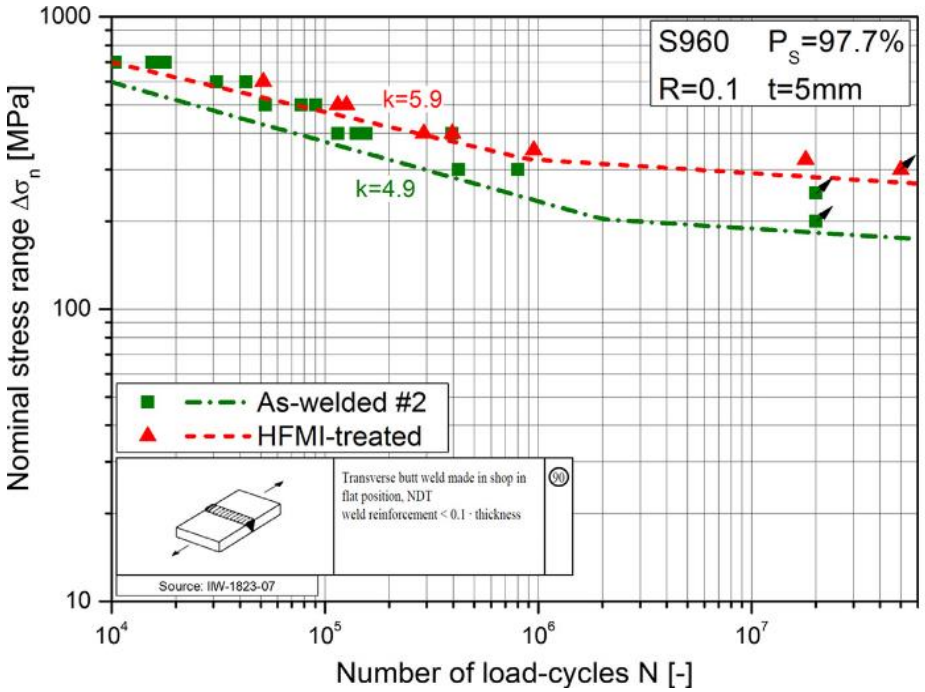

Fig. 3.15. S/N-curves for butt welded joint specimens in as-welded and high frequency mechanical impact (HFMI) treated condition [64].

3.3.4. S-N curve build up

Staircase method can be applied during both the preparation and the evaluation of the HCF test, based on the Japan Society of Mechanical Engineers (JSME) S 002-1981 prescription [65].

In this method (minimum) 8 test specimens should be used in the lifetime region, and (minimum) 6 test specimens in the endurance limit region, so in total (minimum) 14 test

specimens should be tested. Using the method consequently, the limited number of specimens help the reducing of the investigation time, therefore the method can be designated as economic method (see Fig. 3.16).

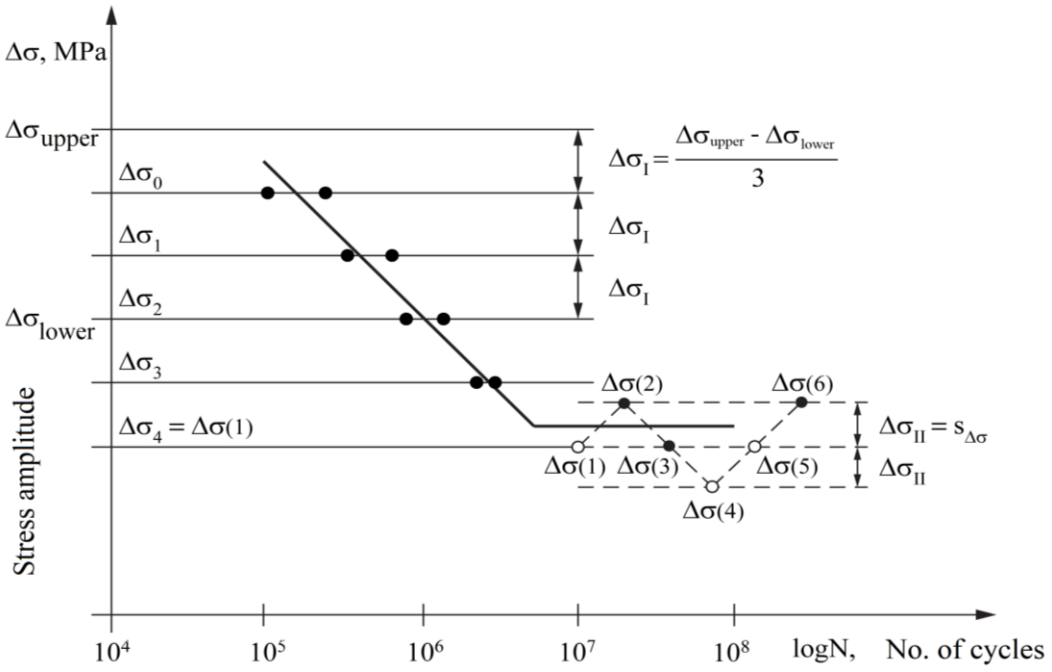

Fig. 3.16. A model of the S-N testing method with 14 specimens (based on [66]).

3.4. Fatigue crack growth (FCG) and characteristics

Most of the failures in the industrial world can be attributed to fatigue and is based on the response of the structural materials to alternating loads that are applied during service. The main failure types are fatigue and fracture [66][67]. The damage progresses through mechanisms starting with crack nucleation, microstructurally small crack growth, followed by linear elastic long crack growth. Each mechanism is associated with a characteristic size, and each characteristic size has its own geometric complexity, constitutive law, and heterogeneity. Fatigue behavior cannot be fully understood and predicted without obtaining information about each of the characteristic sizes [66][68].

Mechanical fatigue of materials can be categorized into the following discrete yet related phenomena [68]:

- initial cyclic damage in the form of cyclic hardening or softening;
- creation of initial microscopic flaws (microcrack initiation),;
- coalescence of these microcracks to form an initial engineering-sized flaw (microcrack growth);
- subsequent macroscopic growth of this flaw (macrocrack growth);
- final failure or instability.

In engineering terms, the first three steps are considered as macrocrack initiation, implying the formation of an (engineering-sized) detectable crack. In welded components, small defects at the weld toe such as undercuts or inclusions can act as initial cracks, and the initiation stage may be short [68]. The total life time of crack clarified in Fig. 3.17 [69].

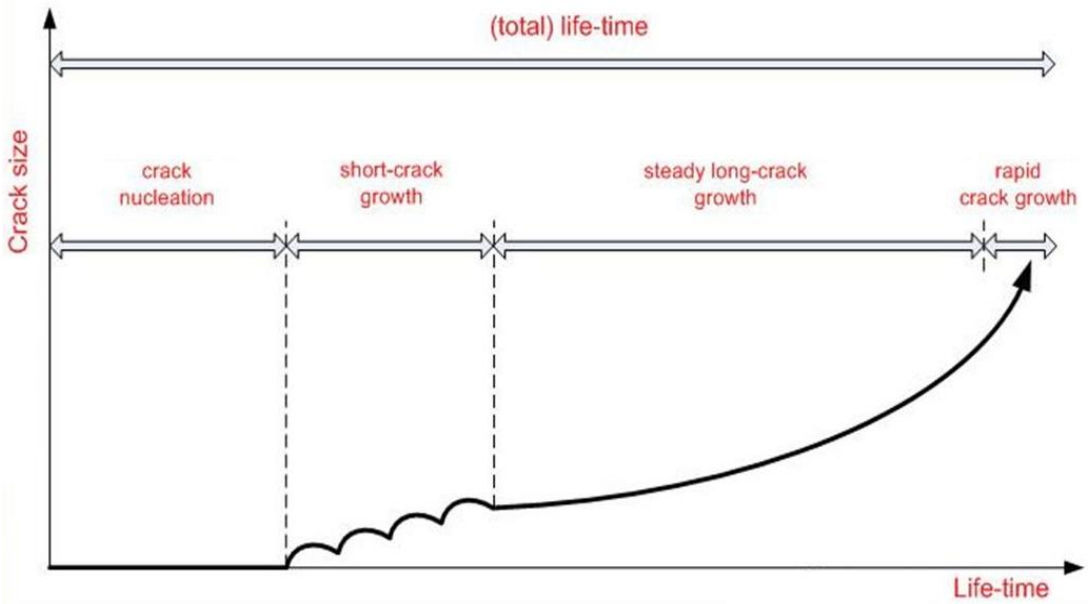

Fig. 3.17. Schematic presentation of the crack - life time connection [69].

There are three characteristics responsible for this behaviour [66]: a) Plastic zone size at the crack tip of a short crack is large with respect to the length of the crack; thus, violating the requirement of linear elastic fracture mechanics; b) Overall applied stress levels may be high with respect to the yield strength of the material; thus, violating the small scale yielding appropriate for linear elastic fracture mechanics; c) Level of crack closure in a state of transition as the crack changes from a short crack to a long crack.

The kinetic diagram of fatigue crack growth can be seen in Fig. 3.18 [70], where both linear elastic and elastic plastic fracture mechanical factors can be seen.

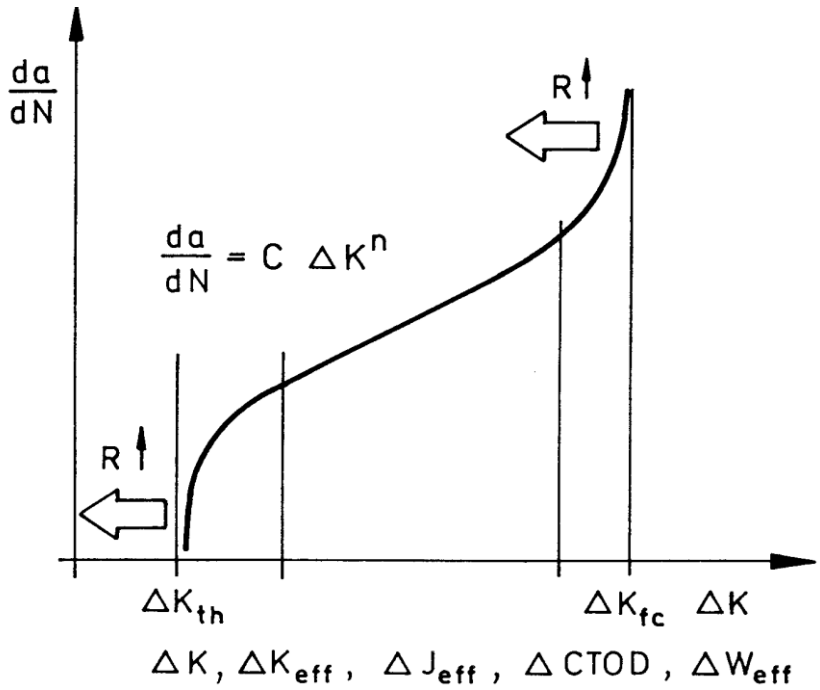

Fig. 3.18. Kinetic diagram of fatigue crack growth (FCG)[70][71].

According to linear elastic fracture mechanics (LEFM) and stress intensity factor (K) theory, the regions of the diagram can be described on different ways. In the first two regions the Klesnil-Lukas equation [72], in the middle part the Paris-Erdogan law [73] and finally, in the second and third regions the Forman's function [74] are the most common used formulae. These equations are as follows, respectively.

$$\frac{da}{dN} = C_m(\Delta K^m - \Delta K_{th}^m)\,, \tag{3.1}$$

$$\frac{da}{dN} = C\Delta K^n\,, \tag{3.2}$$

$$\frac{da}{dN} = \frac{C_p \Delta K^p}{(1-R)K_c - \Delta K}\,, \tag{3.3}$$

where the stress ratio is

$$R = \frac{K_{min}}{K_{max}} = \frac{\sigma_{min}}{\sigma_{max}} = \frac{F_{min}}{F_{max}}\,. \tag{3.4}$$

Beside these formulae further and more complicate possibilities can be found in different sources [53][54]. From an engineering point of view, the Paris-Erdogan law and its modified versions are the most common used equations.

3.4.1. Cases where one strength category of base materials was investigated

– R. T. Yekta, K. Ghahremani and S. Walbridge [75]: $R_{p0.2}$ = 350 MPa). FCG tests were conducted of steel non-load carrying filet welded attachments subjected to ultrasonic impact treatment (UIT) at various levels simulating proper, under-, and over-treatment. Two loading histories were investigated: one with constant amplitude and one with high compressive under-load cycles. UIT significantly improved the fatigue lives of the welded specimens in all cases (compare with subchapter 3.3.3.). The fracture mechanical analysis predicts the fatigue performance of the specimens and finds it to be most sensitive to variations in the residual stresses and initial defect depth (see Fig. 3.19).

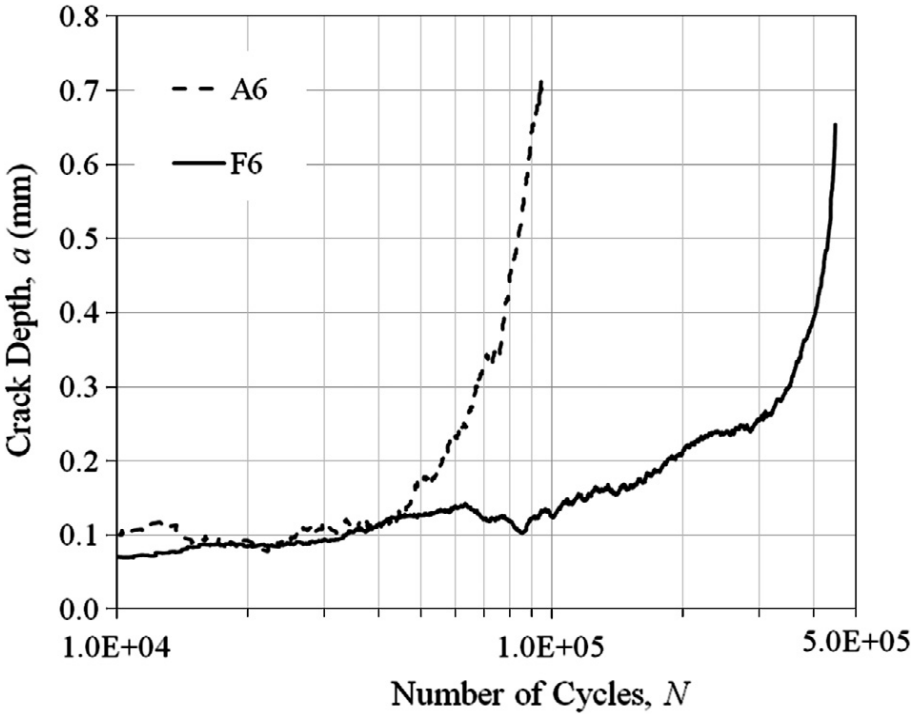

Fig. 3.19. Crack growth curves for specimens as-welded (A6) and treated (F6) [75].

– D. Simunek et al. [76]: $R_{p0.2}$ = 355 MPa). The study focuses on the investigation of flat specimens (two different types of specimens with a width of W = 50 mm and a thickness of t = 12 mm are manufactured) made of mild steel S355 with V-shaped and semi-elliptical notches under constant and variable amplitude fatigue loading to analyze the influence of load sequence effects on fatigue crack growth in order to obtain information about the remaining service life of components. All analytical assessments of V-notched specimen illustrate conservative results compared to testing, and numerical results match experimental investigations well (see Fig. 3.20).

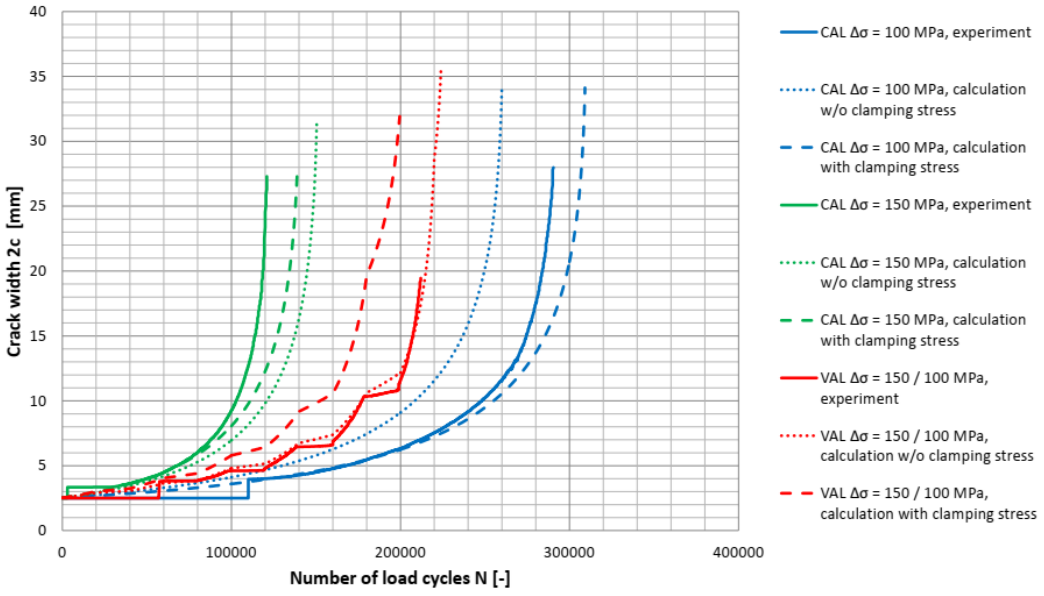

Fig. 3.20. Comparison of numerically and experimentally evaluated fatigue crack growth curves [76].

– J. L. Otegui, U. H. Mohaupt and D. J. Burns [68]: $R_{p0.2}$ = 420 MPa. The propagation of fatigue cracks from weld defects at the toes of manual and automatic T-plate joints in a structural steel was studied. It was found that the evolution of aspect ratios (a/c) and surface growth of cracks are dependent on the mismatch between the planes of adjacent growing surface cracks. Crack mismatch and depth to coalescence were found to be much smaller in the case of automatic welds, which also showed shorter fatigue initiation and propagation lives (see Fig. 3.21).

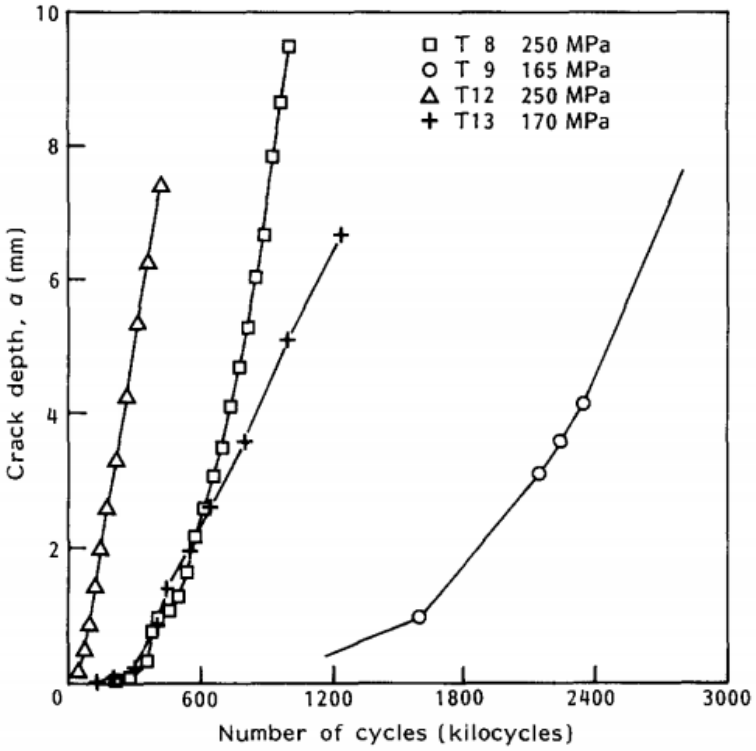

Fig. 3.21. Comparison of the fatigue growth of cracks at the toe of manual (T8, T9) and automatic (T12, T13) T-plate welds [68].

– S. Chattopadhyay [66]: $R_{p0.2}$ = 485 MPa. The proposed fatigue design approach incorporates a distance parameter in conjunction with linear elastic fracture mechanics and effectively integrates long and short crack growth test data. This distance parameter is a material constant, which allows for the effects of large-scale plasticity, crack closure, and fatigue crack threshold. Furthermore, this parameter successfully predicts fatigue crack growth behavior of short cracks. Provides reasonably accurate estimates of fatigue lives and should be an invaluable tool to the designers of industrial machinery and equipment. It is recognizes presence of cracks in structural components. A rational process combining nucleation of a crack on an assumed smooth surface (from a zero to threshold value of crack length) and its subsequent growth to a characteristic dimension is assumed to govern phenomenon of fatigue crack initiation.
– S. Beretta, A. Bernasconi and M. Carboni [77]: $R_{p0.2}$ = 690 MPa. Fatigue crack growth tests were performed on welded joints made of S690 steel. Fatigue tests were run with both constant and variable amplitude loading. The experimental results were compared to predictions obtained by applying local approaches (local stress and local strain) and the

concepts of fracture mechanics. The local stress approach allowed the fatigue strength of joints in constant amplitude loading (for fatigue above 2×10^6) to be predicted, but the assumption of a constant value of the slope k = 3 for all S–N curves led to non-conservative predictions of shorter lives. The local strain approach allowed the fatigue strength of the joints under constant amplitude to be predicted.

- C. Zhang et al. [78]: $R_{p0.2}$ = 690 MPa. A soft buffer layer (BL) between the weld metal and the parent material was introduced in this study. To study the effect of a BL on mechanical properties, two types of joints made from welded HSLA specimens with or without a BL were prepared. The results showed that the presence of a BL significantly improved the fatigue crack growth behavior when a U-notch was in the weld metal. The notch location greatly influenced the fatigue behavior and the surface features of the fatigue fractured specimens.
- Q. Wang et al. [79], $R_{p0.2}$ = 811 MPa. The study was mainly concerned with the long FCG rate of a new generation Ni-Cr-Mo-V high strength steel. The results showed that weld metal possessed better resistance to crack propagation relative to base material under each stress ratio owing to interlocking acicular ferrite microstructure and resultant higher crack closure level. The results obtained helpful in shedding light on the damage tolerance design of the Ni-Cr-Mo-V high strength steel welded joints employed in modern marine structures.
- C. Ni, L. Hua and X. Wang [67]: $R_{p0.2}$ = 835 MPa. To monitor the crack propagation and predict the fatigue life of ferromagnetic material, the metal magnetic memory (MMM) testing was carried out to the single edge notched specimen made from structural alloy steel under three-point bending fatigue experiment. The variation of magnetic memory signal was investigated during the process of fatigue crack propagation. The gradient of magnetic memory signal was investigated and compared with the stress of specimen obtained by finite element analysis. It indicated that the gradient can qualitatively reflect the distribution and variation of stress. The maximum gradient and crack size showed a good linear relationship, which indicated that the crack propagation can be estimated by MMM testing (see Fig. 3.22).

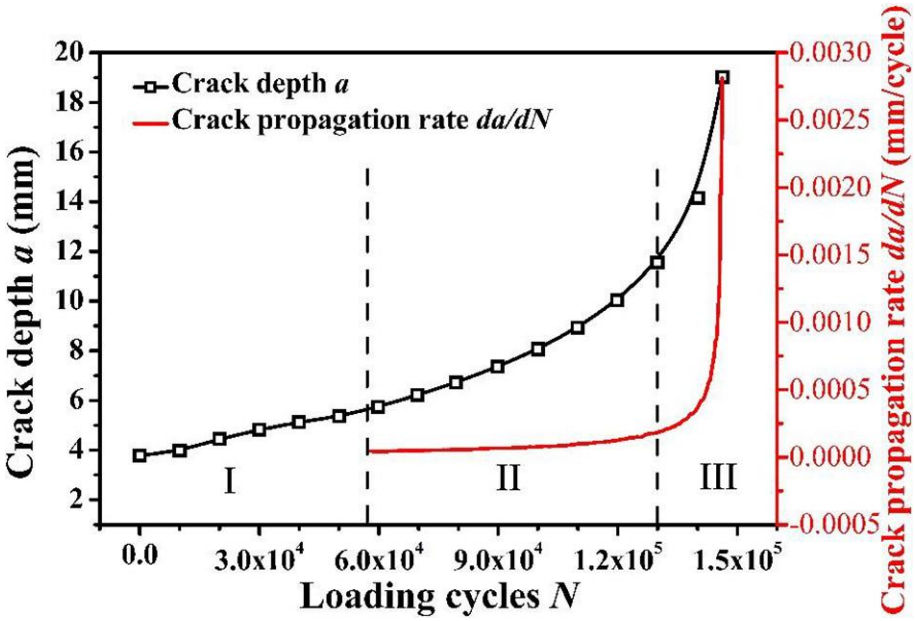

Fig. 3.22. Variation of crack depth a and crack growth rate da/dN along loading cycles [68].

3.4.2. Cases where two strength categories of base materials was investigated

– M. P. de Jesus et al. [80]: yield strength values $R_{p0.2}$ = 355 MPa and $R_{p0.2}$ = 690 MPa. The study presents a comparison of the FCG behavior between S355 mild steel and S690 high strength steel grades, supported by an experimental program of fatigue tests of smooth specimens, performed under strain control, and fatigue crack propagation tests. Results showed that S690 steel grade presents a higher resistance to fatigue crack initiation than S355 steel. Consequently, the design of structural details with S690 steel should avoid sharp notches that significantly reduce the fatigue crack initiation process (see Fig. 3.23).

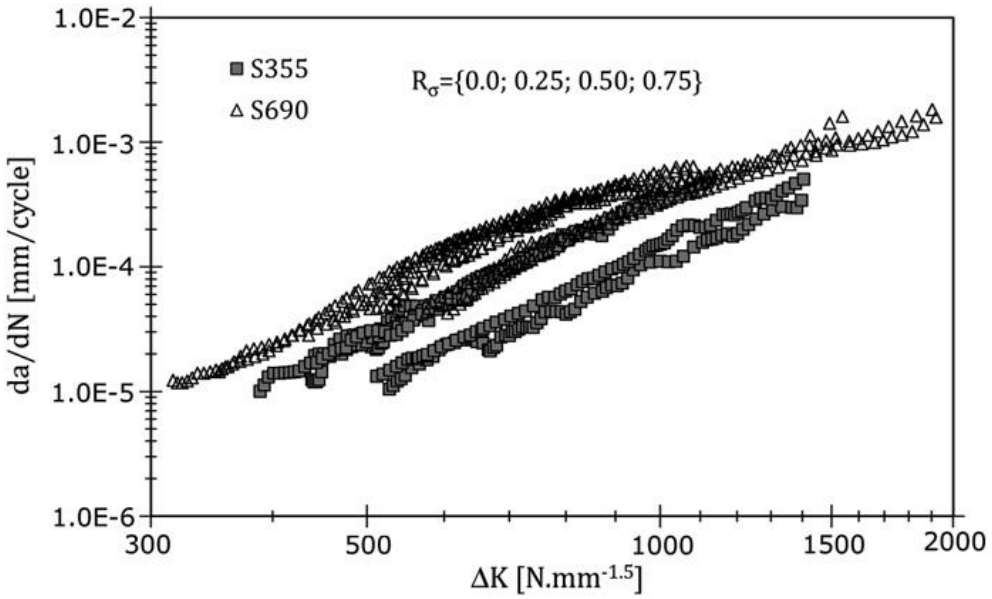

Fig. 3.23. Comparison of all crack growth data obtained for S355 and S690 steel grades [79].

– D. Simunek, M. Leitner and F. Grün [81]: $R_{p0.2}$ = 355 MPa and $R_{p0.2}$ = 960 MPa. An optical measurement system is set-up to analyze crack initiation and growth of high-strength steels compared to common construction mild steels. Constant amplitude tests including overloads are performed for high-strength and common construction mild steel specimens to specify the material's service strength. The crack growth rate is approximately 300 times (9×10^{-6} to 3×10^{-8} mm/cycle) reduced right after the overload at common construction mild steel, whereas crack growth at the high-strength steel is decreased about 50 times (1.5×10^{-4} to 3×10^{-6} mm/cycle). Fig. 3.24 shows the differences of crack initiation and crack propagation phases for the two steel types.

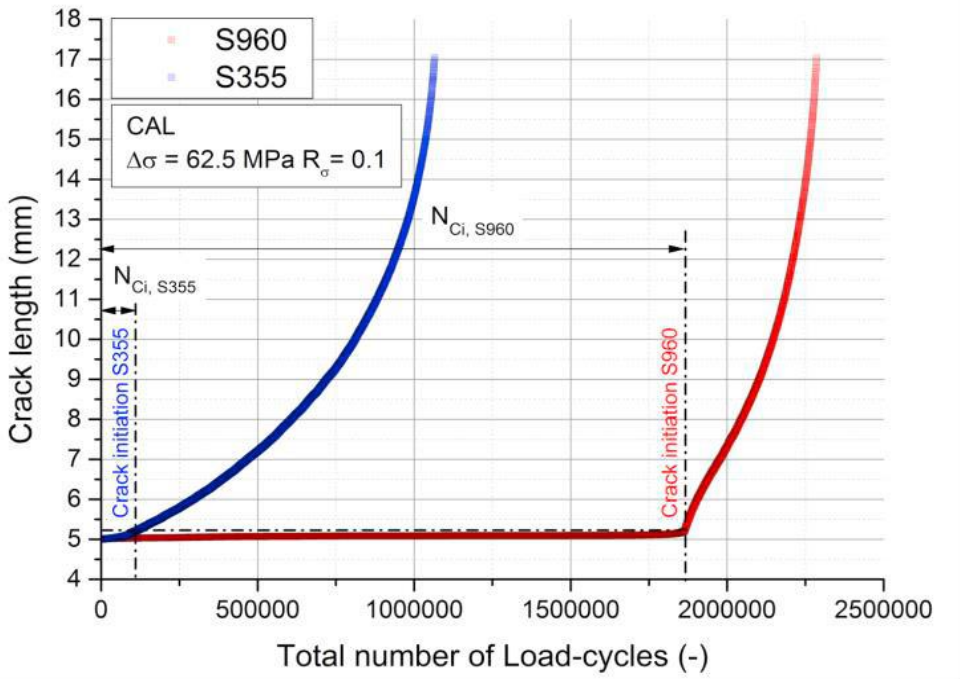

Fig. 3.24. Comparison of crack initiation and crack growth phases for two steel stregth categories [81].

– C. L. Walters [82]: $R_{p0.2}$ = 460 MPa and $R_{p0.2}$ = 980 MPa. The crack length was measured to the nearest 0.001 inches (0.0254 mm) by the DC potential drop method, and the da/dN was calculated according to the incremental polynomial method. The data shows that the low temperature seemed to increase the fatigue crack growth rate for the S980 material but decrease it for the S460 material. The fatigue crack growth rate decreases with lower temperatures until the fatigue ductile-brittle transition (FDBT), and then it increases again (see Fig. 3.25).

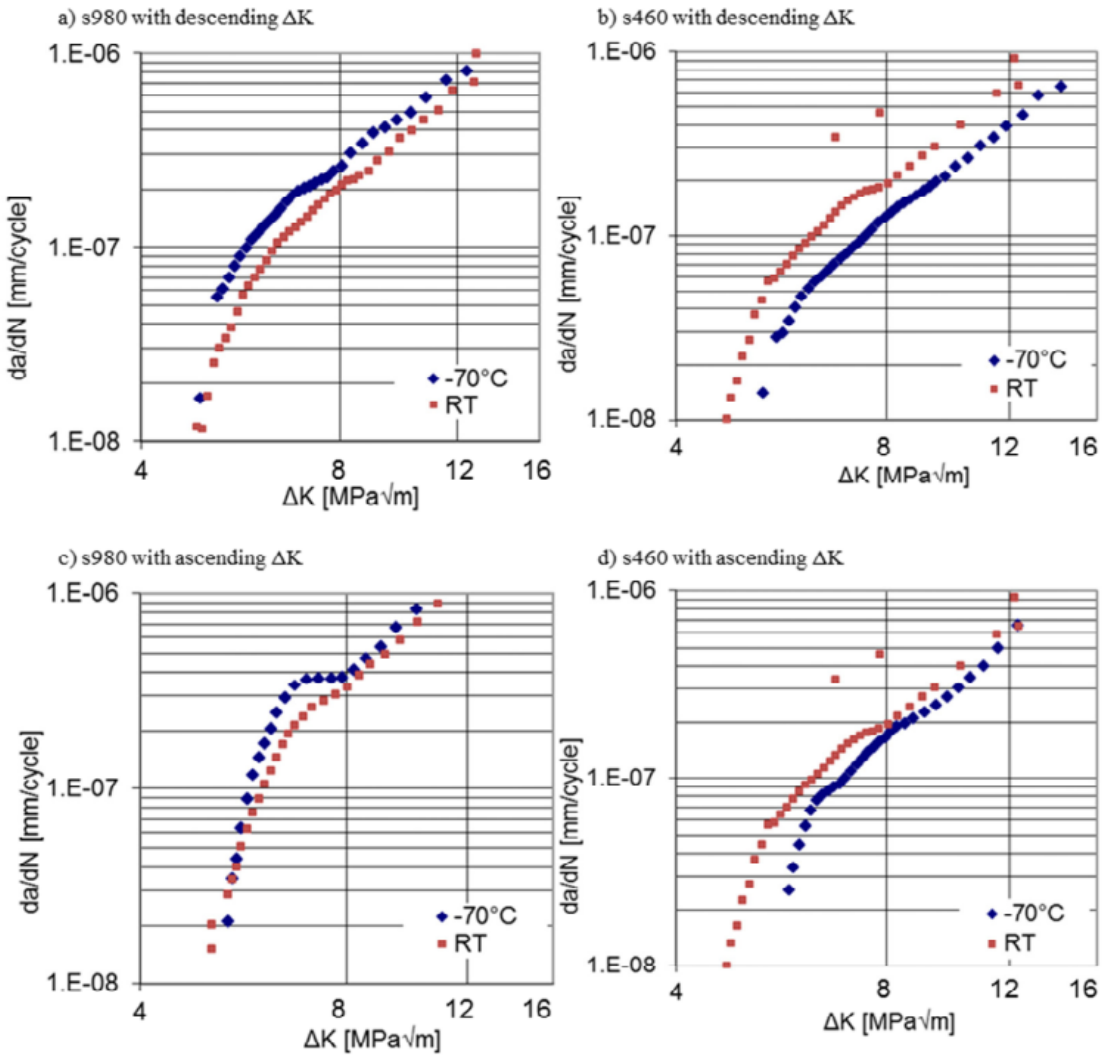

Fig. 3.25. Room temperature fatigue data compared to low-temperature fatigue data for descending values of ΔK (a) and b)) and ascending values of ΔK (c) and d)) for two steel strength categories [82].

3.4.3. Cases where more strength categories of base materials was investigated

- L. Zhen [83]: $R_{p0.2}$ values are 255 MPa, 325 MPa, 450 MPa and 693MPa. Based on the fatigue FCG expression developed by X. Zheng and M.A. Hirt, a new method for the estimation of FCG rate is suggested. It is pointed out that when ΔK_{th} (the FCG threshold) and the mechanism in the intermediate region of FCG are known, the FCG rates can be predicted from tensile properties. In this study, the FCG rate curves of low alloy steels SM50B, HT80, SP42, SPV50 and their welded joints are predicted. It is shown that the predicted lines agree fairly well with the test results. It is also shown that FCG threshold ΔK_{th} is sensitive to stress ratio R but not to weld technology.
- H. Remes et al. [84]: $R_{p0.2}$ values are from 400 MPa to 550 MPa. This study focus on different factors affecting the fatigue strength assessment of thin plates in large structures. Results showed that if the structural analysis considers secondary bending properly, the local elastic fatigue damage parameters such as J-integral range can be used to model fatigue strength at 2-

5 million load cycles. The strain-based crack growth simulations indicate that longer short crack growth period is the reason for the higher slope value.

– S. Ravi, V. Balasubramanian and S. Nemat Nasser [6]: $R_{p0.2}$ values are 560 MPa, 700 MPa, 710 MPa and 810 MPa. The fatigue crack growth experiments were conducted at four different stress levels ($\Delta\sigma$) of 75 MPa, 100 MPa, 125 MPa and 150 MPa. From the crack growth curves (see Fig. 3.26) it is evident the resistance to fatigue crack growth is higher in the overmatched joints and the resistance is lower in the undermatched joints.

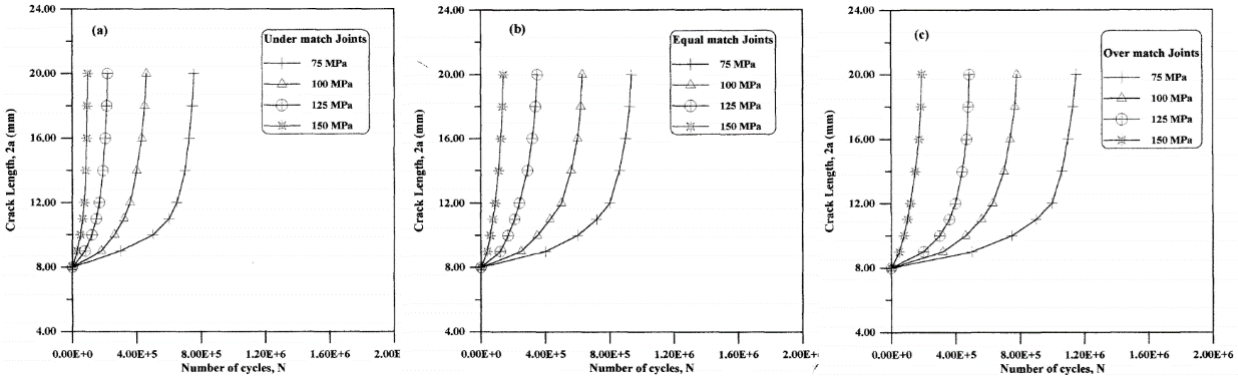

Fig.3.26. Crack growth curves under different stress levels and mismatch conditions [6].

– S. Ravi et al. [39]: $R_{p0.2}$ values are 550 MPa, 560 MPa, 700 MPa, 830 MPa and 840 MPa. Assess the influences of mismatch ratio (MMR), post-weld heat treatment (PWHT) and notch location on fatigue life of HSLA steel welds, Center Cracked Tension (CCT) specimen has been used to evaluate the fatigue life. To assess the influences of mismatch ratio, post-weld heat treatment and notch location on fatigue life strength of mismatched HSLA steel welds, by incorporating response table and response graph, normal probability plot and analysis of variance (ANOVA) techniques.

3.5. Recommendations to the aims

– Statistically relevant number of specimens should be investigated;
– statistical methods should be applied for the evaluation of the testing results;
– in consideration of the numerous influencing factors, the testing circumstances should be specified and should be observed consequently;
– investigation of mismatch phenomenon is necessary, especially in the higher strength categories, because of the strength of the available filler metals;
– the improvement techniques and methods are outside of both the aims and the possibilities of the research work.

4. SUMMARY, SPECIFIC AIMS OF THE RESEARCH WORK

Because the research work is a significant continuation of previous researches, therefore builds upon their experience [11] and uses their measurement results [9][10]. It means that the previous results provide good and reliable basis for the comparison of the research results.

The specific aims of the research work are as follows.

- Carrying out high cycle fatigue investigations on differently mismatched butt welded joints with different crack paths made by different strength categories of high strength steels.
- Studying the influence of welding heat input on high cycle fatigue resistance of the thermomechanically rolled high strength steel type.
- Development a generally usable method for determination of fatigue strength curves, and determination of the curves for all investigated cases.
- Carrying out fatigue crack growth investigations on differently mismatched welded joints with different notch locations made by different strength categories of high strength steels.
- Studying the influence of welding heat input influence on fatigue crack growth resistance of the thermomechanically rolled high strength steel type.
- Analysing the usability of previously developed method for the determination of fatigue crack propagation design or limit curves for high strength steels and their welded joints, furthermore determination of the curves for all investigated cases.

5. CIRCUMSTANCES OF THE INVESTIGATIONS

5.1. Characteristics of the base materials and filler metals

Chemical composition of the base materials and filler metals, and the mechanical properties can be seen based on quality certificates in Table 5.1 and Table 5.2, respectively (see Fig. 2.2).

Table 5.1. The chemical composition of the base materials and the filler metals (weight%)

Material designation	**C**	**Si**	**Mn**	**P**	**S**
Optim 700QL	0.16	0.31	1.01	0.010	0.001
INEFIL NiMoCr	0.80	0.50	1.60	0.007	0.007
Weldox 700E	0.14	0.30	1.13	0.007	0.001
Union X85	0.07	0.68	1.62	0.010	0.010
Union X90	0.10	0.8	1.8	N/A	N/A
Weldox 960E-BM/WJ*	0.16/0.16	0.22/0.23	1.24/1.25	0.009/0.008	0.001/0.001
OK Tubrod 14.03	0.08	0.51	1.16	N/A	N/A
Alform 960M	0.084	0.329	1.65	0.011	0.0005
Union X96	0.1	0.81	1.94	0.015	0.011
Material designation	**Cr**	**Ni**	**Mo**	**V**	**Ti**
Optim 700QL	0.61	0.21	0.205	0.010	0.016
INEFIL NiMoCr	0.30	1.50	0.250	0.09	N/A
Weldox 700E	0.30	0.04	0.167	0.011	0.009
Union X85	0.29	1.73	0.61	<0.01	0.08
Union X90	0.35	2.3	0.6	N/A	N/A
Weldox 960E-BM/WJ*	0.19/0.20	0.05/0.04	0.581/0.605	0.041/0.04	0.004/0.004
OK Tubrod 14.03	0.02	2.27	0.55	0.01	N/A
Alform 960M	0.61	0.026	0.29	0.078	0.014
Union X96	0.52	2.28	0.53	<0.01	0.06
Material designation	**Cu**	**Al**	**Nb**	**B**	**N**
Optim 700QL	0.015	0.041	0.001	0.0015	0.003
INEFIL NiMoCr	0.12	N/A	N/A	N/A	N/A
Weldox 700E	0.01	0.340	0.001	0.002	0.003
Union X85	0.06	<0.01	N/A	N/A	N/A
Union X90	N/A	N/A	N/A	N/A	N/A
Weldox 960E-BM/WJ*	0.01/0.01	0.056/0.06	0.016/0.016	0.001/0.001	0.003/0.003
OK Tubrod 14.03	0.02	N/A	N/A	N/A	N/A
Alform 960M	0.016	0.038	0.035	0.0015	0.006
Union X96	0.06	< 0.01	N/A	N/A	N/A

INEFIL NiMoCr is I.N.E, OK Tubrod 14.03 is ESAB, UNION X85, UNION X90 and UNION X96 are Böhler products.

Table 5.2. The mechanical properties of the examined base materials and filler metals

Material designation	**$R_{p0.2}$ (MPa)**	**R_m (MPa)**	**A (%)**	**CVN impact energy (J)**
Optim 700QL	809	850	17.0	-40 °C:106
INEFIL NiMoCr	750	820	19.0	-40 °C: 60; -20 °C: 90; 20 °C: 120
Weldox 700E	791	836	17.0	-40 °C: 165
UNION X85	≥ 790	≥ 880	≥ 16.0	-50 °C: ≥ 47; 20 °C: ≥ 90
UNION X90	≥ 890	≥ 950	≥ 15.0	-50 °C: ≥ 47; 20 °C: ≥ 90
Weldox 960E-BM/WJ*	1007/1007	1045/1053	16.0/16.0	-40 °C: 141 / 105
OK Tubrod 14.03	757	842	23	71
Alform 960M	1051	1058	16.9	-40 °C: 40
UNION X96	≥ 930	≥ 980	≥ 14.0	-50 °C: ≥ 47; 20 °C: ≥ 80

* Two different Weldox 960E base material samples were used for the investigations: "Weldox 960E-BM" was used for base material tests and "Weldox 960E-WJ" was applied for the preparing and testing of welded joints.

Mismatched welded joints are joints in which yield strength and/or microstructure of weld metal will be different from base material and HAZ. The factors, which are responsible for heterogeneities, are welding process, consumables, joint design and weld thermal cycle. Undermatched joints are used in repair welding, welding of bridges, pressure vessels and penstocks, etc. It is used to prevent cracks in the welds, for example an undermatched cap pass reduces weld toe cracking from cyclic plastic bending during reeling. Similarly, overmatched joints are used in pipeline girth welds, welded offshore structures, cladding and hardfacing etc., for effectively preventing weld metal failure by small cracks found in weld metal [85].

The mishmatch conditions when high strength steels are used in welded structures the selection of filler metal is a crucial point. It is necessary to consider that in terms of the examined steels – based on the ratio of the base material and the filler metal mechanical properties – undermatching (UM), matching (M) and overmatching (OM) filler metals can be applied.

In case of matching condition, the evolved mechanical properties of the weld metal are equal or nearly the same as the base material. In undermatching case, the strength properties of the weld metal are lower, while in case of overmatching condition the strength properties of the weld metal are higher than the base material characteristics. The matching of the base materials and the filler metals cannot be described only with the (tensile) mechanical properties, but other characteristics should be also considered, such as the toughness or the cracking sensitivity. Furthermore, absolute matching might be almost impossible in case of high strength steels. The comparison can be done by the (tensile) mechanical properties, for example the minimum yield strength or the minimum tensile strength. It is important to note at matching condition, the equality of all mechanical properties can be hardly achieved. This is due to the fact, the ratio between the yield strength and tensile strength (Y/T ratio) is usually smaller at the base materials, than in the case of the filler metals [18].

General principle, that in case of hot rolled conventional steels, equal or slightly higher strength matching filler metals are used. It is necessary to calculate with high residual stresses in

case of higher strength overmatching filler metals, which can be unfavorable regarding the operation of the welded joint. In case of high strength steels, with yield strength over 700 MPa, it may be more beneficial to use undermatching filler metals. Despite of the lower strength of the welded joint, these filler metals may have many advantages, which can be utilized effectively in advanced high strength steels. The higher toughness of the weld metal, the higher resistance to hydrogen induced cracking or the smaller residual stresses of the welded joint can be considered as relevant unambiguous effects. In many cases high strength weld metal is demanded, therefore overmatching filler metals are used. In that case, the higher yield strength of the welded joint is more beneficial, despite of the slightly higher residual stresses or the lower toughness [86].

The development of high strength low alloy steels, micro-alloyed steels and quenched and tempered steels as well as new fabrication techniques changed the engineers to design the structures on the basis of yield strength and fracture toughness instead of only yield strength or tensile strength. With the increased use of high strength base materials, it is very difficult to produce matching (M) and overmatching (OM) welding consumables because strength and toughness cannot increased simultaneously. Sometimes, the yield strength of weld metal used for joining plates is lower undermatched (UM) than the yield strength of the base material [85].

In the base material, HAZ and weld metal combinations, mismatch constraint is caused by both global mismatch and local mismatch. Global mismatch is defined as the ratio of yield strength of weld metal to base material, whereas local mismatch is defined as the ratio of yield strength of weld metal to HAZ. The mechanical factors responsible for producing global strength mismatch of weldments are base material yield strength, weld metal yield strength, base material tensile strength and weld metal tensile strength. The net section yielding occurs when plastic deformation is localized to the defective cross section. The gross section yielding occurs when applied stress exceeds material yield strength, i.e. when yield strength of weld metal exceeds base material. In general, large defects trend to produce net section yielding, whereas small defects are beneficial for obtaining gross section yielding [6].

Based on the above mentioned facts, matched (M), undermatched (UM) and overmatched (OM) filler metals were chosen for our experiments. The base material-filler metal pairing can be seen in Table 5.3, M/OM means matched root and undermatched filler layers.

Table 5.3. Mismatch characteristics: the applied base materials and filler metals pairing

Base material	**Mismatch type**	**Filler metal**
Optim 700QL	matching (M)	INEFIL NiMoCr
Weldox 700E	matching (M)	UNION X85
	overmatching (OM)	UNION X90
	matching / overmatching (M/OM)	UNION X85/UNIONX90
Weldox 960E	matching (M)	UNION X96
	undermatching (UM)	OK Tubrod 14.03
Alform 960M	matching (M)	UNION X96
	undermatching (UM)	UNION X90

5.2. Testing matrix

The testing matrix, the summary of the investigated groups and comparison possibilities were summarized in Table 5.4.

Table 5.4. The testing matrix: summary of the investigated groups and demonstration of the comparison possibilities

Base material	**Matching condition and heat input**	**HCF tests**		**FCG tests**	
		Previous studies	**Own investigations**	**Previous studies**	**Own investigations**
Optim 700QL*	M – Medium	SP	–	SP	–
Weldox 700 E	M – Medium	SP	BWJ	SP	–
	OM – Medium	SP	–	SP	–
	M / OM – Medium	–	BWJ	–	SP
Weldox 960E*	M – Medium	SP	–	–	–
	UM – Medium	SP	–	SP	–
Alform 960 M	M – High	SP	BWJ	–	SP
	M – Medium	SP	BWJ	SP	–
	M – Low	SP	–	–	–
	UM – High	–	–	–	SP
	UM – Medium	–	BWJ	SP	–

* Only for comparisons.

SP means that specimens were cat in full from the welded joint, all surfaces were cut (see Fig. 6.2 and Fig. 7.1), and will be designated as WJ.

BWJ means that only the side surfaces of the specimens were cut, the weld faces were not machined (see Fig. 6.3).

Based on Table 5.4. there are different comparison possibilities, such as comparison of base materials, mismatch conditions, heat inputs, and finally, comparison of specimens (SP) and welded joints (WJ).

5.3. Welding circumstances

During our experiments, 15 mm thick plates were used for welding and base materials and welded joints investigations of Weldox 700E and Alform 960M material grades. 30 mm thick plates were used for the investigations of Optim 700QL base material and welded joints, during a previous research. 15 mm Weldox 960E plate was tested during base material examinations (designated Weldox 960E-BM) in previous research; furthermore, 20 mm thick plates welded and investigated (designated Weldox 960E-WJ) in previous research as well. INEFIL NiMoCr, OK Tubrod 14.03, also UNION X85, UNION X90 and UNION X96 filler metals used for production of welded joits (see Tables 5.1-5.3, too).

The dimensions of the welded workpieces were 300 mm x 125 mm. For the equal stress distribution X-grooved (double V-grooved) welding joints were used, with 80° opening angle, 1 mm land thickness, and 2 mm gap between the two plates. The welding equipment was a Daihen Varstroj Welbee Inverter P500L (WB-P500L) MIG/MAG power source; 1.2 mm diameter solid wires and 18% CO_2 + 82% Ar gas mixture (M21) were applied. The root layers (2 layers) were made by a qualified welder, while the filler layers (18 layers for 30 mm thick plates or 10 layers for 20 mm thick plates or 6 layers for 15 mm thick plates) by an automated welding car, in all cases. During the welding process, a welding monitoring system [87] was used and the workpieces were rotated systematically, after each layer. Fig. 5.1 shows the structure of the welded joints for 15 mm and 30 mm thick plates.

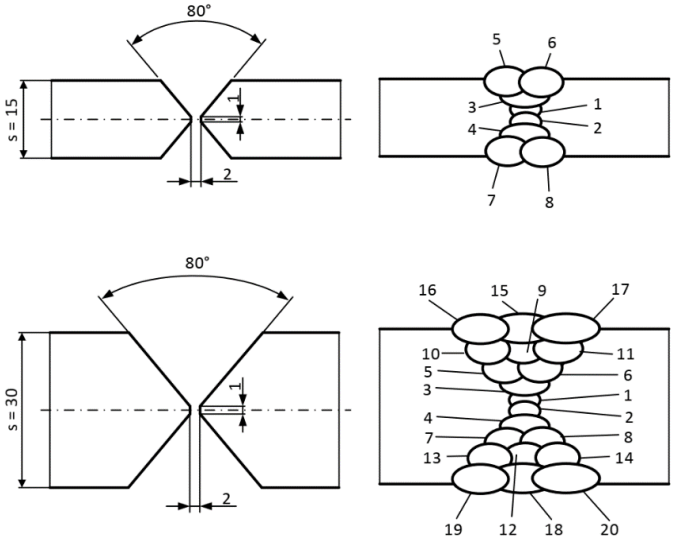

Fig. 5.1. The structure of the welded joints [9].

The welding parameters were selected based on both theoretical considerations and real industrial applications [13][27][28][87][88][89] and those can be found in Table 5.5, using the registered data. The table shows the welding current (I), the voltage (U) and the welding speed (v_w), also the preheating (T_{pre}) and the interpass (T_{ip}) temperatures, with the calculated linear energy (E_v) and the calculated critical cooling time ($t_{8.5/5}$) values.

Table 5.5. Applied welding parameters

Base material designation	**Heat input**	**Layer**	**T_{pre}, T_{ip} (°C)**	**I (A)**	**U (V)**	**v_w (cm/min)**	**E_v* (J/mm)**	**$t_{8.5/5}$** (s)**
Optim 700QL	medium	root: 1-2	150, 180	130-145	19.0-20.0	20	610-680	5.0-6.0
		filler: 3-20		260-275	28.5-29.5	35-40	880-950	7.5-9.0
Weldox 700E	medium	root: 1-2	150, 180	145-155	20.5-21.5	20	700-800	5.5-7.0
		filler: 3-8		255-295	26.5-29.0	40	830-1010	7.0-8.5
Weldox 960E	medium	root: 1 / 2	200 / 180	96 / 194	17.3 / 22.0	11 / 27	727 / 764	6.7 / 6.5
		filler: 3-12	150	298-308	29.0-31.0	45	940-1000	7-8
Alform 960M	medium	root: 1-2	70, 180	135-150	20.0-20.7	20	675-740	4.9-6.3
		filler: 3-8		290-295	27.5-29.0	40	900-1020	7.5-9.0
	high	root: 1-2	70, 300	135-145	17.5-18.0	20	565-630	4.0-9.6
		filler: 3-8		270-300	27.5-29.0	40	890-1050	14.5-18.0

* $E_v = \eta \frac{UI}{v_w}$ (5.1)

** $t_{8.5/5} = (6700 - 5T_{ip}) E_v \left(\frac{1}{500 - T_{ip}} - \frac{1}{850 - T_{ip}} \right) F_3$ (5.2)

The deformation of whole welded workpieces after the welding was measured by two different methods using vernier caliper and ZEN softvare (see Fig. 5.2 and Fig. 5.3).

Fig. 5.2. Deformation scaling by vernier caliper.

Fig. 5.3. Workpiece photo for the ZEN software analysis.

The measured values, which were measured in all four corners, were summarized in Tables 5.6-5.7 and demonstrated in Figs. 5.4-5.5. D634, D906 and D908 workpiece codes can be identified using Appendix A1, D632 and D905 workpieces have been prepared for further investigations. Welding circumstances of D634 and D632 workpieces were the same, and D905 workpiece has been welded using low linear energy.

Table 5.6. Deformation of the welded workpieces scaling by vernier caliper

D632		**D634**		**D905**		**D906**		**D908**	
mm	**degree**	**mm**	**degree**	**mm**	**degree**	**mm**	**degree**	**mm**	**degree**
0.75	0.407	2.30	0.941	1.75	0.811	2.55	1.173	3.35	1.572
0.05	0.027	2.15	0.879	0.90	0.417	2.85	1.311	4.20	1.971
0.05	0.027	1.85	0.757	0.75	0.347	3.25	1.495	2.35	1.103
0.65	0.353	2.05	0.838	1.40	0.649	1.85	0.851	3.75	1.760

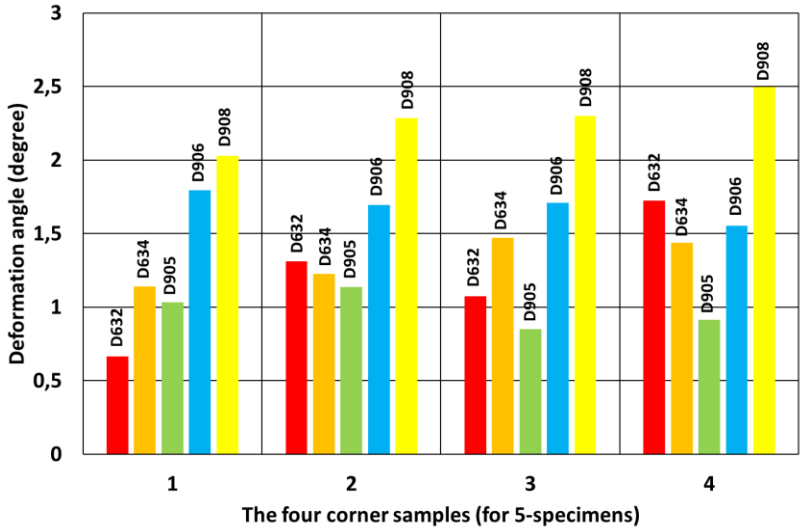

Fig. 5.4. Deformation of workpieces measured by vernier caliper.

Table 5.7. Deformation of the welded workpieces scaling by ZEN software

D632		D634		D905		D906		D908	
mm	**degree**	**mm**	**degree**	**mm**	**degree**	**mm**	**degree**	**mm**	**degree**
1.227	0.666	2.789	1.141	2.229	1.033	3.899	1.793	4.32	2.027
2.416	1.311	3.001	1.227	2.451	1.136	3.683	1.694	4.868	2.284
1.98	1.075	3.597	1.471	1.831	0.849	3.716	1.709	4.900	2.299
3.178	1.725	3.513	1.437	1.971	0.914	3.374	1.552	5.324	2.498

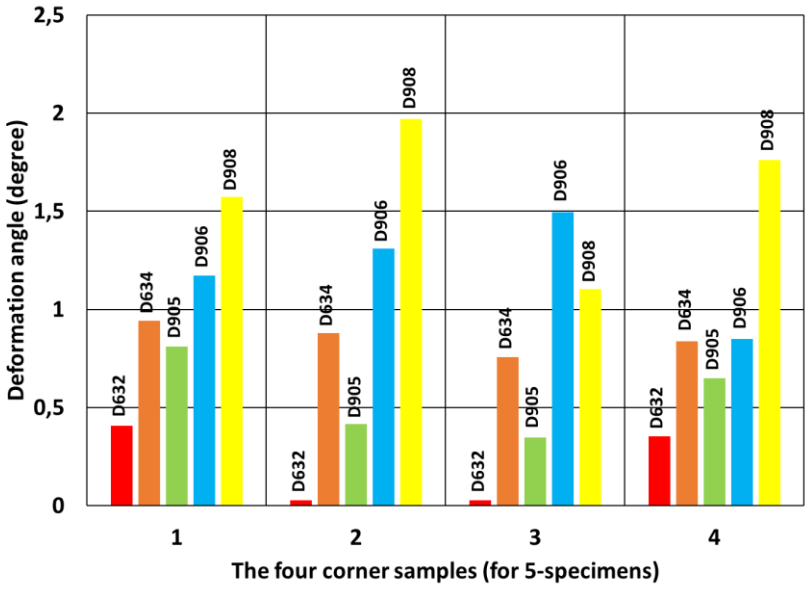

Fig. 5.5. Deformation of workpieces measured by ZEN software.

Based on the results, it can be stated that both methods are applicable for the measurements because the results are close to each other. The deformations do not exclude the workpieces from the further investigations because small deformation degrees were measured and narrow specimens were used.

5.4. Results of hardness testing, the hardness distributions

HV10 hardness values were measured along two lines, a sub-surface and a root lines, using Reicherter UH250 hardness tester. Specimens prepared for FCG tests were used for the measurements, and both types of specimens (T-L/21W, T-S/23W, see 7.1. subchapter) were applied. The macro-structure of the M/OM welded joint with a notch location and hardness indentations can be seen in Fig. 5.6. Figs. 5.7-5.9 show the hardness distributions.

Fig. 5.6. Macro-structure of the M/OM welded joint with a notch location and hardness indentations.

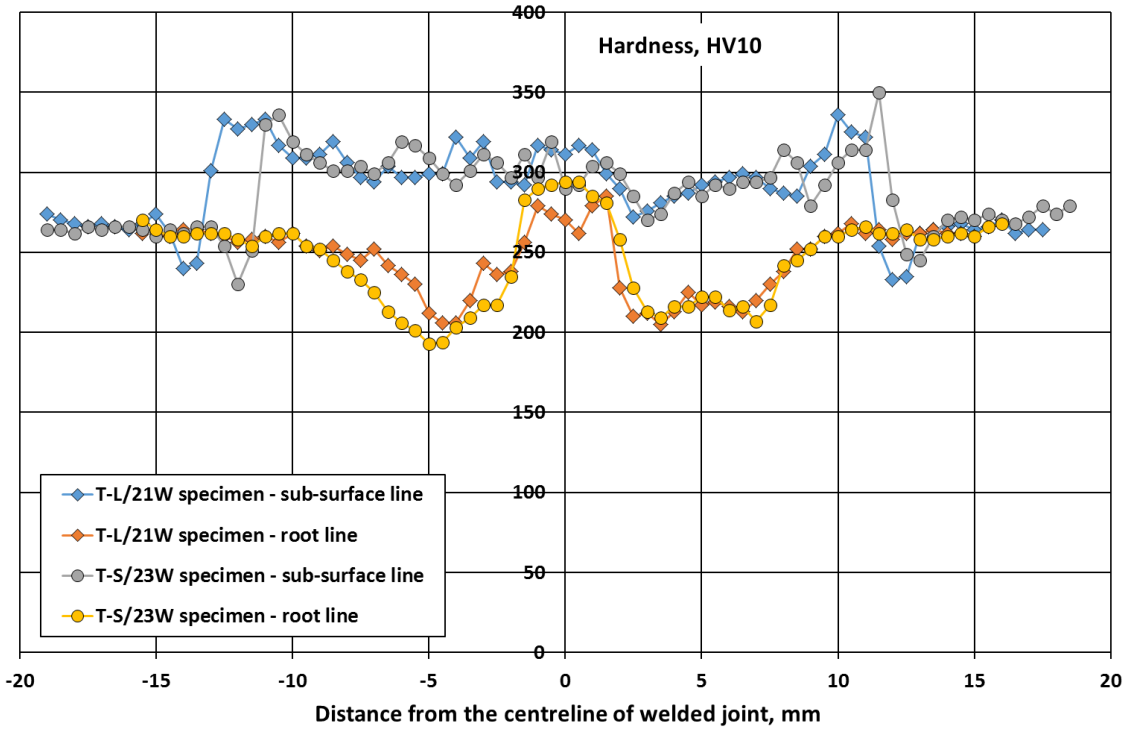

Fig. 5.7. Hardness distributions measured on Weldox 700E / UNIONX85/UNION X90 (M / OM) specimen.

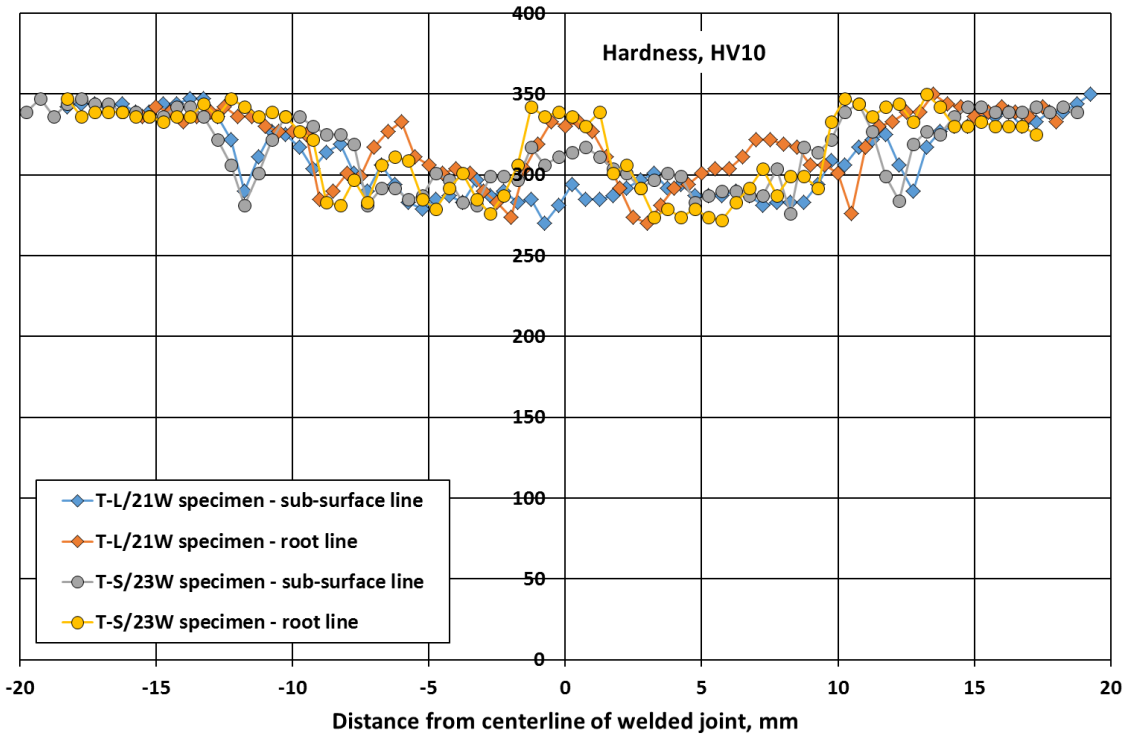

Fig. 5.8. Hardness distributions measured on Alform 960M / UNION X90 (UM) specimen (medium heat input = collective of applied linear energy and interpass temperature).

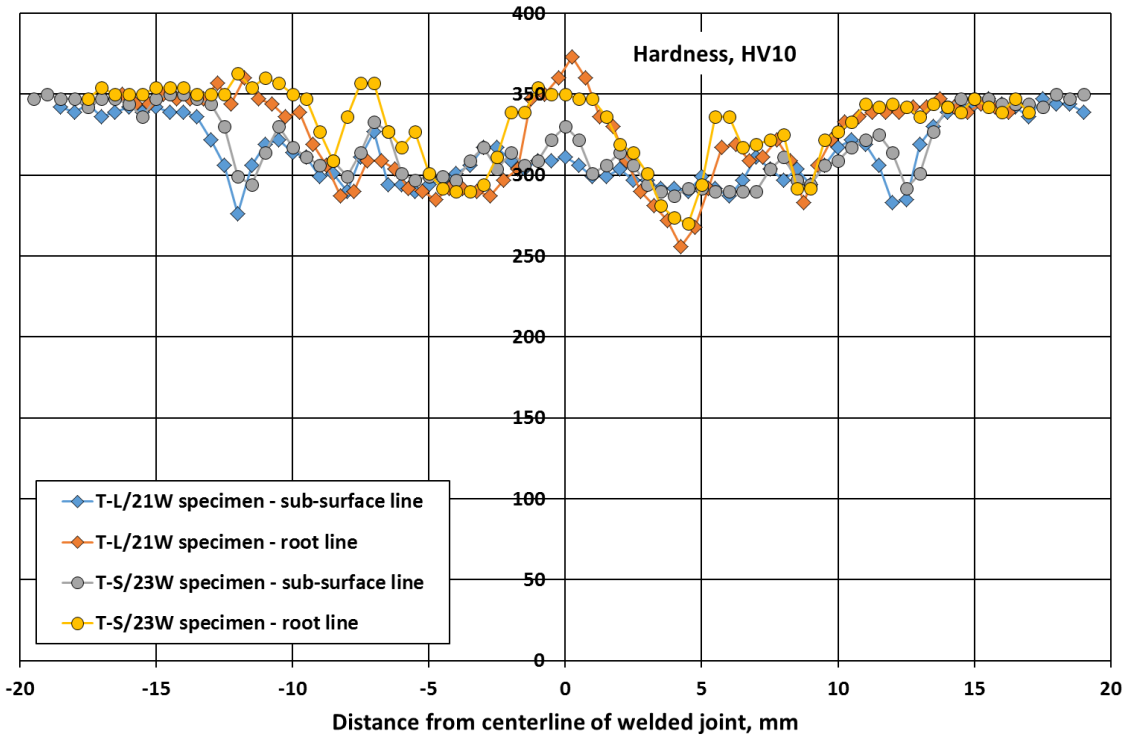

Fig. 5.9. Hardness distributions measured on Alform 960M / UNION X96 (M) specimen (high heat input = collective of applied linear energy and interpass temperature).

All three figures show the expected characteristics. Fig. 5.7 demonstrates the hardness difference between matching and overmatching filler metals, Fig. 5.8 shows lower hardness values in the weld metal and HAZ subsequent upon the undermatched filler metal, and finally, Fig. 5.9 illustrates both the matching and the high heat input (collective of linear energy and interpass temperature) effects.

Fig. 5.10 compares the hardness distributions for matched (M) and undermatched (UM) welded joints of Alform 960M base material, applying high (h) heat input (collective of linear energy and interpass temperature).

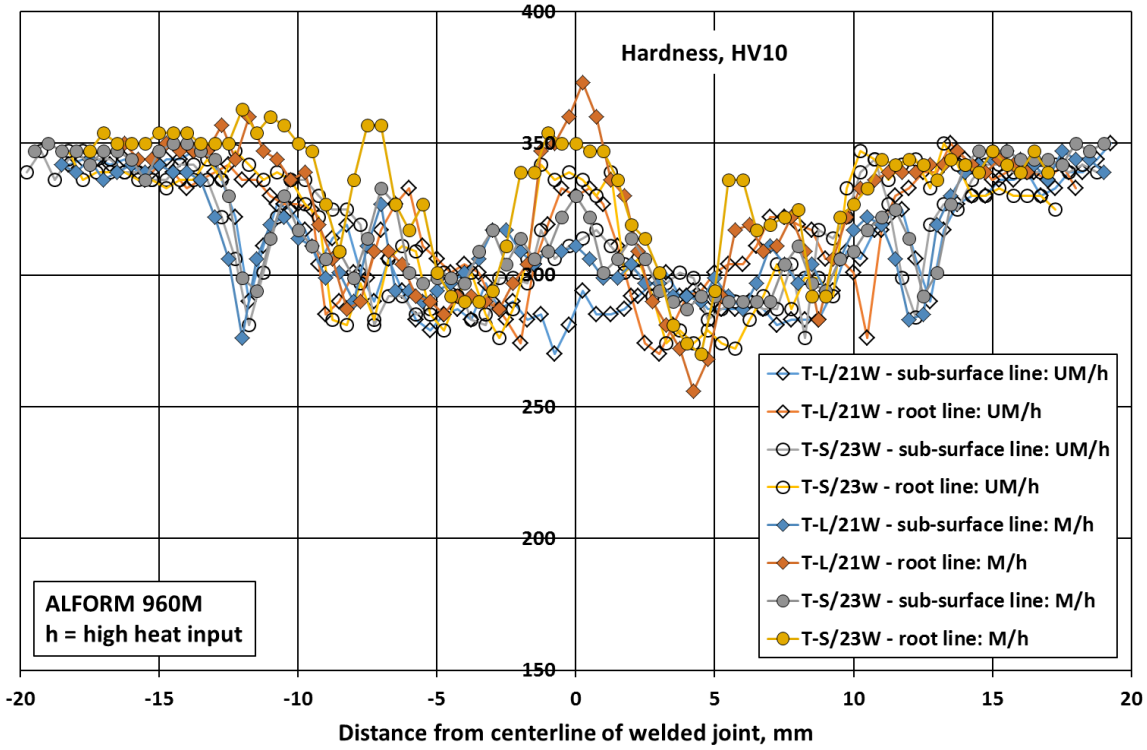

Fig. 5.10. Hardness distribution comparison for undermatching (UM) and matching (M) cases, applying high (h) heat input (collective of linear energy and interpass temperature).

Fig. 5.10 shows the characteristic differences between matched (M) and undermatched (UM) welded joints, applying same heat input.

Based on the results of all cases, important conclusion that hardness values characteristically do not exceed 350HV10 value, only a few measured values were greater than 350HV10.

6. HIGH CYCLE FATIGUE (HCF) TESTS

6.1. Testing characteristics

Wide variety of machines, equipment and structures are usually designed for long operation, high cycle fatigue is considered when the loading is relatively low, and the number of cycles is relatively high, between 10^4 (5×10^4) cycles and 10^8 (10^9) cycles. The cyclic loading of the components, structural elements and structures can be very different, from simple mechanical stresses (tensile, tensile-compression, bending, such as in plane, out of plane and rotating bending, torsion) to complex stresses (for example tensile and bending), furthermore, cyclic thermal and/or environmental stresses can also occur [90].

The results of the measurements can be significantly affected by numerous factors. This clearly means that under the same testing conditions, both more test specimens and mathematical statistical methods should be applied due to the relative high standard deviation of the test results and for the correct evaluation of the results. When specimens from the whole welded joints are examined, the effects of the welding process further increase the uncertainty. The statistical approach (e.g. specimen location) is already recommended in the preparation phase of the experiments, so the validity range of the results can be widened and the reliability can be increased [91].

HCF experiments were performed on butt welded joints, with an MTS 810 type electro-hydraulic materials testing equipment (see Fig. 6.1), at room temperature and in laboratory environment. Flat test specimens and constant load amplitude were applied during the tests, with R = 0.1 stress ratio, f = 30 Hz loading frequency, and sinusoidal loading wave form.

The geoemetry and directions of the specimens cut from base materials and welded joints can be seen in Fig. 6.2 [14]. The investigation and their results executed on these specimens were used for comparison. The shape and the dimentions of the investigated butt welded joint specimens can be seen in Fig. 6.3, the axis of the specimens was perpendicular to the weld line.

Appendix A1 summarizes the charachteristics of the HCF tests and the primary results, such as number of cycles to failure, location of the fracture and the survivar specimens.

6.2. Results of HCF tests, „Mean" S-N curves

Considering the large number of test specimens and striving after reliability, applying of a statistical approach was necessary. Staircase method was applied during both the preparation and the evaluation of the HCF test, based on the JSME (Japan Society of Mechanical Engineers) S 002-1981 prescription [65]. In this method (minimum) 8 test specimens must / should be used in the lifetime or finite life region, and (minimum) 6 test specimens in the endurance limit or infinite life region, so in total (minimum) 14 test specimens must / should be tested.

Fig. 6.1. MTS type electro-hydraulic testing system equipped for the HCF investigation of butt welded joint specimen.

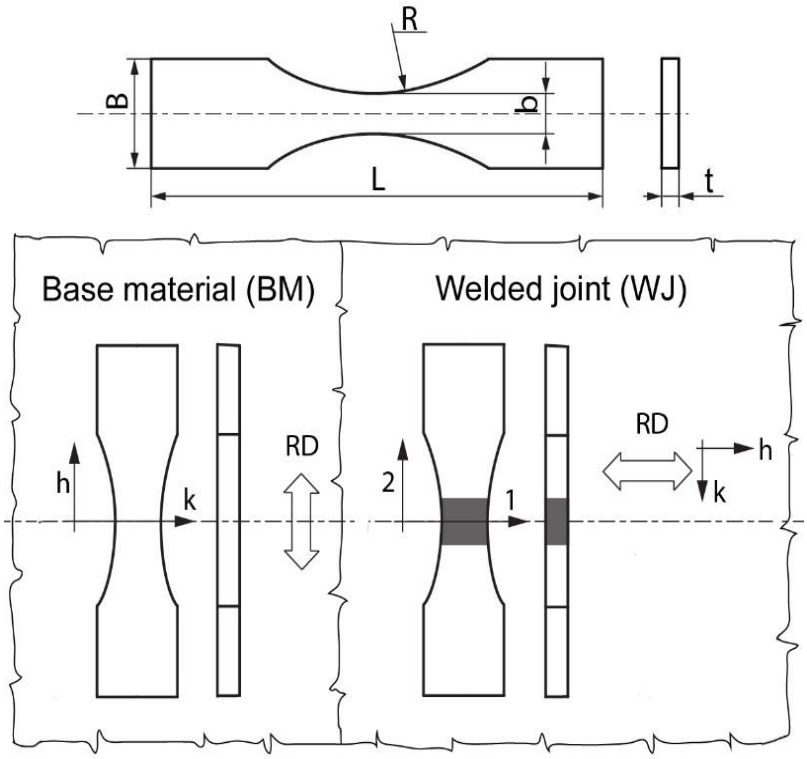

Fig. 6.2. The geometry, the location and the designation of the HCF test specimens for base materials (BM) and welded joints (WJ).

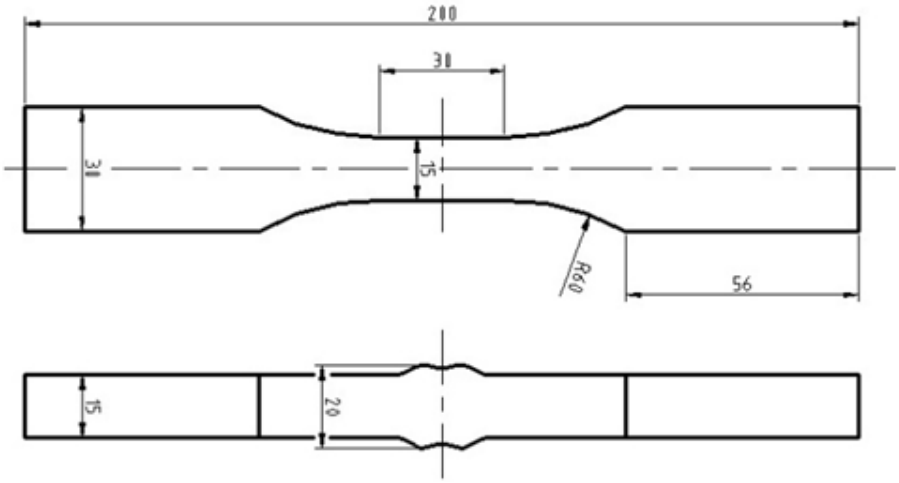

Fig. 6.3. Shape and geometry of the HCF test specimens for butt welded joints (BWJ).

Figs. 6.4-6.7 demonstrates the testing results based on previous [9][10] and our investigations, including the main characteristics of the investigations. Both measured values and "Mean" S-N curves were presented, arrows indicate the survived specimens. In the figures, x/y = center line of the specimen/crack growth direction, h = parallel to the rolling direction, k = perpendicular to the rolling direction, v = thickness direction, 1W = center line of the welded joint, 3W = thickness direction in the welded joint.

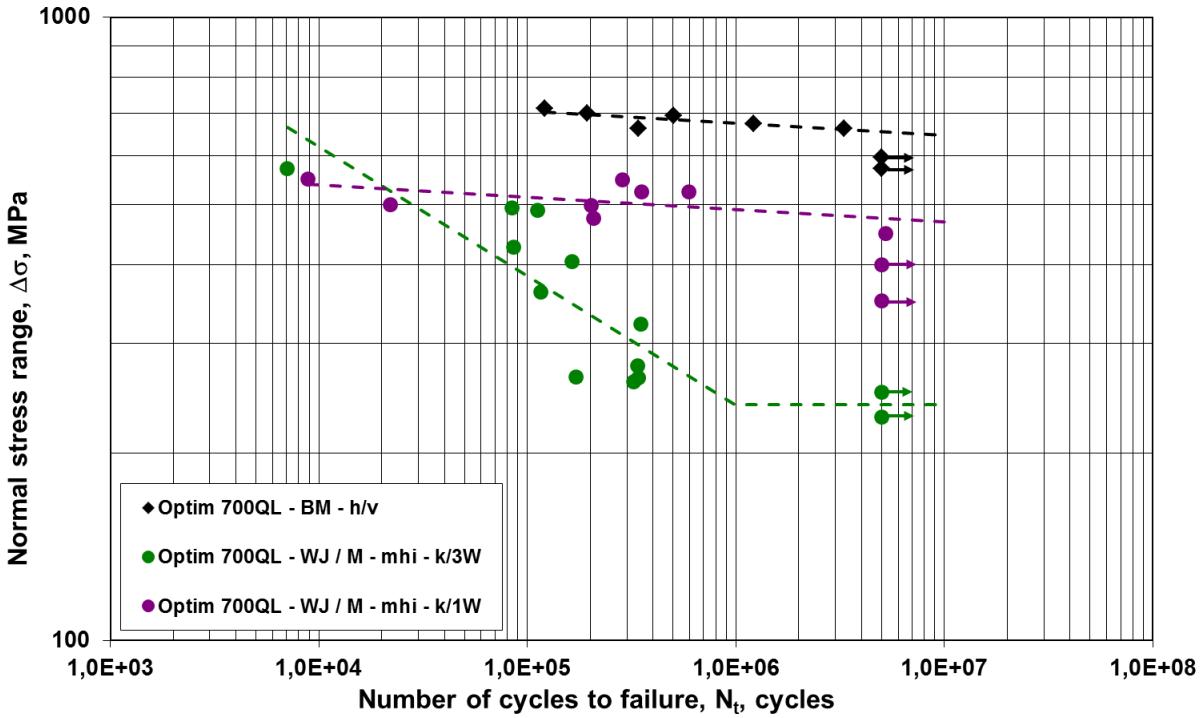

Fig. 6.4. Measured values and „Mean" S-N curves for Optim 700QL base materials (BM) and its welded joints (WJ).

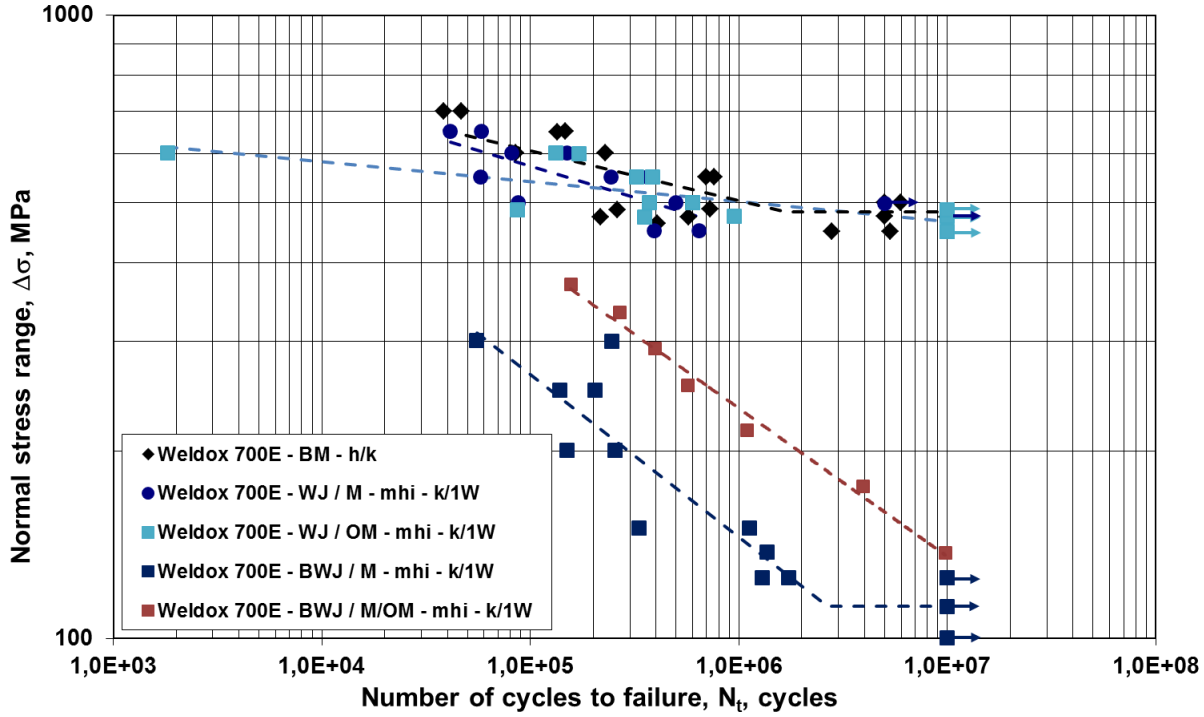

Fig. 6.5. Measured mean values and „Mean" S-N curves for Weldox 700E base materials (BM) and its welded joints (WJ) and butt welded joints (BWJ).

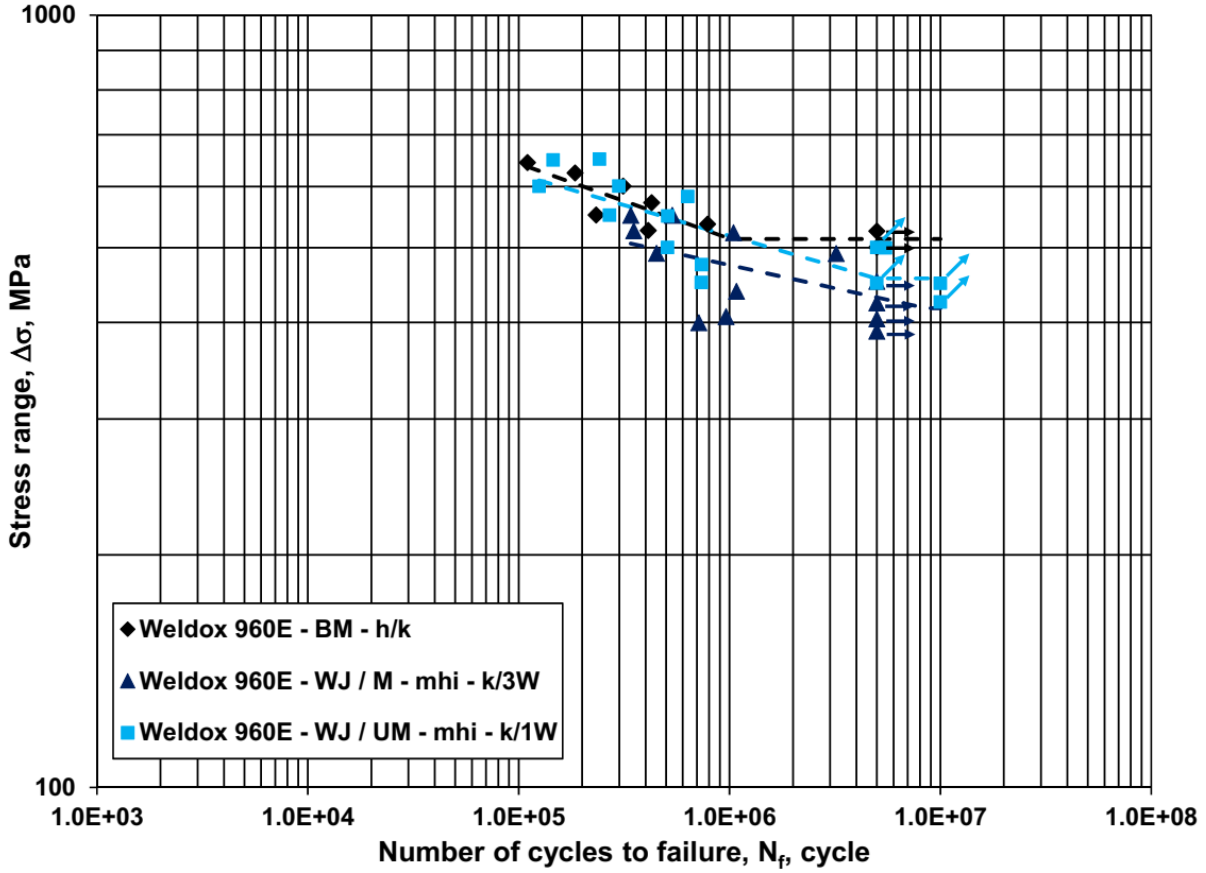

Fig. 6.6. Measured values and „Mean" S-N curves for Weldox 960E base materials (BM) and its welded joints (WJ).

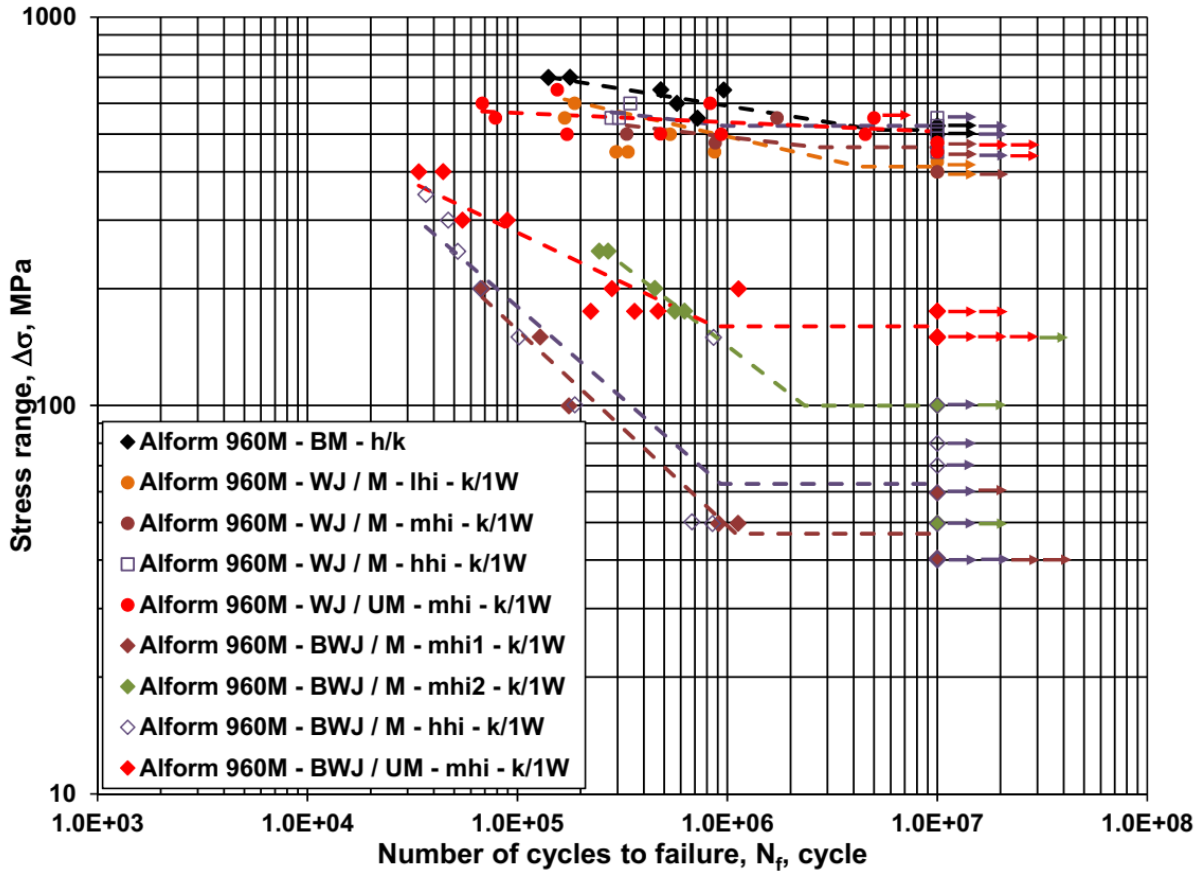

Fig. 6.7. Measured mean values and „Mean" S-N curves for Alform 960M base materials (BM) and its welded joints (WJ) and butt welded joints (BWJ).

The parameters of the "Mean" S-N curves were calculated using the Basquin equation [14]

$$N * \Delta\sigma^m = a\,, \tag{6.1}$$

and summarized in Table 6.1. In the table N_k value is the number of cycles for the break point of the S-N curve, the $\Delta\sigma_D$ is the fatigue limit, and the $\Delta\sigma_{1E07}$ is the stress range belonging to 1×10^7 cycles in the cases, when the horizontal (endurance limit) part of the curves cannot be determined, *m* and *a* are material constants [24].

As we can see in the Table 6.1, in six cases the endurance limit part of the curves was not determined. In five cases the high fatigue resistance is the reason for this; in the sixth case (Weldox 700E WJ / M k/1W), the available data were not enough for the determination of the second part of the S-N curve. In this case, the $\Delta\sigma_{1E07}$ stress values cannot be also determined.

In case of the Weldox 700E at lower number of cycles (approximately under 2×10^5), namely at higher load levels, the fatigue resistance of the overmatched welded joint (WJ) is lower than the matched welded joint, however at higher number of cycles the overmatched welded joint has better fatigue characteristics. If the loading force is not too large, the crack initiation and propagation difficultly happen, while at large loading conditions (at lower number of cycles) the brittle behavior of overmatched filler metal can lead to cracking [24].

Table 6.1. Parameters of high cycle fatigue (HCF) curves: "Mean" S-N curves

Base material	Manufacturing and orientation	Heat input	m	log(a)	N_k	$\Delta\sigma_D$	$\Delta\sigma_{1E07}$	Source
			(–)	(–)	(cycle)	(MPa)	(MPa)	
Optim 700QL	BM-h/v	N/A	51.282	151.109	–	–	646	[9]
	WJ/M-k/3W	medium	4.826	17.476	9.893 E05	239	–	
	WJ/M-k/1W		50.251	141.26	–	–	470	
Weldox 700E	BM-h/k	N/A	12.453	39.650	1.677 E06	483	–	[9]
	WJ/M-k/1W	medium	9.960	32.469	–	–	–	
	WJ/OM-k/1W		31.250	90.415	–	–	467	
	BWJ/M-k/1W		3.831	14.285	2.660 E06	113	–	OWN
	BWJ/M/OM-k/1W		4.207	15.966	–	–	136	
Weldox 960E	BM-h/k	N/A	10.288	33.887	1.014 E06	513	–	[10]
	WJ/M-k/3W	medium	16.722	50.754	8.535 E06	417	–	
	WJ/UM-k/1W		12.594	40.185	4.944 E06	456	–	
Alform 960M	BM-h/k	N/A	11.494	37.855	5.122 E06	513	–	[9]
	WJ/M-k/1W	low	8.130	27.893	4.270 E06	412	–	
	WJ/M-k/1W	medium	16.129	49.413	2.681 E06	462	–	
	WJ/M-k/1W	high	15.385	47.838	9.693 E05	525	–	
	WJ/UM-k/1W	medium	41.667	119.723	–	–	507	
	BWJ/M-k/1W	medium*	1.984	9.354	1.099 E06	47	–	OWN
	BWJ/M-k/1W	medium*	2.392	11.153	2.336 E06	100	–	
	BWJ/M-k/1W	high	2.123	9.787	9.307 E05	63	–	
	BWJ/UM-k/1W	medium	3.891	14.515	8.701 E05	160	–	

* Same welding characteristics but different butt welded joint geometry.

In case of the Weldox 700E, the fatigue resistance of the matched/overmatched butt welded joint (BWJ) is higher than the matched butt welded joint, and both matched and matched/overmatched butt welded joints have lower fatigue resistance than welded joints (WJ).

The high cycle fatigue resistance of the examined Weldox 960E steel is better, than the literature data in the same category. The high cycle fatigue resistance of this steel is higher in the undermatched welded joint (WJ), than in case of the matched joint [24].The high cycle fatigue resistance of the Alform 960M base material is higher, than the examined Weldox 960E, furthermore higher than the overall literature data. In case of the Alform 960M the effect of $t_{8.5/5}$ cooling time was also investigated. By the increase of linear heat input (so the $t_{8.5/5}$ cooling time) the endurance limit of the welded joint improves, however the strength characteristics reduce at the same time. It may be explained by the lack of hardened zones in the welded joint at higher cooling time. At Alform 960M during the application of undermatching filler metal and medium heat input higher endurance limit was found than with matching filler metal. In the wider range of the lifetime section similarly positive effect of the undermatching filler metal was noticed.

In case of the Alform 960M, same tendencies cab be found at butt welded joints (BWJ) and welded joints (WJ). Both the mismatch condition and the heat input have the same influence on the fatigue characteristics. However, the results of investigated butt welded joints under matched condition and medium heat input have clearly demonstrated the influence of the weld toe geometry (two "Mean" curves). The high cycle fatigue resistance of the butt welded joints were lower than the welded joints, which has been detected at Weldox 700E material, too.

6.3. Determination of high cycle fatigue strength curves

The "Mean" S-N curves determined based on JSME prescription [65] can be completed with standard deviation (*SD*) values and these curves ("Mean-2SD" S-N curves) can be used as high cycle fatigue strength curves, in other words high cycle fatigue design or limit curves (see Fig. 6.8 and compare with Fig. 3.16).

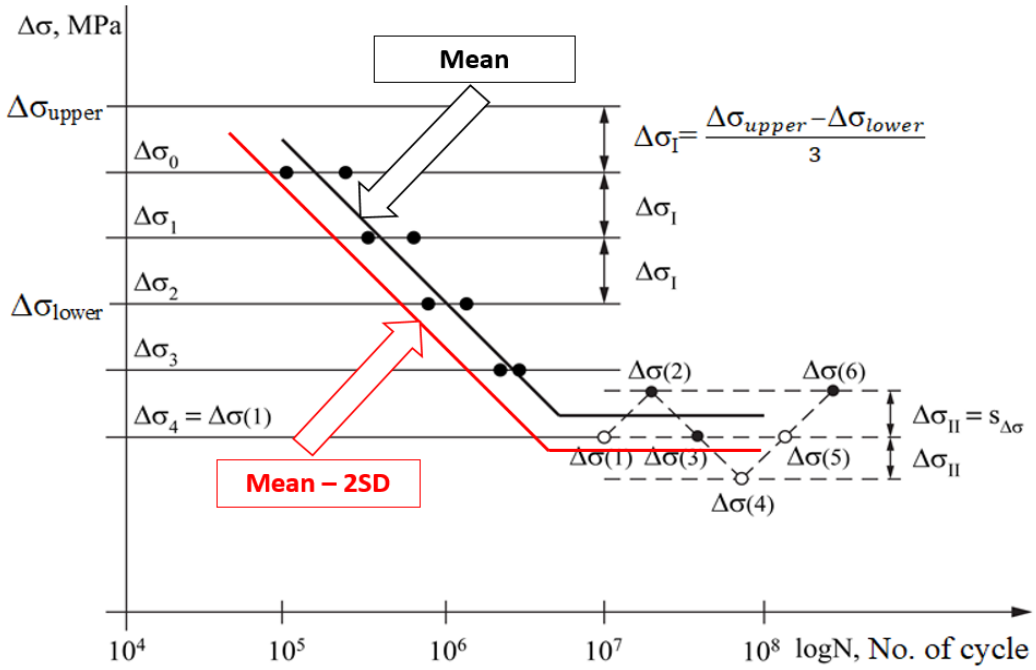

Fig. 6.8. Determination of high cycle fatigue strength curves, „Mean-2SD" S-N curves.

On the one hand, it is known that HCF test results have greater uncertainty, standard deviation and lower reliability than static test results, therefore "Mean" values and "Mean" S-N curves reflect unacceptable risks. On the other hand, the application of 3SD value – based on the three-sigma (3σ) rule – is unjustified because the excessively low allowable strength values. It means that 2SD and "Mean-2SD" S-N curves result in a good compromise between the acceptable risk and the required reliability.

The calculated parameters of the "Mean-2SD" S-N curves for both steel categories (690 MPa and 960 MPa) and for all types (base material (BM), welded joint (WJ), butt welded joint (BWJ)) investigated are presented in Table 6.2.

Table 6.2. Parameters of high cycle fatigue (HCF) strength curves: "Mean-2SD" S-N curves

Base material	**Manufacturing, orientation and heat input***	**m**	**log(a)**	**N_k**	**$\Delta\sigma_D$**	**$\Delta\sigma_{1E07}$**
		(–)	**(–)**	**(cycle)**	**(MPa)**	**(MPa)**
Optim 700QL	BM-h/v	51.282	150.186	–	–	620
	WJ/M-k/3W	4.826	16.762	9.893 E05	170	–
	WJ/M-k/1W	50.251	138.732	–	–	418
Weldox 700E	BM-h/k	12.453	38.557	1.677 E06	395	–
	WJ/M-k/1W	9.960	31.739	–	–	–
	WJ/OM-k/1W	31.250	88.311	–	–	400
	BWJ/M-k/1W	3.831	13.752	2.660 E06	82	–
	BWJ/M/OM-k/1W	4.207	15.822	–	–	126
Weldox 960E	BM-h/k	10.288	33.473	1.014 E06	467	–
	WJ/M-k/3W	16.722	49.063	8.535 E06	331	–
	WJ/UM-k/1W	12.594	39.173	4.944 E06	379	–
Alform 960M	BM-h/k	11.494	37.207	5.122 E06	450	–
	WJ/M-k/1W lhi	8.130	26.723	4.270 E06	296	–
	WJ/M-k/1W	16.129	48.012	2.681 E06	379	–
	WJ/M-k/1W hhi	15.385	47.226	9.693 E05	479	–
	WJ/UM-k/1W	41.667	116.389	–	–	422
	BWJ/M-k/1W	1.984	9.175	1.099 E06	38	–
	BWJ/M-k/1W	2.392	11.103	2.336 E06	95	–
	BWJ/M-k/1W hhi	2.123	9.107	9.307 E05	30	–
	BWJ/UM-k/1W	3.891	13.957	8.701 E05	115	–

* Only low and high heat inputs (collective of linear energy and interpass temperature) were designated, lhi and hhi, respectively.

Figs. 6.9-6.12 show the previously determined „Mean" high cycle fatigue S-N curves (see Figs. 6.4-6.8) and the calculated „Mean-2SD" high cycle fatigue strength S-N curves, for all cases, systematically.

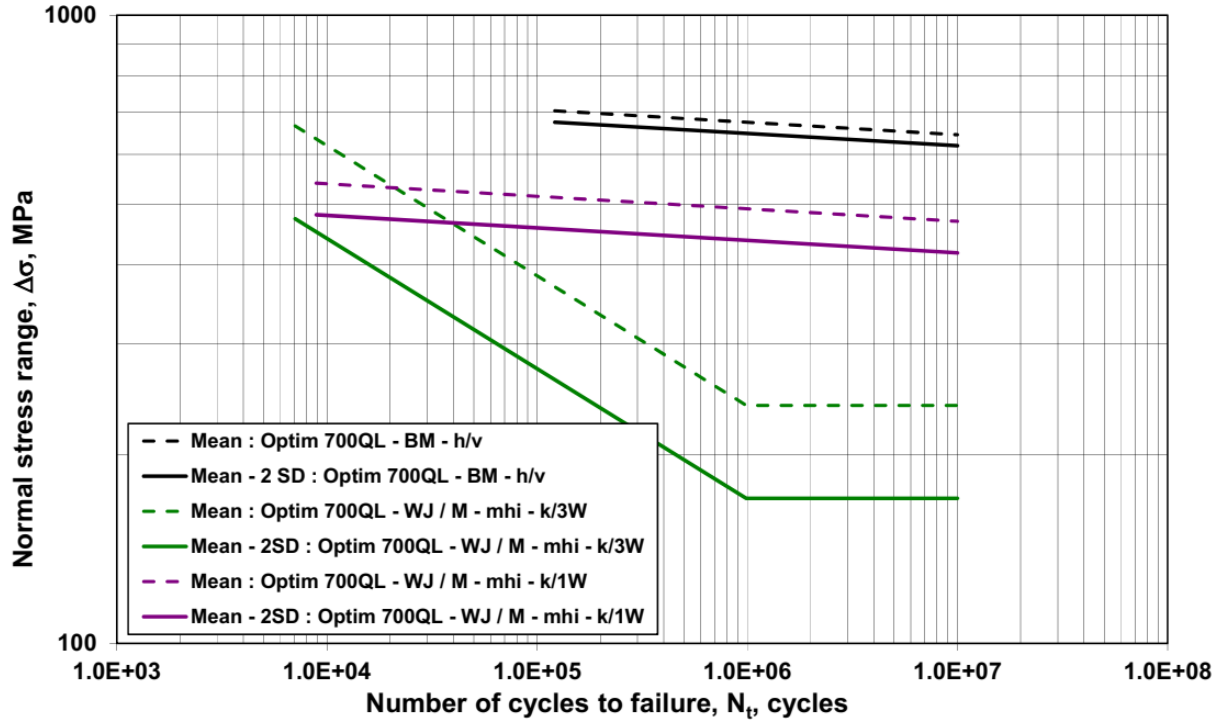

Fig. 6.9. „Mean" S-N curves and determined "Mean-2SD"high cycle fatigue strength curves for Optim 700QL base material (BM) and its welded joints (WJ).

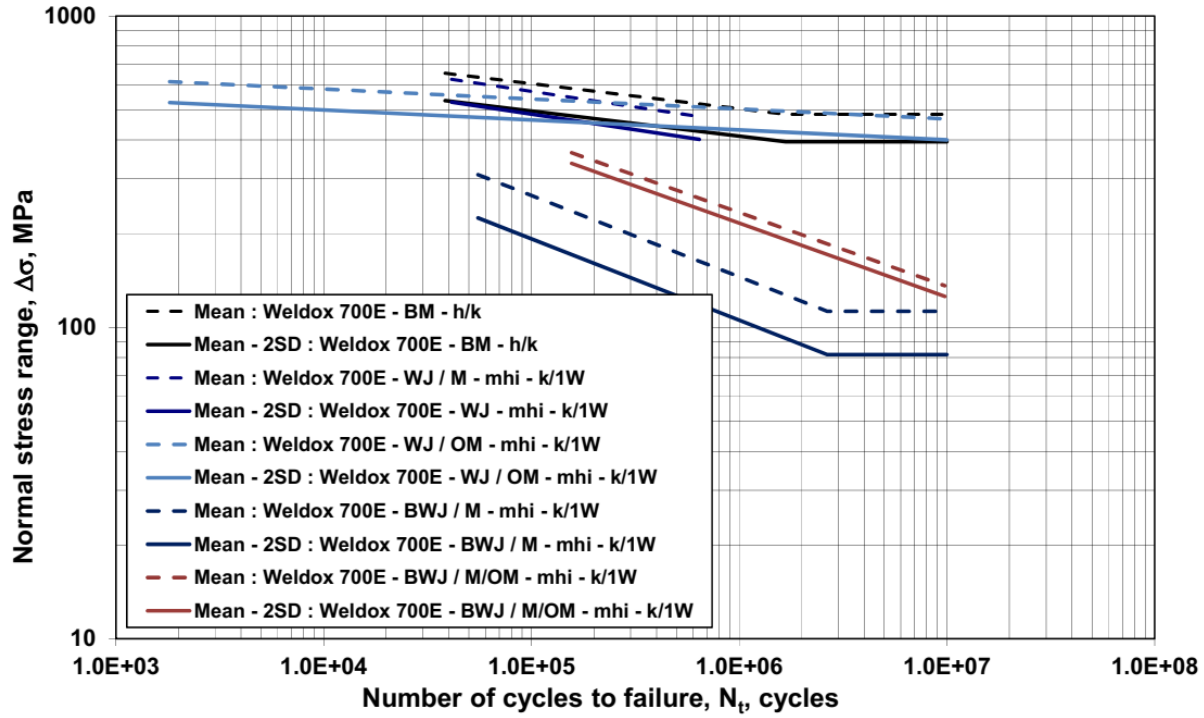

Fig. 6.10. „Mean" S-N curves and determined "Mean-2SD"high cycle fatigue strength curves for Weldox 700E base material (BM) and its welded joints (WJ) and butt welded joints (BWJ).

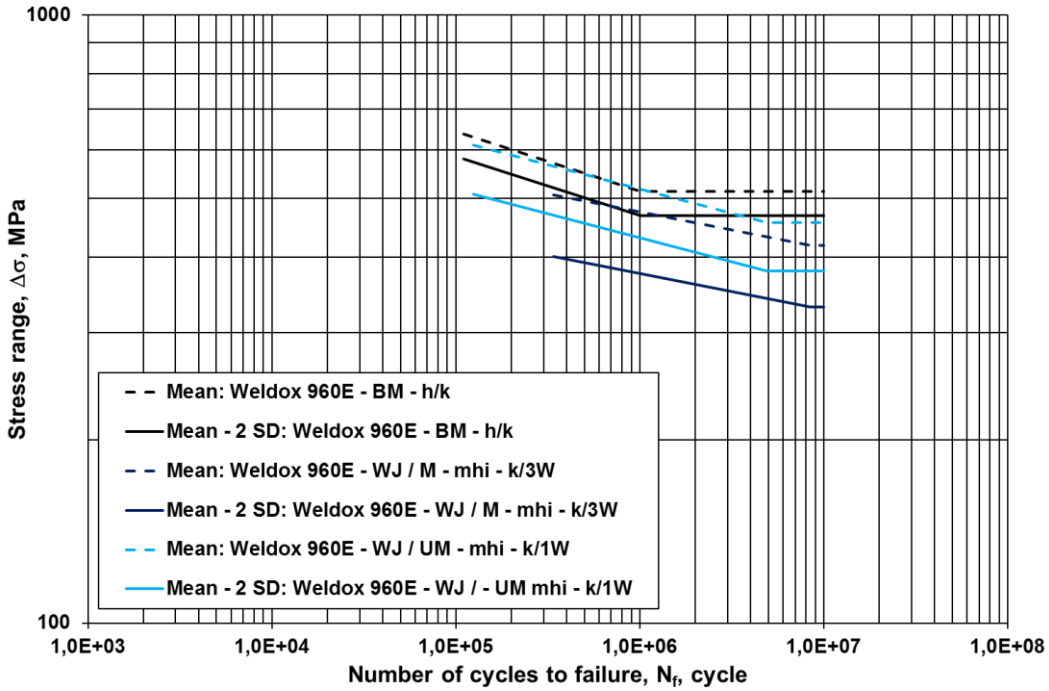

Fig. 6.11. „Mean" S-N curves and determined "Mean-2SD"high cycle fatigue strength curves for Weldox 960E base material (BM) and its welded joints (WJ).

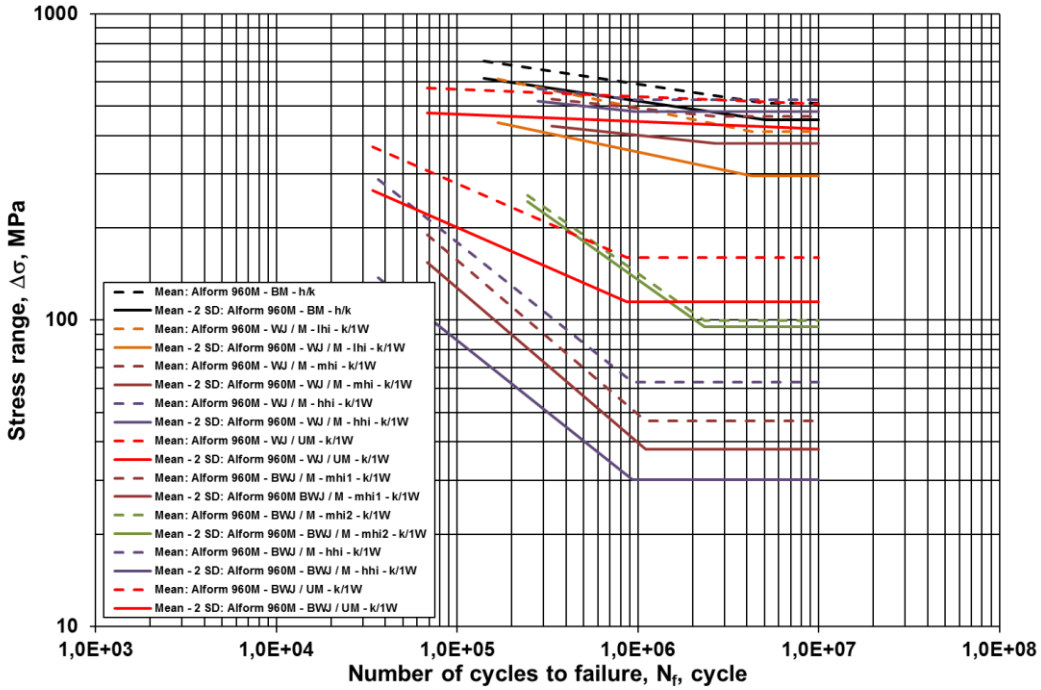

Fig. 6.12. „Mean" S-N curves and determined "Mean-2SD"high cycle fatigue strength curves for Alform 960M base material (BM) and its welded joints (WJ) and butt welded joints (BWJ).

6.4. Conclusions

Based on our investigations and their results, comparing them with previous researches, the following conclusions can be drawn.

- Applying the developed welding technologies eligible welded joints can be produced, where the appropriate quality contains the eligible resistance to high cycle fatigue. This statement has good correspondence with previous experiments can be found in the literature [25][91].
- The results of the executed investigations justified the necessity of the statistical approaches, especially referring to directions of base materials (h, v and k), the welded joints and the butt welded joints (k, 1W and 3W) and the determination of the number of the tested specimens. The crack paths have influence on the high cycle fatigue resistance of base materials and welded joints, the thickness direction is more unfavourable than the other directions.
- The resistance of the base materials to high cycle fatigue is more advantageous than the resistance of the welded joints. The welding causes unfavourable effects on the high cycle fatigue resistance of the investigated high strength steels.
- The matching phenomenon has influence on the high cycle fatigue resistance of high strength steel welded joints, depending on the strength category. In the case of the Weldox 700E base material, the effect of the filler metal depends on the loading magnitude; while in the case of the Weldox 960E, the undermatching filler metal has the higher fatigue resistance. The Alform 960M base material with undermatching filler metal has a relatively high fatigue resistance, but in the case of matching filler metals, the resistance depends on the heat input (collective of linear energy and interpass temperature) during welding; the best results obtained with the higher heat input.
- Based on the Basquin equation calculated high cycle fatigue S-N curves, called "Mean" S-N curves, can be used for the determination of high cycle fatigue strength curves (design or limit curves) called "Mean-2SD" S-N curves.
- Interesting observation that the base material grade in the same type has characteristic influence on the high cycle fatigue resistance of the base material and their gas metal arc welded joint (see Fig. 6.13).

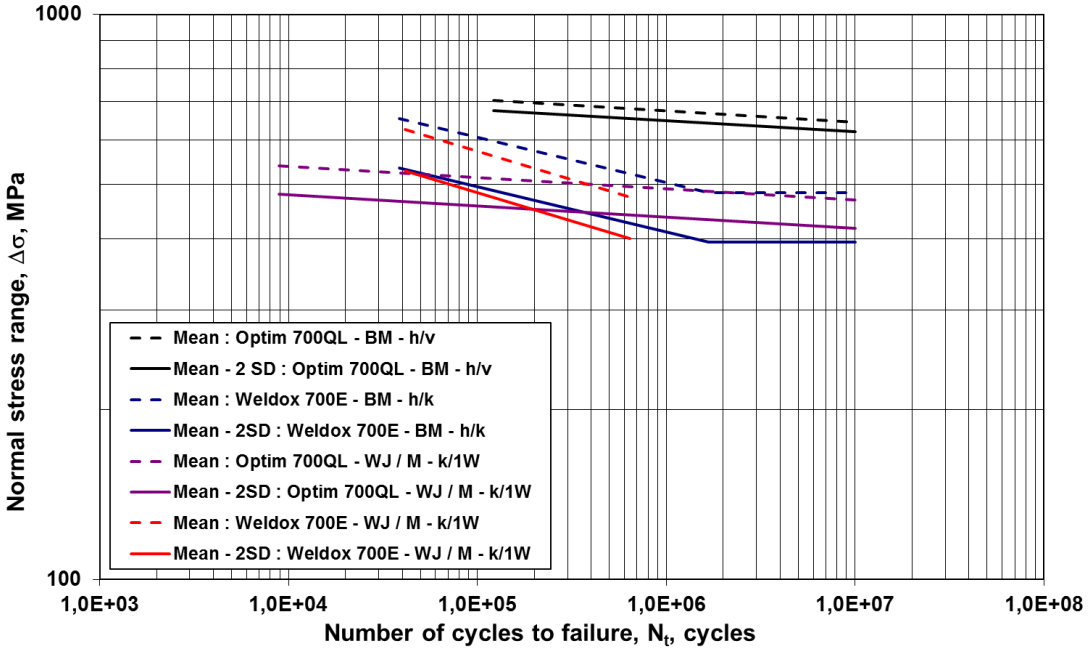

Fig. 6.13. Comparison of the high cycle fatigue "Mean" and "mean-2SD" curves for the two investigated S690Q type base materials and their gas metal arc welded joints.

7. FATIGUE CRACK GROWTH (FCG) TESTS

7.1. Testing characteristics

The FCG tests were executed on three-point bending (TPB) specimens, nominal W values were W = 26 mm (t = 15 mm), and W = 28 mm (t = 30 mm or t = 20 mm), and W = 13 mm (t = 15 mm) and W = 18 mm (t = 20 mm) for the base materials and the welded joints, in the 21 and 23 directions, respectively. The position of the notches correlated with the rolling direction (T-L, L-T and T-S). The positions of the cut specimens from the welded joints are shown in Fig. 7.1, 21 and 23 directions (21W and 23W) were used [92].

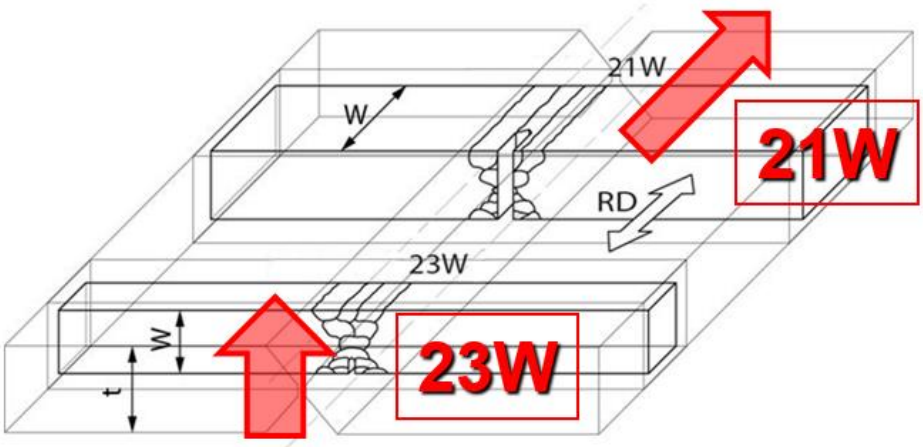

Fig. 7.1. TPB specimen locations in welded joint with notch directions (RD = rolling direction).

The notch locations, the notch distances from the centreline of the welded joints (Fig. 7.2), were different, therefore the positions of the notches and the crack paths represent the most important and the most typical crack directions in a real welded joins (see Fig. 5.6, too).

The FCG examinations were performed with tensile stress, R = 0.1 stress ratio, sinusoidal loading wave form, at room temperature, and on laboratory air, using MTS type electro-hydraulic testing equipment (see Fig. 7.3). The loading frequency was f = 20 Hz for two-thirds of the growing crack's length, approximately, and it was f = 5 Hz for the last third. The propagating crack was registered with optical method, using video camera and hundredfold magnification (N = 100x).

Post-weld treating (thermal and/or mechanical) was not applied after welding of gas metal arc welded joints (investigations in as-welded condition).

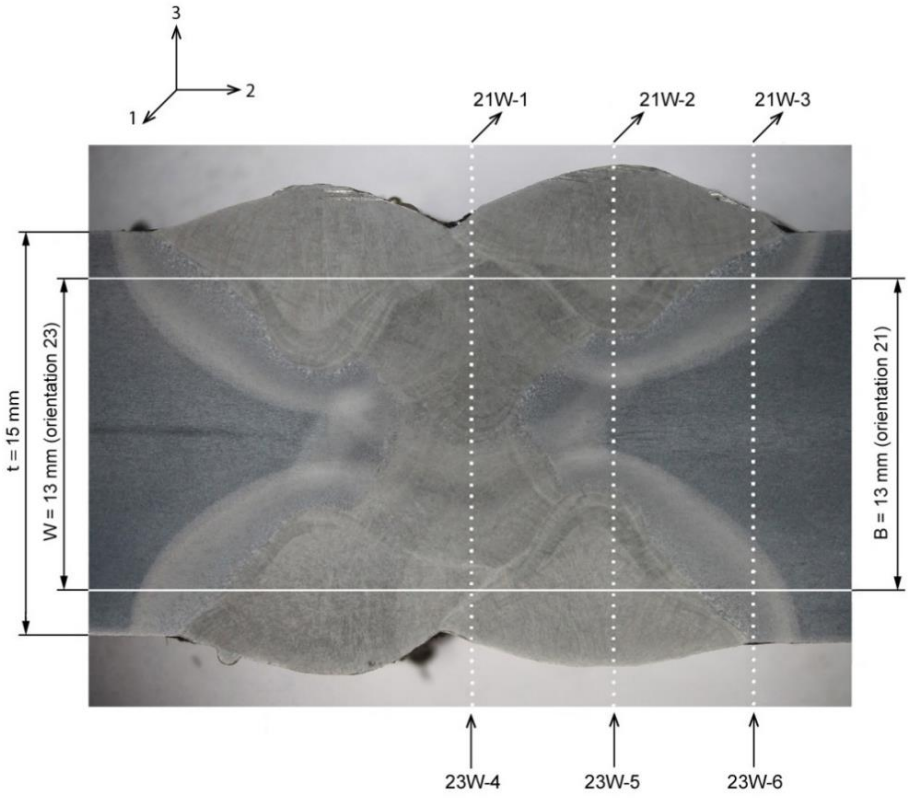

Fig. 7.2. Notch locations and crack paths in the welded joints.

Fig. 7.3. MTS type electro-hydraulic testing system equiped for FCG investigation.

7.2. Results of FCG tests

The crack length vs. number of cycles curves can be seen in different orientations for Weldox 700E / UNIONX85/UNION X90, matching / overmatching (M / OM) condition, welded with medium heat input in Fig. 7.4 and Fig. 7.5; Alform 960M / UNION X90, undermatching (UM) condition, welded with high heat input in Fig. 7.6 and Fig. 7.7; Alform 960M / UNION X96,

matching (M) condition, welded with high heat input in Fig. 7.8 and Fig. 7.9. Heat input includes both the linear energy and the interpass temperature.

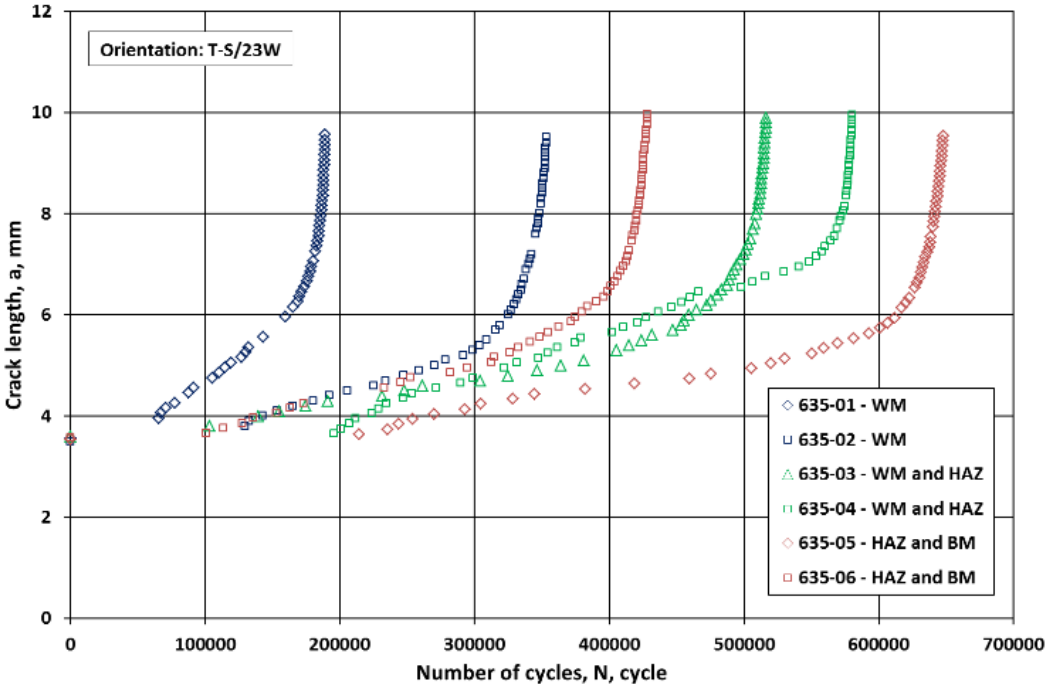

Fig. 7.4. Crack length vs. number of cycles curves in T-S/23W orientation (Weldox 700E / UNIONX85/UNION X90, matching / overmatching, medium heat input).

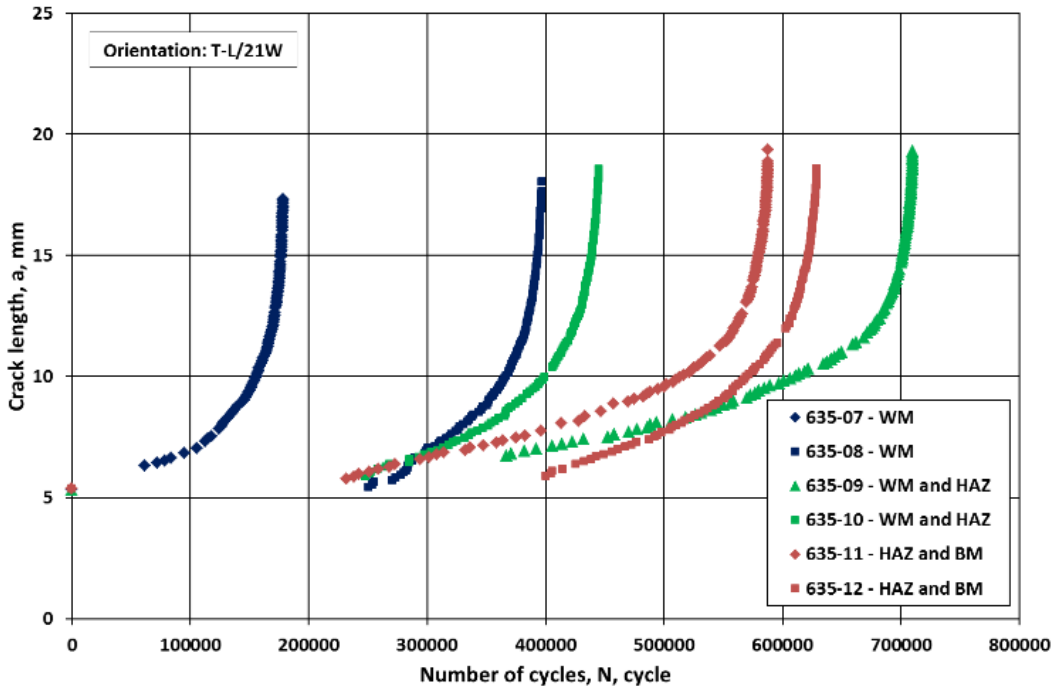

Fig. 7.5. Crack length vs. number of cycles curves in T-L/21W orientation (Weldox 700E / UNIONX85/UNION X90, matching / overmatching, medium heat input).

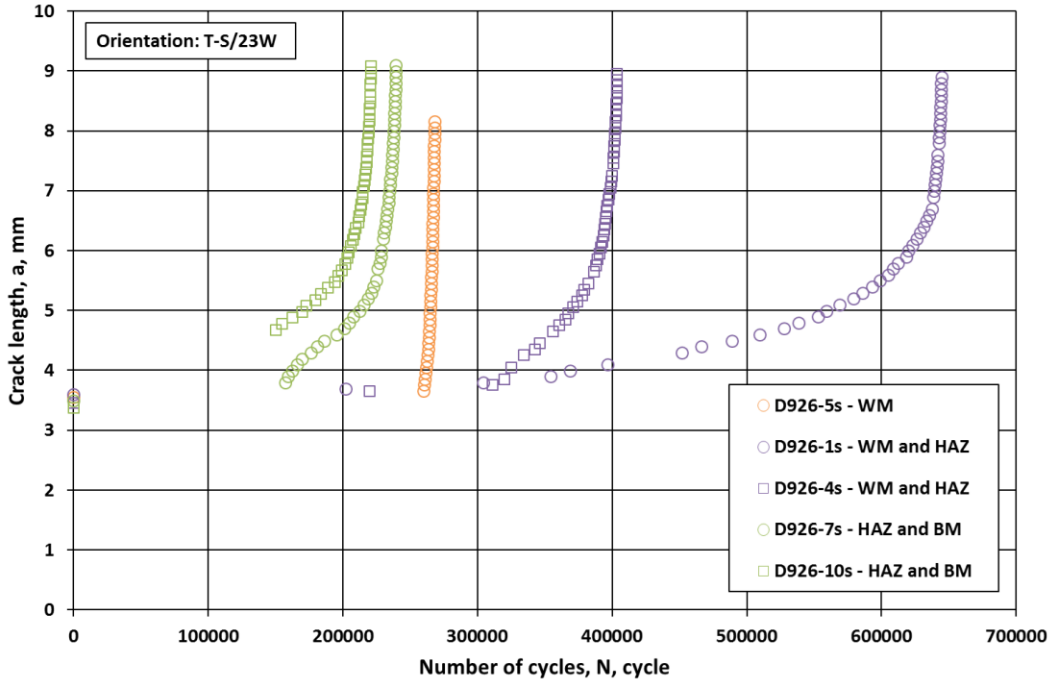

Fig. 7.6. Crack length vs. number of cycles curves in T-S/23W orientation (Alform 960M / UNION X90, undermatching, high heat input).

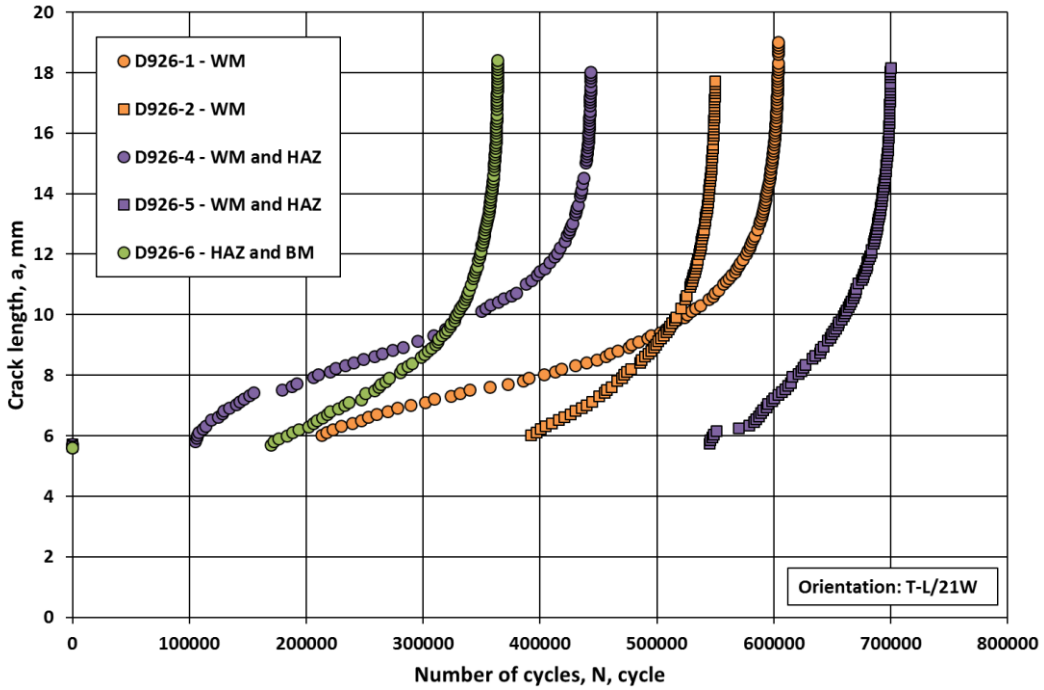

Fig. 7.7. Crack length vs. number of cycles curves in T-L/21W orientation (Alform 960M / UNION X90, undermatching, high heat input).

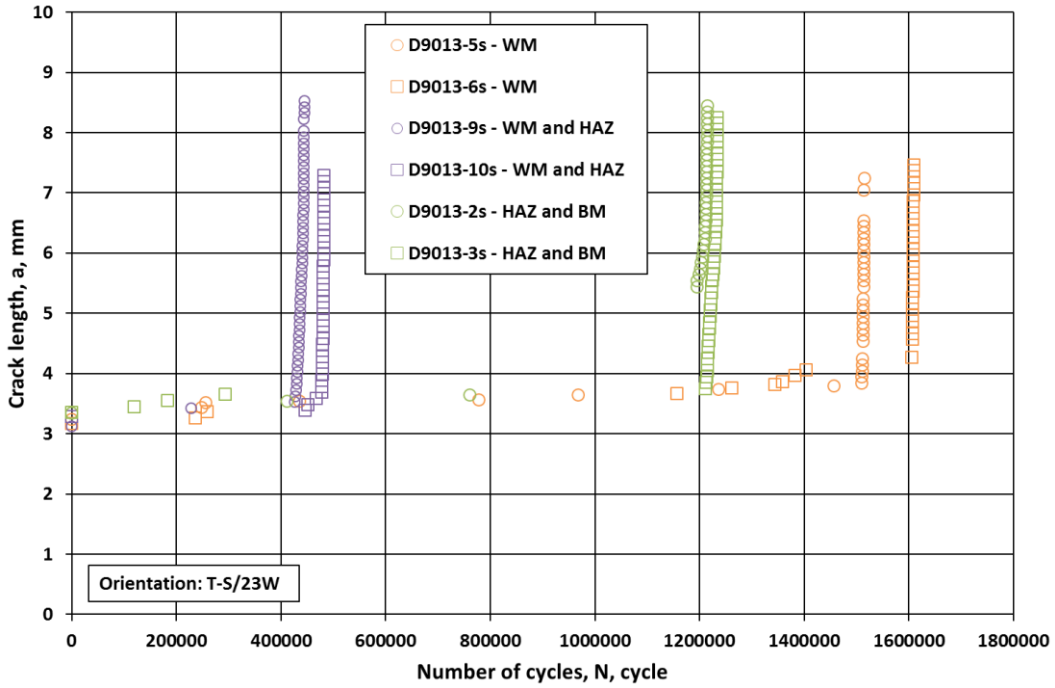

Fig. 7.8. Crack length vs. number of cycles curves in T-S/23W orientation (Alform 960M / UNION X96, matching, high heat input).

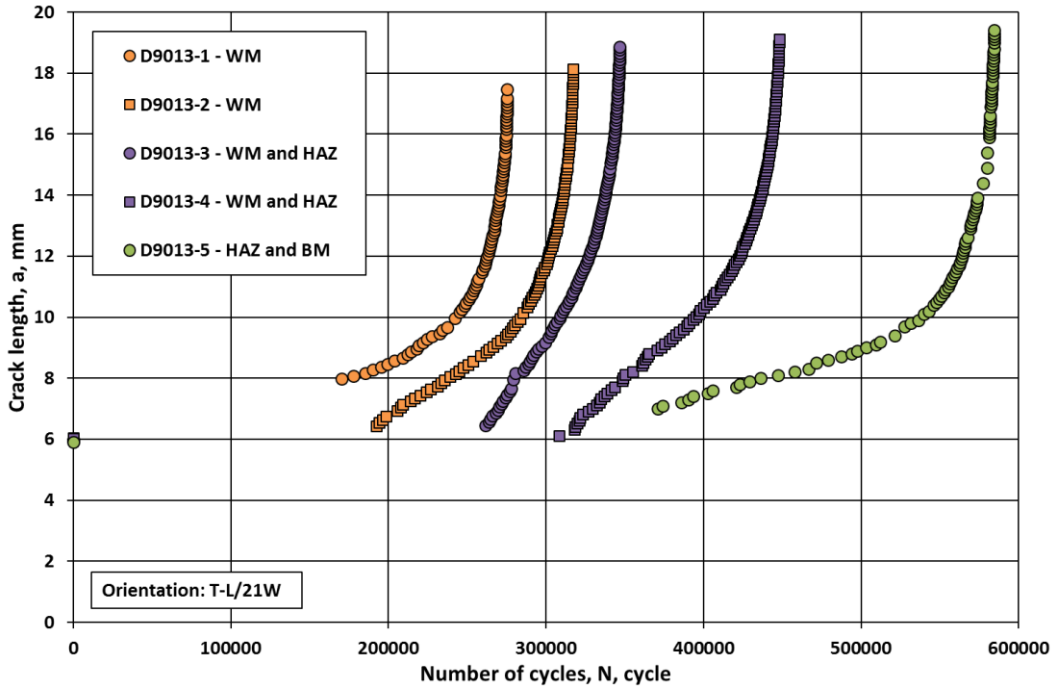

Fig. 7.9. Crack length vs. number of cycles curves in T-L/21W orientation (Alform 960M / UNION X96, matching, high heat input).

Secant method [93] was used to evaluate the fatigue crack growth data.. The calculated stress intensity factor range vs. fatigue crack growth rate values, the kinetic diagrams of FCG, are shown in Figs. 7.10-7.12.

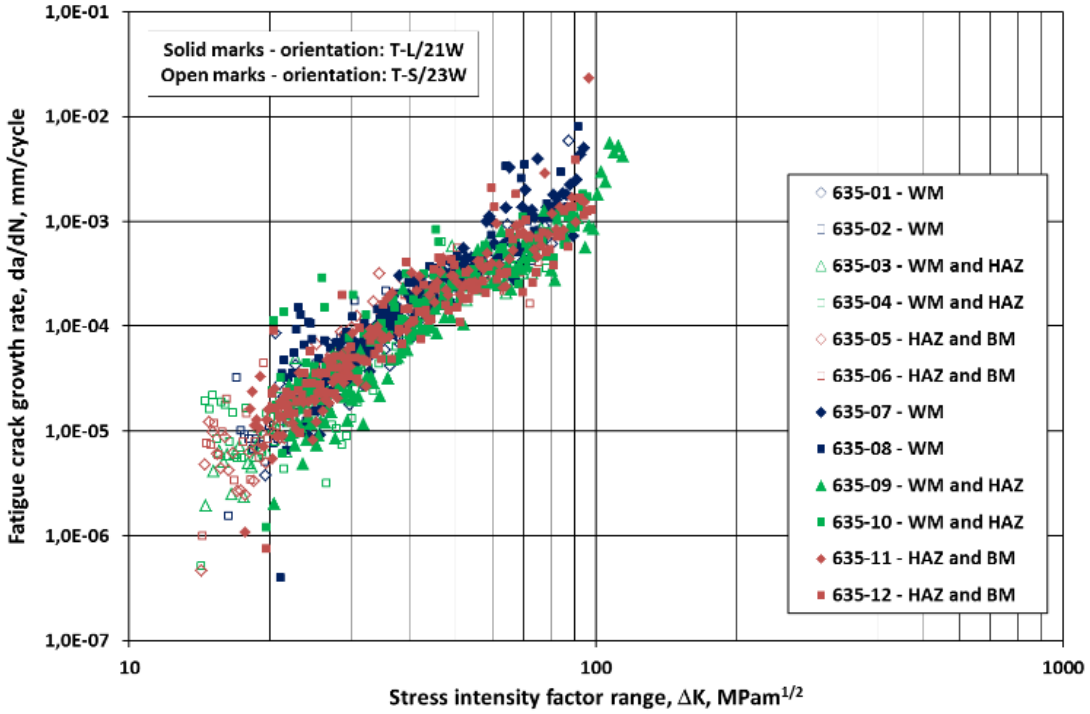

Fig. 7.10. Kinetic diagrams of FCG tests on Weldox 700E / UNIONX85/UNION X90 welded joints (altogether12 specimens).

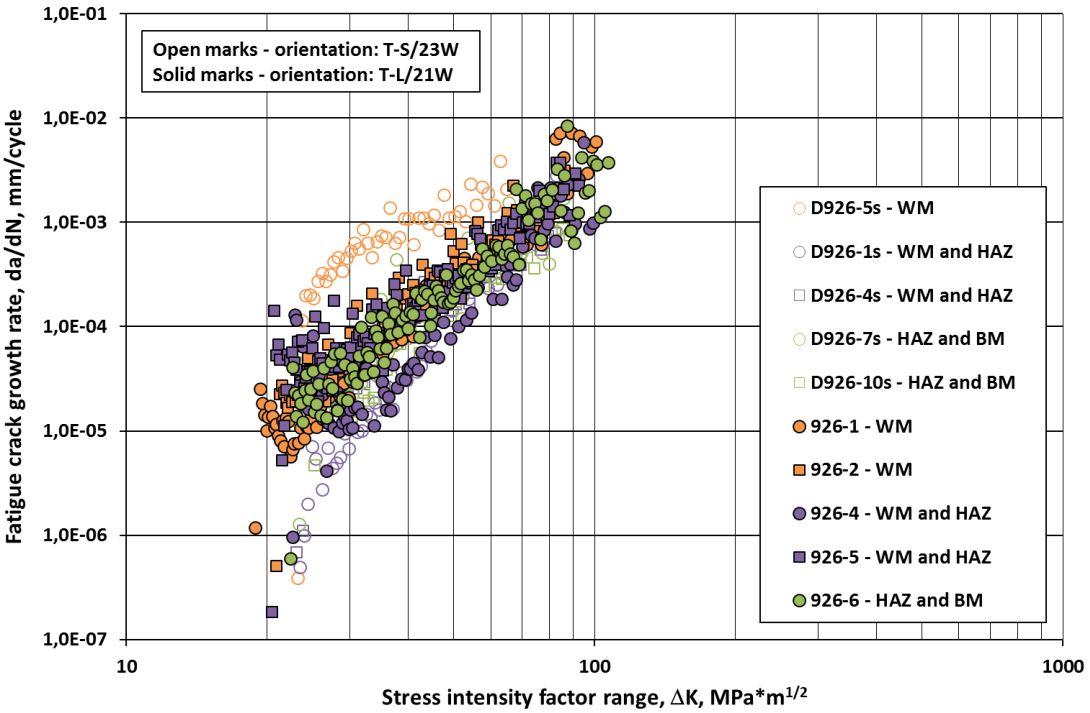

Fig. 7.11. Kinetic diagrams of FCG tests on Alform 960M / UNION X90 welded joints (altogether 10 specimens).

The constants (C and n) of the Paris-Erdogan relationship [73] were calculated using the least squares regression method. The data do not belong to the stage II of the kinetic diagram of

fatigue crack propagation have been eliminated during the least square regression analysis, for each specimen, systematically.

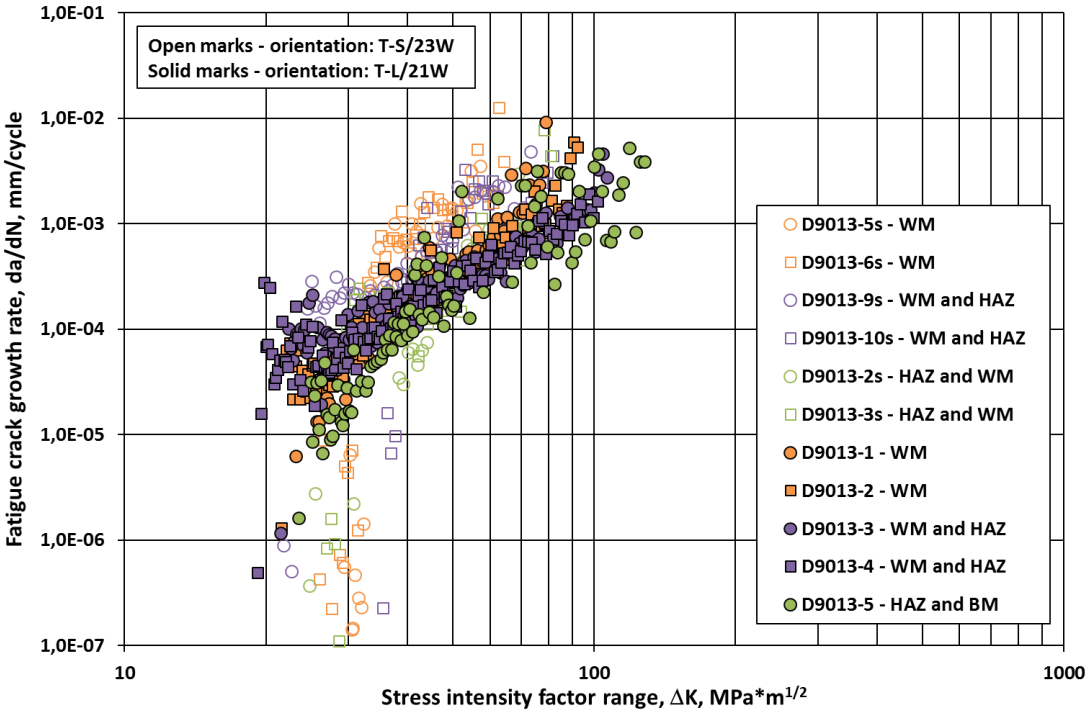

Fig. 7.12. Kinetic diagrams of FCG tests on Alform 960M / UNION X96 welded joints (altogether 11 specimens).

The fatigue fracture toughness (ΔK_{fc}) values were determined using the crack length on the crack front measured by stereo microscope. The calculated n, C and ΔK_{fc} values were summarized in Tables 7.1-7.3.

Table 7.1. FCG test results: Weldox 700E / UNIONX85/UNION X90, matching / overmatching, medium heat input

Specimen ID	**Crack path**	**n**	**C**	**Correlation coefficient**	**ΔK_{fc}**
		(mm/cycle, MPam$^{1/2}$)		**(–)**	**(MPam$^{1/2}$)**
Specimen location: T-S/23W					
D635-01	WM	3.30	5.23E-10	0.9549	91.3
D635-02	WM	3.21	8.03E-10	0.9496	76.2
D635-03	WM and HAZ	3.43	3.45E-10	0.9632	80.1
D635-04	WM and HAZ	3.27	4.62E-10	0.9205	82.1
D635-05	HAZ and BM	3.61	2.20E-10	0.9372	68.1
D635-06	HAZ and BM	2.94	2.13E-09	0.9309	82.9
Specimen location: T-L/21W					
D635-07	WM	3.44	4.42E-10	0.9454	95.7
D635-08	WM	2.97	2.72E-09	0.9274	96.0
D635-09	WM and HAZ	3.36	2.88E-10	0.9599	117.0
D635-10	WM and HAZ	2.76	5.07E-09	0.9285	98.8
D635-11	HAZ and BM	3.20	8.64E-10	0.9613	102.9
D635-12	HAZ and BM	2.94	2.23E-09	0.9354	100.0

Table 7.2. FCG test results: Alform 960M / UNION X90, undermatching, high heat input

Specimen ID	Crack path	n	C	Correlation coefficient	ΔK_{fc}
		(mm/cycle, MPam$^{1/2}$)		(–)	(MPam$^{1/2}$)
Specimen location: T-S/23W					
D926-5s	WM	2.108	3.605E-07	0.9134	66.9
D926-1s	WM and HAZ	5.122	2.450E-13	0.9768	86.2
D926-4s	WM and HAZ	3.282	4.885E-10	0.9549	88.5
D926-7s	HAZ and BM	3.298	5.483E-10	0.9202	92.5
D926-10s	HAZ and BM	3.982	2.709E-11	0.9642	91.9
Specimen location: T-L/21W					
D926-1	WM	3.855	6.831E-11	0.9795	103.1
D926-2	WM	3.362	6.727E-10	0.9727	87.8
D926-4	WM and HAZ	4.499	2.739E-12	0.9674	101.3
D926-5	WM and HAZ	3.024	2.372E-09	0.9446	94.4
D926-6	HAZ and BM	3.588	2.031E-10	0.9636	109.2

Table 7.3. FCG test results: Alform 960M / UNION X96, matching, high heat input

Specimen ID	Crack path	n	C	Correlation coefficient	ΔK_{fc}
		(mm/cycle, MPam$^{1/2}$)		(–)	(MPam$^{1/2}$)
Specimen location: T-S/23W					
D9013-5s	WM	3.075	7.816E-09	0.8141	67.6
D9013-6s	WM	3.281	4.266E-09	0.8266	66.2
D9013-9s	WM and HAZ	2.960	8.105E-09	0.9330	75.7
D9013-10s	WM and HAZ	2.530	3.834E-08	0.7156	84.0
D9013-2s	HAZ and BM	5.181	3.626E-13	0.9154	80.9
D9013-3s	HAZ and BM	2.348	3.152E-08	0.8080	83.5
Specimen location: T-L/21W					
D9013-1	WM	3.933	7.859E-11	0.9526	81.9
D9013-2	WM	3.104	1.678E-09	0.9666	94.1
D9013-3	WM and HAZ	2.331	2.983E-08	0.9579	108.7
D9013-4	WM and HAZ	2.564	1.106E-08	0.9670	104.1
D9013-5	HAZ and BM	3.365	3.709E-10	0.9056	131.3

Appendix A3 summarizes the statistical samples of Paris-Erdogan exponent values (n) and their characteristics.

7.3. Determination of fatigue crack propagation design or limit curves

Reliability of a structural element having crack or crack-like defect under cyclic loading conditions is determined by the geometrical features of the structural element and the flaws, the loading conditions, as well as the material resistance to fatigue crack propagation. There are different documents [94][95][96], standards and recommendations [96][97][98] containing fatigue crack propagation limit or design curves and rules for the prediction of the crack growth [98]. The background of the fatigue crack propagation limit curves and the calculations consist

of two basic parts: statistical analysis of numerous investigations (fatigue crack propagation tests) and fatigue crack propagation law, frequently the Paris-Erdogan law (see Equation (3.2)).

Kinetic diagrams of fatigue crack growth can be simplified and described using both simple and two-stage crack growth relationships, as it can be seen in Fig. 7.13, based on BS 7910 [98].

According to the main aim of our research work, the simple crack growth relationship was selected and used.

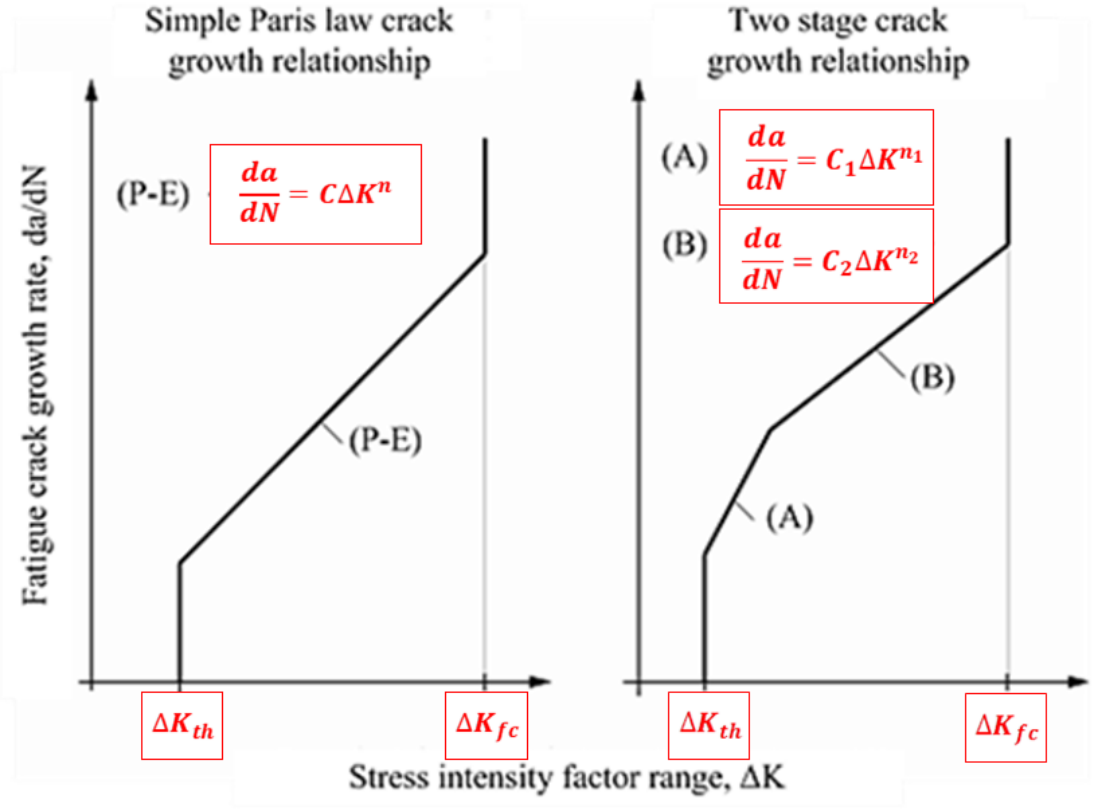

Fig. 7.13. Simple and two-stage fatigue crack growth relationships, based on [98].

Based on the experimental data and results, fatigue crack propagation limit curves can be determined. Generally, the determination of the fatigue design curves consists of six steps, as follows [99].

First step: determination of measuring values, the threshold stress intensity factor range (ΔK_{th}), if available, the two parameters of the Paris-Erdogan law (in our case C and n) and the fatigue fracture toughness (ΔK_{fc}).

Second step: classification of measured values into statistical samples, on the basis of calculated test results, applying Wilcoxon matched pairs test.

Third step: selection of the distribution function type using Shapiro-Wilk, Kolmogorov-Smirnov and chi square (χ^2) goodness of fit tests (testing if sample data fits a distribution from a certain population, i.e. a population with a normal or a Weibull distribution), at a level of significance $\varepsilon = 0.05$. After the analysis, it was concluded, that only the three parameter Weibull-distribution function is suitable for describing all the configured samples.

Fourth step: calculation of the parameters of the three parameter Weibull-distribution functions. The parameters of the distribution functions were calculated for all the configured samples using the

$$F(x) = 1 - \exp\left[-\left(\frac{x - N_0}{\beta} \right)^{1/\alpha} \right] \tag{7.1}$$

equation, where N_0 is the threshold parameter, α is the shape parameter and β is the scale parameter.

Fifth step: selection of the characteristic values of the distribution functions. Considering the influencing effects of the material parameters on the lifetime estimation, characteristic values of ΔK_{th}, n and ΔK_{fc} were selected. The threshold stress intensity factor range (ΔK_{th}) is that value which belongs to the 95% probability, the exponent of the Paris-Erdogan law (n) is that value which belongs to the 5% probability and the fatigue fracture toughness (ΔK_{fc}) is that value which belongs to the 5% probability of the relevant Weibull-distribution function. The Paris-Erdogan constant (C) can be calculated on the material group (in our case steels or more accurately high strength steel) dependent correlation between C and n. The described fifth step can be seen in Fig. 7.14, schematically.

Sixth step: calculation of the parameters of the fatigue crack propagation design or limit curves.

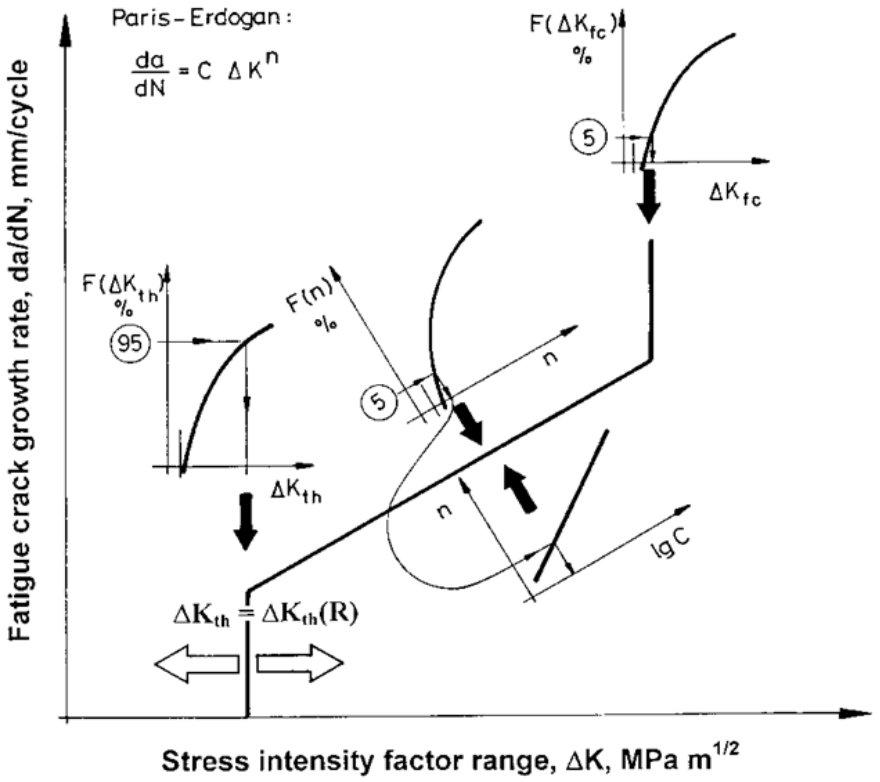

Fig. 7.14. The previously proposed method for determination of fatigue crack propagation limit curves [99].

Fig. 7.15 shows the connection between the Paris-Erdogan exponent (n) and constant (C) for the investigated welded joints, where the correlation index (0.9815) demonstrates close and reliable connection.

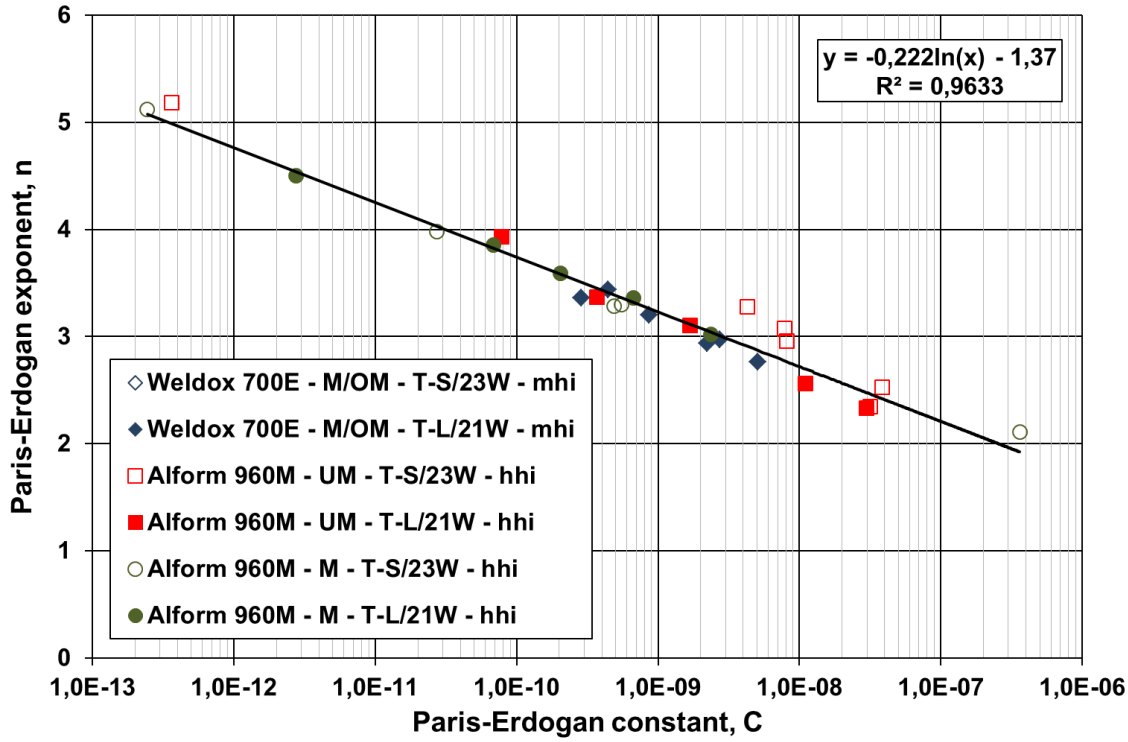

Fig. 7.15. Connection between the two parameters of Paris-Erdogan equation for the investigated welded joints.

The main characteristics of the determined fatigue crack propagation design or limit curves can be found in Table 7.4, using the data can be found in Appendix A3 too.

In those cases, when the orientation and/or the path of the propagating crack is known, the values in Table 7.4 can be directly used. In those cases, when n and ΔK_{fc} values calculated in different directions (T-L and L-T vs. T-S, or 21W vs. 23W) are significantly different, and the orientation and/or the growing crack path is not known, the lowest value should be considered from the related ones.

The unambiguous determination of the design curves in the near threshold region (near ΔK_{th}) is difficult. On the one hand, if the threshold stress intensity factor range value (ΔK_{th}) is not known, values can be found in the literature (e.g. [100][101][102]) are usable; furthermore, in special or particular cases, results of virtual testing [103] can be applied, too. On the other hand, the threshold stress intensity factor range value (ΔK_{th}), must be reduced by tensile residual stress field and may be increased by compressive residual stress field (e.g. welding residual stresses).

Fig. 7.16 and Fig. 7.17 summarize and demonstrate the calculated fatigue crack propagation design or limit curves for 690 MPa and 960 MPa strength categories, respectively.

Table 7.4. Characteristics of the determined fatigue crack propagation design or limit curves.

Base material	Mismatch type and heat input*	Orientation	n	C	ΔK_{fc}	Source
			(MPam$^{1/2}$, mm/cycle)		(MPam$^{1/2}$)	
Optim 700QL	M	T-S	1.20	6.52E-06	93	[14]
Weldox 700E	BM	T-L and L-T	1.70	8.09E-07	101	[9]
		T-S	1.50	2.06E-06	75	
	M	T-L/21W	4.10	1.12E-11	105	[9]
		T-S/23W	2.30	4.93E-08	80	
	OM	T-L/21W	1.85	4.02E-07	96	[9]
		T-S/23W	1.90	3.19E-07	61	
	M/OM	T-L/21W	2.67	8.88E-09	90	OWN
		T-S/23W	2.85	3.87E-09	67	
Weldox 960E	BM	T-S, L-S and T-L	1.80	3.50E-07	94	[103]
	M	T-L/21W and T-S/23W	2.75	1.03E-08	93	[104]
Alform 960M	BM	T-L and L-T	1.82	4.63E-07	116	[9]
		T-S	1.75	6.41E-07	87	
	UM	T-L/21W	2.40	3.10E-08	115	[105]
		T-S/23W	2.15	9.93E-08	67	
	UM – hhi	T-L/21W and T-S/23W	2.65	1.65E-08	81	OWN
	M	T-L/21W	1.90	3.19E-07	114	[9]
		T-S/23W	2.75	6.06E-09	82	
	M – hhi	T-L/21W and T-S/23W	2.25	9.45E-08	65	OWN

* Only high heat input (collective of linear energy and interpass temperature) was designated, hhi.

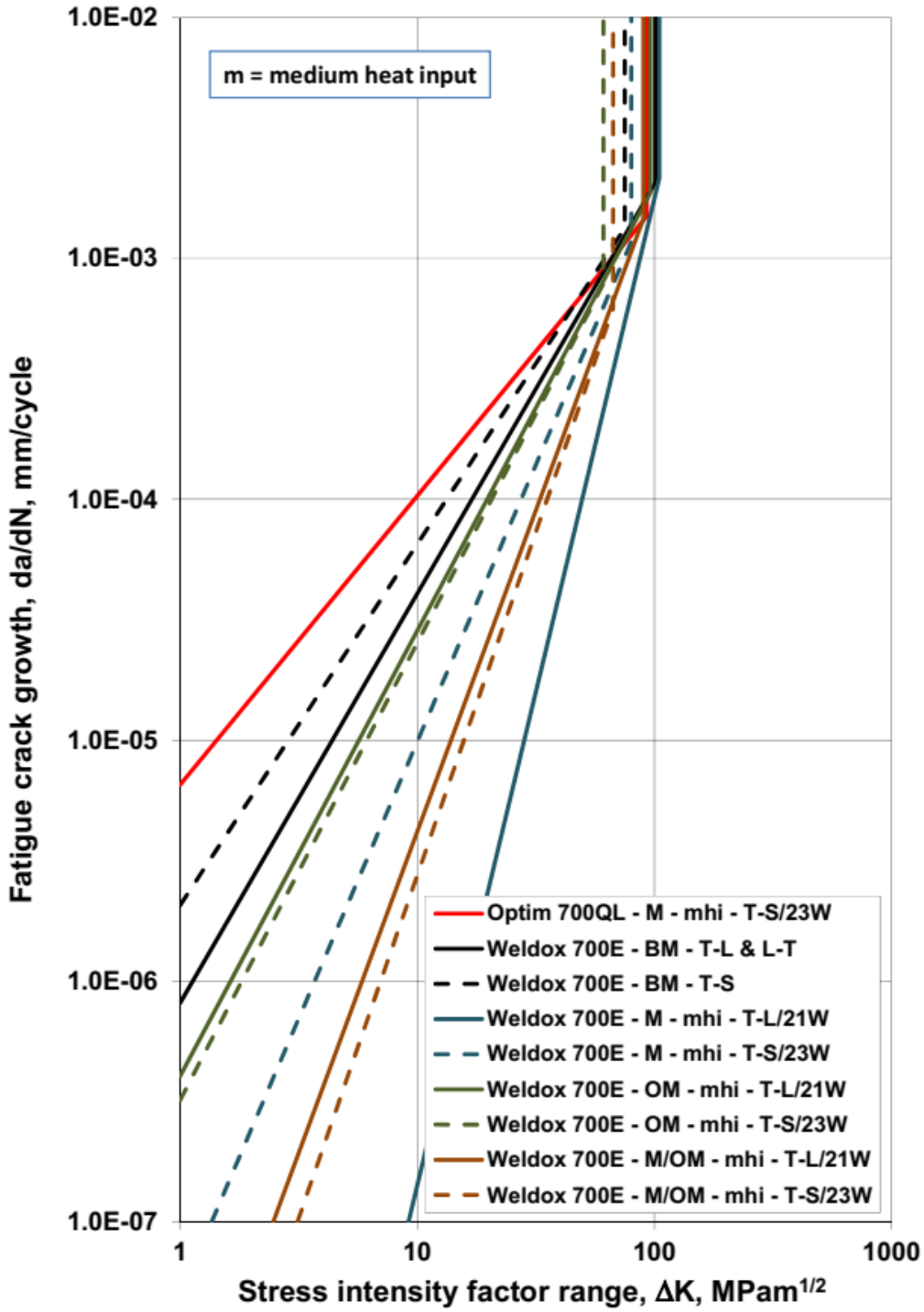

Fig. 7.16. Characteristics of the determined fatigue crack propagation limit curves for 690 MPa strength category.

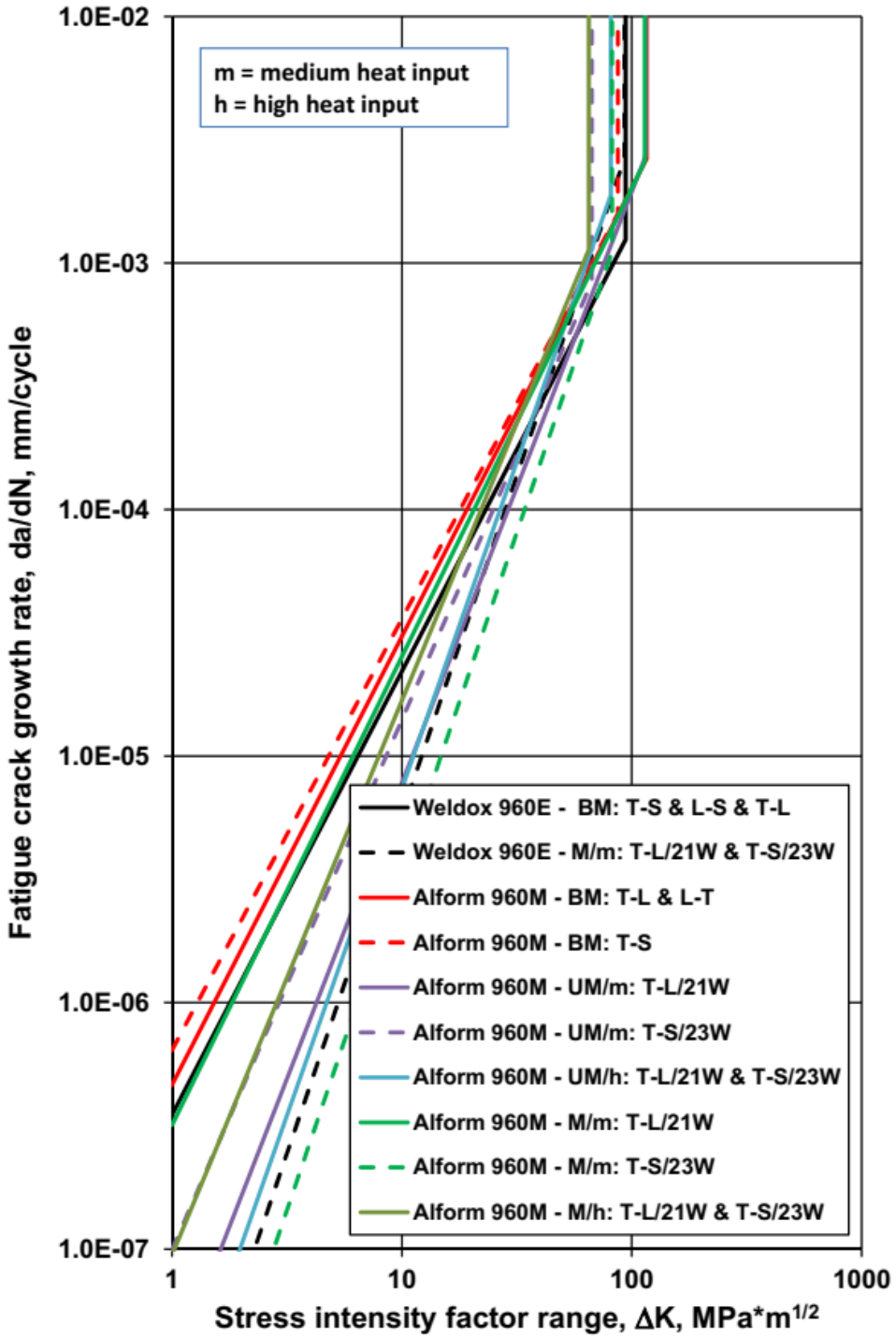

Fig. 7.17. Characteristics of the determined fatigue crack propagation limit curves for 960 MPa strength category.

7.4. Conclusion

Based on our investigations and their results, comparing them with previous researches, the following conclusions can be drawn:

– Applying the developed welding technologies eligible welded joints can be produced, where the appropriate quality contains the eligible resistance to fatigue crack propagation.

- The results of the executed investigations justified the necessity of statistical approaches, especially referring to the directions of the base materials (T-L, L-T, T-S and L-S) and the welded joints (21W and 23W), and the determination of the number of the tested specimens.
- The determined results fundamentally refer to reliable and reproducible examinations. Unfortunately, the standard deviation coefficients are in some cases too high (Paris-Erdogan exponent (n), T-S, 21W and 23W orientations).
- The mismatch phenomenon (matching (M), undermatching (UM) and matching/overmatching (M/OM)) has characteristic influence on the FCG resistance. The mismatch phenomenon has different influence on various crack paths or crack propagation directions. The reliability of the test results is different in case of different matching conditions.
- The average values of the Paris-Erdogan exponents (n) of Weldox 700E and Alform 960M base materials in the T-L and L-T directions and of the Weldox 960Q base material in the T-S and L-S directions are significantly not different, which means equal fatigue crack growth resistance in these orientations. The average values of the Paris-Erdogan exponent (n) of Weldox 700E and Alform 960M base materials in T-S orientation and of Weldox 960Q base material in the T-L orientation are significantly different. The fatigue crack growth resistance of the Weldox 700E material is more unfavourable in T-S direction. The material strength category (in our case 690 MPa or 960 MPa) and the production condition (in our case Q+T or TM) cause significant effect on the fatigue crack growth resistance, too.
- The average values of Paris-Erdogan exponents (n) of matching (M), overmatching (OM), matching / overmatching (M/OM) and undermatching (UM) conditions of the investigated welded joints were statistically higher than the exponents of the concerning base materials.
- The average value of the Paris-Erdogan exponent (n) of the overmatching (OM) welded joint of the Weldox 700E is lower than the exponent of both the matching (M) and the matching/overmatching (M/OM) conditions. It means that the matching/overmatching (M/OM) mismatch type is more beneficial than the overmatching (OM) type.
- The average value of the Paris-Erdogan exponent (n) of the matching (M) welded joint of Alform 960M is lower than exponent of the undermatching (UM) condition. The fatigue crack growth resistance under matching (M) condition is lower than undermatching (UM) condition.
- The heat input (collective of linear energy and interpass temperature) has characteristic influence on fatigue crack propagation resistance and the differences depend on the mismatch condition, which can be seen for Alform 960M welded joints in Fig. 7.18.

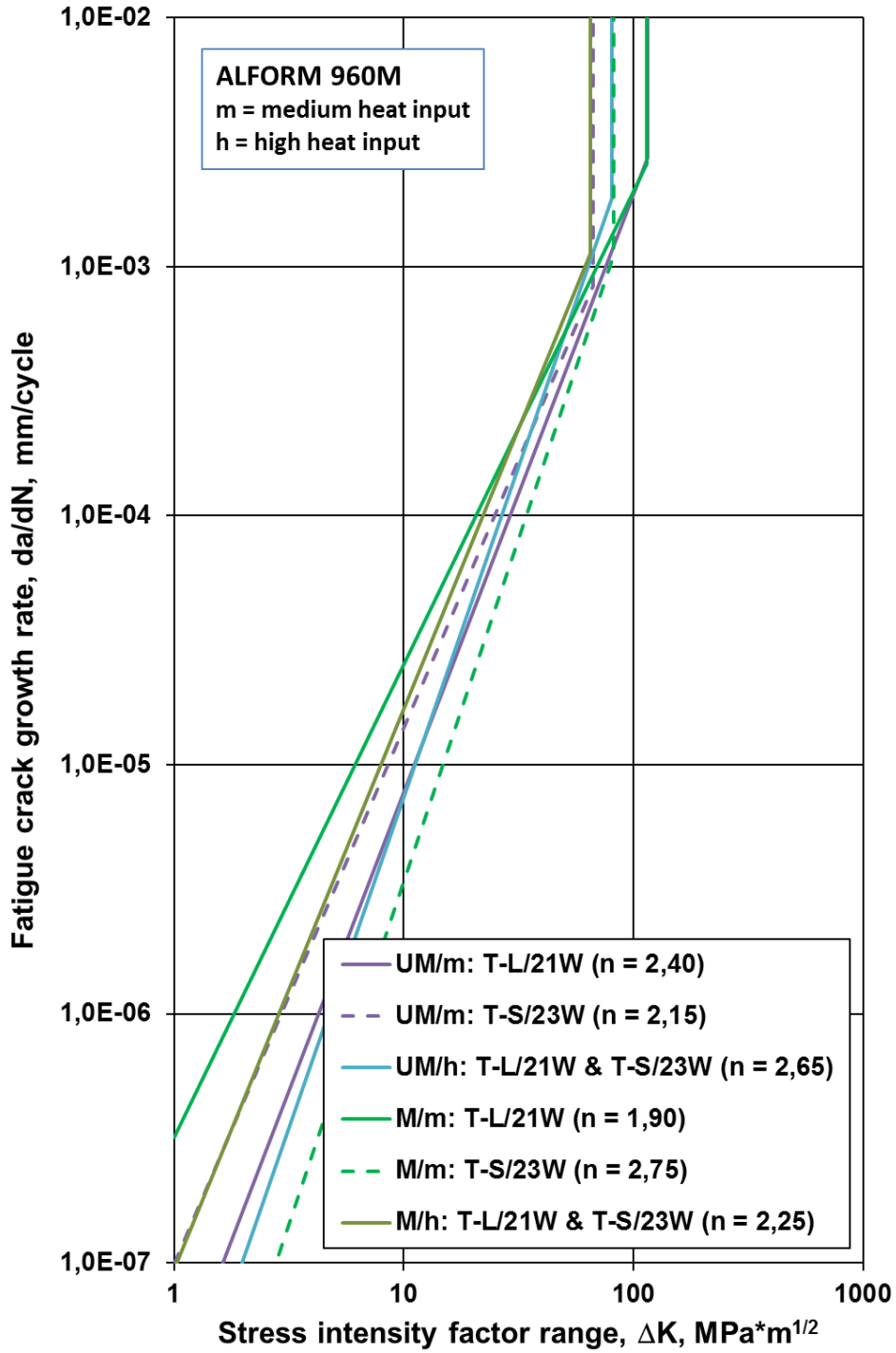

Fig. 7.18. Heat input (collective of linear energy and interpass temperature) influence on the determined fatigue crack propagation limit curves for ALFORM 960M welded joints: medium and high heat input.

Based on these results and the used methods fatigue crack propagation limit curves can be determined for the investigated high strength base materials and their gas metal arc welded joints, using simplified method [98]. The limit curves on the one hand correctly reflect the fatigue crack growth characteristics of both the base materials and the welded joints, on the other hand are usable for engineering critical assessment (ECA) and structural integrity calculations

8. THESES – NEW SCIENTIFIC RESULTS

T1. For reliable assessment of high cycle fatigue and fatigue crack growth resistance of high strength steels and their welded joints statistical approaches must be used. On the one hand, different crack paths and notch locations must be applied; on the other hand, sufficient number of specimens must be tested in order the correct applications of evaluation methods. I have proved this statement with executed and/or analysed high cycle fatigue and fatigue crack growth tests. (2) (3) (7) (10) (11) and (9)

T2. Both the high cycle fatigue and the fatigue crack growth resistance of the investigated high strength steels and their welded joints characteristically depend on the crack growth directions; the thickness direction is more unfavourable than the other directions. I have proved this statement with executed and/or analysed high cycle fatigue and fatigue crack growth tests. (4) (6) (10) (12) and (9)

T3. The linear energy and the interpass temperature during the welding of the thermomechanically rolled Alform 960M steel have collectively characteristic influence on the high cycle fatigue resistance of butt welded joints and the fatigue crack growth resistance of welded joints, which have to take into consideration during the specification of welding technology. I have proved this statement with executed and/or analysed high cycle fatigue and fatigue crack growth tests. (8) (10)

T4. With common application of the JSME investigation method resulting “Mean” S-N curves and “-2SD” philosophy, “Mean-2SD” S-N curves can be calculated, which can be used as high cycle fatigue strength curves. I have proved this statement with executed and/or analysed high cycle fatigue tests and with calculated “Mean” and “Mean-2SD” S-N curves. (7)

T5. The matching phenomenon has characteristic influence on the high cycle fatigue resistance of both Weldox 700E and Alform 960M high strength steel butt welded joints, depending on the strength category. In case of Weldox 700E the matching/overmatching (M/OM) condition is better than matching (M), while in the case of the Alform 960M the undermatching (UM) is better than matching (M). The statement justifies the specific role of the 690 MPa strength category in the mismatch phenomenon. I have proved this statement with executed and analysed high cycle fatigue tests. (2) (3) (4) (11)

T6. The mismatch phenomenon (matching (M), undermatching (UM), matching/overmatching (M/OM) and overmatching (OM)) has characteristic influence on the fatigue crack growth resistance of investigated high strength steel welded joints. The average values of Paris-

Erdogan exponents (n) of mismatch conditions of the investigated welded joints were statistically higher (Weldox 700E, Alform 960M thickness direction) or lower (Alform 960M longitudinal and transversal direction) than the exponents of the concerning base materials. I have proved this statement with executed and analysed fatigue crack growth tests. (6) (7) (8) (10) (12) and (9)

T7. The average value of the Paris-Erdogan exponent (n) of the matching/overmatching (M/OM) welded joint of Weldox 700E is lower than the exponent of both the overmatching (OM) and the matching (M) conditions; the matching (M) mismatch type is more efficient than both the overmatching (OM) and the matching/overmatching (M/OM) types. The average value of Paris-Erdogan exponent (n) of the matching (M) welded joint of Alform 960M is lower than the exponent of the undermatching (UM) condition and independent of the collective of linear energy and interpass temperature; the undermatching (UM) mismatch type is more efficient than the matching (M) type, independently of the collective of linear energy and interpass temperature. The statement justifies the specific role of the 690 MPa strength category in the mismatch phenomenon, too. I have proved this statement with executed and/or analysed fatigue crack growth tests. (5) (6) (10)

9. SUMMARY

The significant of the research work and the obtained results of the dissertation clarify that if we go back to the previous century then we can recognize and realize huge problems of applications and failures of the others and the most important is the big size of death of humans because of these problems and failures. There are many examples of accidents was occurred during the earlier period in many applications and in several countries (see section 3.1), but here I would like to mention one of the famous of these is "Aloha Airlines Flight 243 - Aircraft Accident" where the fatigue is 55% from total failure frequency of aircraft components. Due to of these accidents many humans losing life and also injure other many of them, as well as losing money from safety companies and manufacturing companies for these applications as well.

One of the important aims of this dissertation is how to develop a structure against fatigue problem. In an accurate sentence, we realized that the significant role of structural steel in manufacturing field and also during the previous study and literature survey we found limited knowledge and results about the new version of high strength structural steel experiments.

The processes of joining technology are one of the important methods applied in structural steel during their production and right now have many types. Since our work related with high strength structural steel which is used now in many applications (see section 2.3) and as it was mentioned earlier due to the knowledge limited and the necessity for new results of new types of structural steels due to appear new higher strength categories of structural steels. There is still a limited experiment in this field, and due to the required demand for new results of these new versions of structural steel categories as well as manufacturing of these types of steels is costly and the fatigue and then failure (God forbid!) is too complicated and tough because of the higher production cost, thus one of our research work to covered and supplied new information and results to support both of scientific research area and production field as well.

The two different categories of structural steels (690 MPa and 960 MPa) have different characteristics (see Figs. 2.1 and 2.2), where the weldability and the behaviour under cyclic loading conditions of quenched and tempered (Q+T) and thermomechanically rolled (TM) high strength steels, applied in medium plate thickness, are different.

One issue are weldability questions, so it can be stated, that these steels required a complex welding technology. The TM steels have favourable mechanical and toughness properties, furthermore, the weldability is much easier than the Q+T steels, because of the microstructure and the applied alloying elements (see Figs. 2.10 and 2.16). The other issue is a mismatching condition, so we used different cases (overmatching / matching / undermatching / merge of both matching/overmatching) because there are different characteristics of the investigated base materials and their welded joints due to different strength categories of both base materials with different mechanical properties of the filler materials that are available and approximately same (or harmony) with base materials specification which was used to prepare welded joints samples. Also, there are different heat input values, which were applied during welding aspect.

According to this variety in characteristics of base materials strength categories, filler metals properties and then different mismatching case of the welded joints as well as different heat input applied during welding aspect, then obviously many different results obtained during many investigations. Since the base materials and then welded joints what was cut by water jet from whole samples were investigated to evaluate and assess the result of the investigations.

The statistical data of fracture damages of engineering structures is noteworthy: 59% during high cycle fatigue (HCF) and fatigue crack growth (FCG) from all other types of failure in the structures. Thus the importance of the investigation and evaluation is to describe, predicate and recognise the results for the whole welded structure by investigating small specimens (before applying in real structure i.e. mobile crane, shovel, excavators, ship, offshore and so on) to avoid consuming time and reduce raw materials consumption and then cost reduction. Also, the handling with specimens is easier than the whole structure in the fact not just because of the small size of specimen just but also it easier to dominate on surrounding condition of the experimental field for these specimens.

It was shown, that the HCF properties of the examined base materials are always succeeded in the welded joints properties. In the case of lower cyclic numbers (under 2×10^5 cycles) with higher loading condition, the overmatching welded joints have worse fatigue properties than the matching joints; while in case of higher cyclic numbers, the overmatching joints had the better properties. So when the loading of the welding joint is not so high, the fatigue crack initiation and propagation is more difficult, while in case of higher loading, the more brittle behaviour of the overmatching filler metal is the determinant. In the case of Alform 960M base material, with the increases of the heat input, the HCF limit is increased as well, while the mechanical properties practically remained the same. One possible explanation for this is the grain size changes; with the high heat input caused coarse grain microstructure the cracks can be propagated with large difficulties, so the fatigue limit can be increased.

The FCG experiments show, that in the case of Weldox 700E and Alform 960M base materials, the crack growth is significantly same in the L-T and T-L directions, but significantly different in the T-S direction. In the case of the welded joints, the crack growths are significantly different from the base materials, in both directions and all of the matching circumstances. The FCG resistance of the welded joints is the same the examined 21W and 23W orientations, in three cases, but the Alform 960M matching welded joint has different properties. The fatigue fracture toughness value is smaller in the 23W direction, in all of the welded joints. The fatigue fracture toughness value of the Weldox 700E welded joints is higher than the same of the base material, while the Alform 960M welded joints value is lower than the base material. Overall, it can be summarised, that the Weldox 700E matching welded joint has better FCG properties than the overmatching joint, and the Alform 960M undermatching welded joints have better properties than the matching joints, independently of the orientations.

Based on the measured, calculated and analysed results, both high cycle fatigue strength and fatigue crack propagation design curves were developed for the investigated high strength steels and their GMAW joints. The curves can be applied during the whole lifetime of cyclic loaded structural elements and structures.

Finally, our obtained results were compared with other previous results and we have published and it demonstrates more reliable, acceptable and satisfying and there are seven new scientific results (see section 8) in this field, so these are justified the importance of many experiments during the research to reach the higher quality results.

10. APPLICATION POSSIBILITIES OF THE RESULTS

Nowadays, the reliability of a structural element or a structure is one of the most important, if not the most important feature of the structural element or the structure itself. This is a requirement on the one hand; on the other hand, this is a task for the structural and technological designers, manufacturers, operators and maintainers of the structure. The regrettable accidents always draw attention to this fact, and summary studies about these form global messages from which all stakeholders can learn.

At the same time, the behaviour of HSSS differs fundamentally from that of conventional steels, both as a result of manufacturing technologies and in static and dynamic stresses. As a result, it is not possible to make general recommendations for all high strength steels. Therefore, one of the basic aims of this dissertation is to summarize knowledge that provides useful information to industry professionals by experimenting multi (mismatching and heat input) with different characteristics of BM and FM. The data and case studies presented in the sections on the determination of welding working ranges can provide useful insights for engineers manufacturing welded structures.

There are different characteristics of HSSS friend of the environment and then achieve sustainable development, as follows. Economy: by increasing the strength of steel, then the structural section can be reduced by 20 to 30%. Architecture: by reducing the size of structural elements with higher-performing steel products, strong, thin and lightweight. Environment (resources): by construction with less steel, reduced consumption of our world's scarce resources. Safety: by ensured high safety of the structures both in the fabrication and application.

Significant reduction of the structure's dead weight, material and labour consumption are the main advantages of using these steels. They influence economic and operational efficiency by reducing the costs of production, operating and maintenance. Further development of the innovative HSSS, determination of their performance and improvement joining technology are associated with the necessity to perform further studies.

Survive of structures against different hard weather conditions without or less repairing process it's also achieved by obtained results which will also help for conservative raw materials in nature and decrease production cost.

High performance is obtained of these new generations of high strength steel categories of welded joints in many application fields than these previous applications of lower steel categories. Also continuous and survival HSSS applications for the long term than the previous other applications. Thus the results increased performance of applications i.e. ships, offshore, heavy vehicle equipment and machinery now are better than old applications.

In predominantly cases, service loads have variable characteristics. For this reason, it is necessary to perform numerous investigations of the HSSS welded joints determining their mechanical properties, especially fatigue characteristics and behaviour. During the research, despite a large number of experiments and specimens, it was not possible to fully investigate the

steels. Fatigue strength and limit curves were determined for the conditions of HCF and FCG, for both investigated base materials and welded joints, and for each mismatch. Fatigue strength curves were calculated for comparative materials, too. These boundary curves, in their specific or generic form, can be used to evaluate the integrity of welded structures, estimate lifetime and/or residual lifetime, and perform comparative calculations. These curves carry important data and information for the interested researchers, manufacturing companies and so on.

The materials from the grade of HSSS are increasingly used in welded structures e.g. telescopic jibs and chassis of mobile cranes, gantries frames, pressure vessels, offshore platforms or bridge structures including the military mobile bridges. For example, in the vehicle industry, one of the fundamental trends in the environmental load reduction through weight reduction, this can be achieved by the application of high strength materials.

The publishing results via articles of researchers, dissertations of both masters and PhD students as well as different of other studies have a contributing role to start a new generation of manufacturing with new joining welding technology applied on higher steel categories these make our life more pleasant and easier.

The importance of investigation and then the results obtaining for welded joints specimens what was studied in two different categories and comparison with previous investigated work is necessary during mismatch phenomenon of welded joints which characteristic influence both on the HCF and on the FCG resistance. Thus in case of different matching conditions, the reliability of the test results will be different, and this justifies the necessity of applying many experimental investigation works to collect more reliable results which will serve the people who are interested with this science area, and finally developing of application field and enhance the products.

Welding technology is improved by supporting these results which applied for joining HSSS in different types of applications and by developing the characteristics of welding aspect and testing methodology so the results of researchers or manufacturing products will be in higher level in the near future. Applying the developed welding technologies adequate with HSSS base materials produced, appropriate quality contains the eligible resistance to HCF and FCG.

The results of researcher help reduce the number of pieces of equipment working in the projects like the increase in the capacity of the loader, shovel and cranes using higher steel categories with developed welding process help decreasing the number of them in the working land.

Increasing productivity of buildings and towers by the increasing number of floors and length of towers using the new results of welded of high strength steel categories in construction of these buildings and towers and then increases green land and supporting sustainable development issue.

Miskolc, 12th June 2020

Haidar Faisal Helal Mobark
Agriculture and Machinery Equipments Engineering Techniques (BSc)
Machine Design (MSc)

ACKNOWLEDGEMENTS

First of all, I am thankful to Allah, for everything He gave me, for everything He did not give me, for everything He protected me from that which I know and that which I am not even aware of, thanks for blessings that I did not even realize were blessings much more than I deserve, and thanks for everything else because no matter how many things I try to list, I cannot even come close to thanking Him enough. The one who is most deserving of thanks and praise from people is Allah, may He be glorified and exalted, because of the great favours and blessings that He has bestowed upon His slaves in both spiritual and worldly terms. Allah has commanded us to give thanks to Him for those blessings, and not to deny them. ”my success is only by blessings of Allah”.

I would like to say a big thank you for all Ahl al-Bayt, the “People of the House”, or the family of Messenger Muhammad and they are successors of Messenger Muhammad. I requested them many times to solve different of my problems and the solutions occur by their good and blessings of them from Allah.

I would like to thank my supervisor, Dr. János Lukács, professor for his help in the dissertation's professional content, his continuous guidance, his constructive critical comments, and his many years of active joint publishing. In particular, I would like to emphasize your help in the areas of high-cycle fatigue tests and fatigue crack testing, where he assisted in the evaluation of the results with his extensive professional consultation.

I am grateful to Dr. Ádám Dobosy, a distinguished university teacher for his help in carrying out welding processing of high strength steel. I would like to emphasize his tireless work with which he regularly helped me in mechanical properties tests and welding aspects.

I would like to express my gratitude to my all respected teachers who they thought me different subjects during 2nd and 3rd semesters, they are Dr. András Balogh (Welding process and welding technology), Dr. Mihály Komócsin (Welding Theory) and Dr. Marcell Gáspár (Weldability), for whom I owe my commitment to teach me welding processing and they develop my knowledge in welding of steel.

I would like to thank Prof. Dr. Miklós Tisza, who, as head of the institutional department and previous head of the István Sályi Doctoral School of Mechanical Sciences, he is my teacher during the 1st semester taught me (Fundamentals of Materials Science). And also I do not forget my thank you to the current head of the István Sályi Doctoral School of Mechanical Sciences Prof. Dr. Gabriella Vadaszne Bognar.

I would like to express my gratitude to the workshop and laboratory staff at the Institute of Materials Science and Technology. I would like to highlight András Petrovics a welder without whom the welding experiments would not have been possible. I would like to thank the workshop manager Sándor Kecskés-Kristóf for his precise work, who provided tremendous help in the production of specimens. Thanks are due to László Szentpéteri and Géza Csukás for their

assistance in carrying out long and laborious measurements, and for Ágnes Csurilláné Balogh for her contribution in the preparation of abrasives and shooting digital photos.

I would also like to thank the colleagues of my agriculture college, Dr. Ali Fadhel Merjan, Dr. Ehab Kareem Al-hilly, Mr. Kazem Mahdi Al-saffar, who contributed guarantee command of a financial affair to issue of my scholarship.

And last but not least, I would like to thank my parents, my sisters and brother, special thanks to my wife and kids too for their patience and resistant because they have missed me a lot, also my wife family, all of my uncles, aunts and cousins, relatives and friends for their versatile support during my studies and preparation of my PhD dissertation.

I would like to thank Stipendium Hungaricum Scholarship for this chance by covered the academic courses fee and the living costs and for their cooperation to receive admission at the University of Miskolc to complete my PhD study in Hungary.

Some publications were carried out as part of the EFOP-3.6.1-16-2016-00011 “Younger and Renewing University – Innovative Knowledge City – institutional development of the University of Miskolc aiming at intelligent specialization” project implemented in the framework of the Széchenyi 2020 program. The realization of this project is supported by the European Union, co-financed by the European Social Fund.

DEDICATION

“To All of My Dears and Lovers”

“Rasul Allah Muhammad Ibn Abdullah Ibn Abd Al-Muttalib Khatam Al-Anbia”

“Umm Abiha Al-Zahra Fatimah Bint Muhammad Sayyidat Al-Nisa”

“Imam Ali Ibn Abi Talib Amir al-Mu'minin”

“Imam Al-Hasan Ibn Ali Al-Mujtaba”

“Imam Al-Husayn Ibn Ali Sayyid Ash-Shuhada”

“Imam Ali Ibn Husayn Al-Sajjad”

“Imam Muhammad Ibn Ali Baqir Al-Ulum”

“Imam Ja'far Ibn Muhammad As-Sadiq”

“Imam Musa Ibn Ja'far Al-Kazim”

“Imam Ali Ibn Musa Ar-Rida”

“Imam Muhammad Ibn Ali Al-Jawad”

“Imam Ali Ibn Muhammad Al-Hadi”

“Imam Hasan Ibn Ali Al-Askari”

“Imam Al-Zaman Hujjat Allah Ibn Al-Hasan Muhammad Al-Mahdi Baqiyyat Allah and His Mother Madam Narjis”

“Qamar Bani Hashim Al-Abbas Ibn Ali and His Mother Madam Umm Ul-Banin”

“Grand Ayatollah Al-Sayyid Ali Al-Husseini Al-Sistani”

REFERENCES

[1] W. Schütz: *A history of fatigue*, Journal of Engineering Fracture Mechanics, Vol. 54, No. 2, pp. 263-300, 1996.

[2] P. C. Paris, M. P. Gomez, W. E. Anderson: *A rational analytic theory of fatigue*, The Trend in Engineering 13, pp. 9-14, 1961.

[3] D. Schroepfer, T. Kannengiesser: *Stress build-up in HSLA steel welds due to material behavior*, Journal of Materials Processing Technology, Vol. 227, pp. 49-58, 2016.

[4] T. Lausch, T. Kannengiesser, M. Schmitz-Niederau: *Multi-axial load analysis of thick-walled component welds made of 13CrMoV9-10*, Journal of Materials Processing Technology, Vol. 213, pp. 1234-1240, 2013.

[5] D. Schroepfer, A. Kromm, T. Kannengiesser: *Improving welding stresses by filler metal and heat control selection in component-related butt joints of high-strength steel*, Welding in the World, Vol. 59, No. 3, pp. 455-464, 2015.

[6] S. Ravi, V. Balasubramanian, S. Nemat Nasser: *Effect of mis-match ratio (MMR) on fatigue crack growth behaviour of HSLA steel welds*, Engineering Failure Analysis, Vol. 11, No. 3, pp. 413-428, June 2004.

[7] H. F. H. Mobark, J. Lukács: *Mismatch effect influence on the high cycle fatigue resistance of S690QL type high strength steels*, 2nd International Conference on Structural Integrity and Durability, Dubrovnik, Croatia, October 2-5, 2018.

[8] J. Kömi: *Hot-rolled ultra-high-strength steels of Ruukki trainers' training*, Raahe, Finland, June 14, 2011.

[9] Á. Dobosy: *Design limit curves for cyclic loaded structural elements made of high strength steels*, PhD Thesis, István Sályi Doctoral School of Mechanical Engineering Sciences, University of Miskolc, Miskolc, 2017 (In Hungarian).

[10] M. Gáspár.: *Welding technology development of Q+T high strength steels based on physical simulation*, PhD Thesis, István Sályi Doctoral School of Mechanical Engineering Sciences, University of Miskolc, Miskolc, 2016 (In Hungarian).

[11] St. Weglowski, M.: *Modern toughened steels – their properties and advantages*, Biuletyn Instytutu Spawalnictwa, No. 2, pp. 25-36, 2012.

[12] K. Richter, F. Hanus, P. Wolf: *Structural steels of 690 MPa yield strengths – A state of art*, High Strength Steel for Hydropower Plants Conference, Graz, 2005.

[13] M. Gáspár, A. Balogh: *GMAW Experiments for advanced (Q+T) high strength steels*, Production Processes and Systems, Vol. 6, No. 1, pp. 9-24, 2013.

[14] A. Balogh, J. Lukács, I. Török (Eds.): *Weldability and the properties of welded joints*, University of Miskolc, Miskolc, 324 p, 2015 (In Hungarian).

[15] J. Kerns: *Advances in metals pave way to lighter vehicles*, Machine Design, Vol. 87, pp. 36-43, (2015).

[16] https://www.machinedesign.com/metals/advances-metals-pave-way-lighter-vehicles

[17] http://www.sagesteelltd.com/dl/Alform/Alform%202016.pdf
[18] M. Fiedler et al.: *The Alfrom welding system. The world first system for high-strength welded structures*, Proceedings of IIW International Conference, Paper IIW 2015 1504, pp. 1-5, 2015.
[19] www.voestalpine.com/grobblech
[20] K. Tatsumi, Y. kouki, A. Hidemi: *Development of high strength H-shapes with excellent toughness manufactured by advanced Thermo-Mechanical Control Process (TMCP)*, Originally Published in JFE Giho No. 16, pp. 30-35, 2011.
[21] M. Toyosada: *Characteristics of TMCP steels and their welded joints used for hull structures*, Proceeding of The Twelfth International Offshore and Polar Engineering Conference, Kitakyuyushu, Japan, 2002.
[22] S. Nobuo, M. Shinji, E. Shigeru: *Recent development in microstructural control technologies through the Thermo-Mechanical Control Process (TMCP) with JFE steel's high-performance plates*, JFE Technical Report, No. 11, 2008.
[23] R. Laitinen: *Welding of high and ultra high strength steels. trainers' training*, Raahe, Finland, June 14, 2011.
[24] H. F. H. Mobark, Á. Dobosy, J. Lukács: *Mismatch effect influence on the HCF resistance of high strength steels and their GMA welded joints*, Vehicle and Automotive Engineering 2 (VAE 2), pp. 755-767, 2018.
[25] R. J. M. Pijpers, et al.: *Fatigue experiments on very high strength steel base material and transverse butt welds*, Advanced Steel Construction Vol. 5, No. 1, pp. 14-32, 2009.
[26] N. Baluch, Z. M. Udin, C. S. Abdullah: *Advanced high strength steel in auto industry*, An Overview Engineering Technology and Applied Science Research, Vol. 4, No. 4, pp. 686-689, 2014.
[27] E. Kalácska, et al.: *MIG-welding of dissimilar advanced high strength steel sheets*, Materials Science Forum, Vol. 885, pp. 80-85, 2017.
[28] K. Májlinger, E. Kalácska, P. R. Spena: *Gas metal arc welding of dissimilar AHSS sheets*, Materials and Design, Vol. 109, pp. 615-621, 2016.
[29] P. Collin, et al.: *Undermatching butt welds in high strength steel*, International Association for Bridge and Structural Engineering, 2009.
[30] Z. Barsoum, M. Khurshid: *Ultimate strength capacity of welded joints in high strength steels*, 2nd International Conference on Structural Integrity, 4-7 September 2017, Funchal, Madeira, Portugal, Procedia Structural Integrity, Vol. 5, pp. 1401-1408, 2017.
[31] J. N. Dupont, S. Babu, S. Liu: *Welding of materials for energy applications*, The Minerals, Metals and Materials Society and ASM International 2013, Metallurgical and Materials Transactions A, Vol. 44a, pp. 3385-3410, 23 February, 2013.
[32] B. Jonsson, et al.: *Implementing high frequency mechanical impact in industrial components: A case study*, 5th Fatigue Design Conference, Procedia Engineering Vol. 66, pp. 202-215, 2013.
[33] Strategic Research Agenda: *A vision for the future of the steel sector*, 2nd ed. European Steel Technology Platform (May 2013). https://www.estep.eu/assets/SRA-2013.pdf, last accessed 2019/09/28.
[34] D. A. Porter: *Weldable high-strength steels: challenges and engineering applications*, Portevin lecture, IIW 2015 International Conference on High Strength Steels –

Challenges and Applications, Helsinki, Finland, 2-3. July 2015, Paper IIW 2015 0102 13p.

[35] Á. Dobosy, J. Lukács: *The effect of the welding parameters on the properties of the thermomechanically rolled high strength steels*, The Publications of the MultiScience - XXX. microCAD International Multidisciplinary Scientific Conference, University of Miskolc, Paper D2_3. 8 p, 2016.

[36] AWS D1.1/D1.1M:2015: *Structural Welding Code – Steel*. 23rd Edition, American Welding Society.

[37] Metals Handbook, Vol. 6: *Welding, Brazing and Soldering*. ASM International, USA (1995).

[38] J. Górka: *Effect of repair welding on the properties of welded joints of steel S700MC*, International Journal of Engineering Science and Innovative Technology (IJESIT), Vol. 2, No. 5, September 2013.

[39] S. Ravi, et al.: *Assessment of some factors influencing the fatigue life of strength mis-matched HSLA steel weldments*, Materials and Design Vol. 25, No. 2, pp. 125-135, April 2004.

[40] A. J. R. Loureiro: *Effect of heat input on plastic deformation of undermatched welds*, Journal of Materials Processing Technology, Vol. 128, No. 1-3, pp. 2490-2496, October 2002.

[41] M. Mirzaei, et al.: *Study of welding velocity and pulse frequency on microstructure and mechanical properties of pulsed gas metal arc welded high strength low alloy steel*, Materials and Design, Vol. 51, pp. 709-713, October 2013.

[42] K. Devakumaran, M.R. Ananthapadmanaban, P.K. Ghosh: *Variation of chemical composition of high strength low alloy steels with different groove sizes in multi-pass conventional and pulsed current gas metal arc weld depositions,* Defence Technology, Vol. 11, No. 2, pp. 147-156, June 2015.

[43] P. Collin, B. Johansson*: Design of welds in high strength steels*, Proceedings of the 4th European Conference on Steel and Composite Structures, Maastricht, Vol. C, pp.89-98, 2005.

[44] E. Harati, et al.: *Applicability of low transformation temperature welding consumables to increase fatigue strength of welded high strength steels,* International Journal of Fatigue, Vol. 97, pp. 39-47, April 2017.

[45] M. Stoschka, et al.: *Effect of high-strength filler metals on fatigue*, Welding in the World, Vol. 56, No. 3-4, pp. 20-29, March 2012.

[46] M. Stoschka, et al.: *Effect of high-strength filler metals on the fatigue behaviour of butt joints*, Welding in the World, Vol. 57, No. 1, pp. 85-96, February 2013.

[47] W. Guo, et al.: *Comparison of microstructure and mechanical properties of ultra-narrow gap laser and gas-metal-arc welded S960 high strength steel*, Optics and Lasers in Engineering, Vol. 91, pp. 1-15, April 2017.

[48] W. Guo, et al: *Microstructure and mechanical properties of laser welded S960 high strength steel*, Materials and Design, Vol. 85, No. 15, pp. 534-548, November 2015.

[49] M. Gáspár, R. P. S. Sisodia: *Weldability analysis of Q+T and TMCP high strength steels by physical simulation*, Proceedings of IIW International Conference, pp. B166-B170, Shanghai, P.R. China, 29-30 June 2017.

[50] D. Radaj: *Review of fatigue strength assessment of nonwelded and welded structures based on local parameters*, International Journal of Fatigue Vol. 18, No. 3, pp. 153-170, April 1996.

[51] J. Schijve: *Predictions on fatigue life and crack growth as an engineering problem. A state of the art survey*, 6th International Fatigue Congress, Berlin, 6-10 May 1996. Eds.: G. Lütjering, H. Nowack, Elsevier, 1996. Vol II, p. 1149-1164.

[52] J. C. Jr. NEWMAN: *The merging of fatigue and fracture mechanics concepts: a historical perspective. Fatigue and Fracture Mechanics*, 28th Volume, ASTM STP 1321. Eds.: J. H. Underwood, B. D. Macdonald, M.R. Mitchell, American Society for Testing and Materials, 1997. p. 3-51.

[53] R. I. Stephens, et al.: *Metal Fatigue in Engineering*, John Wiley & Sons, Inc., 2001. (ISBN 0-471-51059-9)

[54] H. Naubereit, J. Weihert: *Einführung in die Ermüdungsfestigkei,* Carl Hanser Verlag, München - Wien, 1999. (ISBN 3-446-21028-8).

[55] Y. L. Lee, et al.: *Fatigue testing and analysis (Theory and Practice.),* Elsevier Butterworth-Heinemann, 2005. (ISBN-10: 0-7506-7719-8)

[56] C. M. Sonsino: *Effect of residual stresses on the fatigue behaviour of welded joints depending on loading conditions and weld geometry*; Part of special issue: Fatigue assessment of welded connections, International Journal of Fatigue, Vol. 31, No. 1, pp. 88-100, January 2009.

[57] M. J. Ottersböck, et al.: *Effect of weld defects on the fatigue strength of ultra high-strength steels*, Procedia Engineering, XVIII. International Colloquium on Mechanical Fatigue of Metals, Gijón (Spain), Vol. 160, pp. 214-222, September 5-7, 2016.

[58] T. Nykänen, T. Björk: *A new proposal for the assessment of fatigue strength of steel butt welded joints improved by peening*, IIW International Conference, High-Strength Materials - Challenges and Applications, 2-3 July 2015, Helsinki, Finland, 2015.

[59] T. Teng, C. Fung, P. Chang: *Effect of weld geometry and residual stresses on fatigue in butt-welded joints*, International Journal of Pressure Vessels and Piping, Vol. 79, No. 7, pp. 467-482, July 2002.

[60] A. A. Bhatti, et al.: *Fatigue strength improvement of welded structures using new low transformation temperature filler materials*, 5th Fatigue Design Conference, Fatigue Design 2013, Procedia Engineering, Vol. 66, pp. 192-201, 2013.

[61] C. M. Sonsino, T. Łagoda, G. Demofonti: *Damage accumulation under variable amplitude loading of welded medium- and high-strength steels*, International Journal of Fatigue, Vol. 26, No. 5, pp. 487-495, May 2004.

[62] K. J. Kirkhope, et al.: *Weld detail fatigue life improvement techniques. Part 1: review*, Marine Structures, Vol. 12, No. 6, pp. 447-474, July 1999.

[63] S. Cicero, et al.: *Definition of BS7608 fatigue classes for structural steels with thermally cut edges*, Journal of Constructional Steel Research, Vol. 120, pp. 221-231, April 2016.

[64] M. Leitner: *Influence of effective stress ratio on the fatigue strength of welded and HFMI-treated high-strength steel joints*, International Journal of Fatigue, Vol. 102, pp. 158-170, September 2017.

[65] H. Nakazawa, S. Kodama: *Statistical S-N testing method with 14 specimens: JSME standard method for determination of S-N curves*. In: T. Tanaka, S. Nishijima, M. Ichikawa, (Eds.) Statistical research on fatigue and fracture. Current Japanese materials

research, Vol. 2, pp. 59-69, Elsevier Applied Science and The Society of Materials Science, Japan, 1987.

[66] S. Chattopadhyay: *Design fatigue curves based on small crack growth and crack closure*, Journal of Applied Science and Engineering Technology 2008, pp. 9-15, ISSN Print: 1939-8565.

[67] C. Ni, L. Hua, X. Wang: *Crack propagation analysis and fatigue life prediction for structural alloy steel based on metal magnetic memory testing*, Journal of Magnetism and Magnetic Materials, Vol. 462, pp. 144-152, September 2018.

[68] J. L. Otegui, U. H. Mohaupt, D. J. Burns: *Effect of weld process on early growth of fatigue cracks in steel T joints*, International Journal of Fatigue, Vol. 13, No. 1, pp. 45-58, January 1991.

[69] A. C. Pickard: *Component lifing. Materials Science and Technology*, Vol. 3, pp. 743-749, September 1987.

[70] J. Lukács: *Reliability of cyclic loaded welded joints having cracks*, CSc dissertation, Miskolc-Budapest, 1992.

[71] J. Lukács: *Structural integrity, PhD lecture, 5th lecture*, University of Miskolc, 2018.

[72] M. Klesnil, P. Lukas: *Effect of stress cycle asymmetry on fatigue crack growth*, Materials Science and Engineering, No. 9, p. 231-240, (1972).

[73] P. Paris, F. Erdogan: *A critical analysis of crack propagation laws*, Journal of Basic Engineering, Transactions of the ASME, pp. 528-534, December 1963.

[74] R. G. Forman, V. E. Kearney, R. M. Engle: *Numerical analysis of crack propagation in cyclic-loaded structures*, Journal of Basic Engineering, Transactions of the ASME, pp. 459-464, September 1967.

[75] R. T. Yekta, K. Ghahremani, S. Walbridge: *Effect of quality control parameter variations on the fatigue performance of ultrasonic impact treated welds*, International Journal of Fatigue, Vol. 55, pp. 245-256, October 2013.

[76] D. Simunek, et al.: *Fatigue crack growth under constant and variable amplitude loading at semi-elliptical and V-notched steel specimens*, 6th Fatigue Design conference, Procedia Engineering, Vol. 133, pp. 348-361, 2015.

[77] S. Beretta, A. Bernasconi, M. Carboni: *Fatigue assessment of root failures in HSLA steel welded joints: A comparison among local approaches*, International Journal of Fatigue, Part of special issue: Fatigue Assessment of Welded Connections, Vol. 31, No. 1, pp. 102-110, January 2009.

[78] C. Zhang, et al: *Effect of buffer layer and notch location on fatigue behavior in welded high-strength low-alloy*, Journal of Materials Processing Technology, Vol. 212, No. 10, pp. 2091-2101, October 2012.

[79] Q. Wang, et al.: *Understanding of fatigue crack growth behavior in welded joint of a new generation Ni-Cr-Mo-V high strength steel*, Engineering Fracture Mechanics, Vol. 194, pp. 224-239, May 2018.

[80] A. M. P. de Jesus, et al: *A comparison of the fatigue behavior between S355 and S690 steel grades*, Journal of Constructional Steel Research, Vol. 79, pp. 140-150, December 2012.

[81] D. Simunek, M. Leitner, F. Grün: *In-situ crack propagation measurement of high-strength steels including overload effects*, 7th International Conference on Fatigue Design 29-30 November 2017, Senlis, France, Procedia Engineering No. 213, pp. 335-345, 2018.

[82] C. L. Walters: *The effect of low temperatures on the fatigue of high-strength structural grade steels*, Part of special issue: 20th European Conference on Fracture, Procedia Materials Science, Vol. 3, pp. 209-214, 2014.

[83] L. Zhen: *Estimation of fatigue crack propagation rate in steel*, Engineering Fracture Mechanics, Vol. 48, No. 3, pp. 339-345, June 1994.

[84] H. Remes, et al.: *Factors affecting the fatigue strength of thin-plates in large structures*, International Journal of Fatigue, Vol. 101, Part 2, pp. 397-407, August 2017.

[85] H. F. H. Mobark, J. Lukács: *HCF design curves for high strength steel welded joints*, Design of Machines and Structures, Vol. 8, No. 2, pp. 39-51, 2018.

[86] Y. Wang: *Optimizing weld integrity for high-strength steels*, Advanced Welding and Joining Technical Workshop, Boulder, Colorado USA (2009). https://primis.phmsa.dot.gov/rd/mtgs/012506/35_KeynoteWang.pdf, last accessed 29/12/2017.

[87] https://hks-prozesstechnik.de/en/about-hks/

[88] M. Gáspár, A. Balogh, I. Sas: *Physical simulation aided process optimisation aimed sufficient HAZ toughness for quenched and tempered AHSS*, In: Proceedings of IIW 2015 International Conference, Paper IIW 2015 1504, pp. 1-7, 2015.

[89] Á. Dobosy, M. Gáspár, P. Jámbor: *Weldability of S960M thermo-mechanically treated advanced high strength steel*, In: Third Young Welding Professionals International Conference, Halle (Saale), Pages 1-6, 2017.

[90] J. Lukács, et al.: *Selected chapters from structural integrity of engineering structures*, 1st edn. Ed.: Lukács, J. University of Miskolc, Miskolc (2012), (In Hungarian).

[91] I. Marines-García, D. Galván-Montiel, C. Bathias: *Fatigue life assessment of high-strength, low-alloy steel at high frequency*. Arabian Journal for Science and Engineering 33 (1B), 237-247, 2008.

[92] J. Lukács, H. F. H. Mobark: *Mismatch effect on fatigue crack propagation limit curves of S690QL, S960QL and S960TM type base materials and their gas metal arc welded joints*, 72nd IIW Annual Assembly and International Conference 7-12 July 2019 Conference Proceedings, Bratislava Slovakia 2019.

[93] ASTM E647-11e1: *Standard Test Method for Measurement of Fatigue Crack Growth Rate*, ASTM International 2011.

[94] R. J. Allen, G. S. Booth, T Jutla: *A review of fatigue crack growth characterisation by linear elastic fracture mechanics (LEFM). Part I – Principles and methods of data generation*, Fatigue and Fracture of Engineering Materials and Structures, Vol. 11, No. 1, p. 45-69, 1988.

[95] R. J. Allen, G. S. Booth, T Jutla: *A review of fatigue crack growth characterization by linear elastic fracture mechanics (LEFM). Part II – Advisory documents and applications within national standards*, Fatigue and Fracture of Engineering Materials and Structures, Vol. 11, No. 2, p. 71-108, 1988.

[96] A. Ohta, et al.: *Fatigue Crack Propagation Curve for Design of Welded Structures*, Transactions of the Japan Welding Society, Vol. 20, No. 1, April 1989. p. 17-23.

[97] Det norske Veritas: *Classification Notes, Note No. 30.2 Fatigue strength analysis for mobile offshore units*, August 1984.

[98] BS 7910: *Guide on methods for assessing the acceptability of flaws in fusion welded structures*, 1999.

[99] J. Lukács: *Fatigue crack propagation limit curves for different metallic and nonmetallic materials*, Materials Science Forum (2003) Vol. 414-415, pp. 31-36.

[100] R. O. Ritchie: *Near-Threshold Fatigue Crack Propagation in Steels*, International Metals Reviews, Vol. 20 (5/6), 1979, pp. 205-230.

[101] D. Taylor: *Compendium of fatigue thresholds and crack growth rates*, EMAS, Warley, 1985.

[102] D. Taylor, L. Jianchun (Eds.): *Sourcebook on fatigue cack propagation: threshold and crack closure*, EMAS, Warley, 1993.

[103] B. Farahmand: *Multiscale Fatigue Crack Initiation and Propagation of Engineering Materials*, Structural Integrity and Microstructural Worthiness, Solid Mechanics and its Applications 152 Springer, Dordrecht 1, 2008.

[104] J. Lukács, Á. Dobosy: *Matching effect on fatigue crack growth behaviour of high strength steels GMA welded joints*, 1-19. IIW-DOC XIII-2692-17

[105] J. Lukács: *Determination of fatigue crack propagation limit curves and one possibility of their application*, In: K. Jármai, J. Farkas (Eds.) Metal structures: design, fabrication, economy, Proceedings of the International Conference on Metal Structures, Millpress Science Publishers, Rotterdam, pp. 33-38, 2003.

[106] J. Lukács, L. Kuzsella, Zs. Koncsik, M. Gáspár, Á. Meilinger: *Role of the Physical Simulation for the Estimation of the Weldability of High Strength Steels and Aluminum Alloys*, Materials Science Forum, Vol. 812 pp. 149-154 (2015).

[107] https://www.ssab.com/products/brands/strenx/products/strenx-1300

[108] https://www.dillinger.de/d/en/products/heavyplate/highstrength-finegrained/index.shtml

[109] https://www.voestalpine.com/alform/en/Products/x-treme

[110] O. Lagerqvist, et al.: *Efficient lifting equipment with extra highstrength steel*, Contract No 7210-PR/379. Final report, European Commission Technical Steel Research, 2007.

[111] Szunyogh, L. (Ed. in chief): *Welding and related technologies. Gépipari Tudományos Egyesület*, Budapest, 2007 (In Hungarian).

[112] http://www.ruukki.com/optimqc

[113] P. Collin, M. Möller, M. Nilsson, S. Törnblom: *Undermatching butt welds in high strength steels*, 2009. https://www.researchgate.net/publication/233646066_Undermatching_Butt_Welds_in_High_Strength_Steel

[114] R. Wilms: *High strength steels for steel construction*, Nordic Steel Conference publication, pp. 597-604, 2009.

LIST OF PUPLICATIONS RELATED TO THE TOPIC OF THE RESEARCH FIELD

IN ENGLISH

(1) H. F. H. Mobark, Á. Dobosy, J. Lukács: *Mismatch effect influence on the HCF resistance of high strength steels and their GMA welded joints,* Vehicle and Automotive Engineering 2 (VAE 2), pp. 755-767, 2018.

(2) H. F. H. Mobark, J. Lukács: *Mismatch effect influence on the high cycle fatigue resistance of S690QL type high strength steels,* 2nd International Conference on Structural Integrity and Durability, Dubrovnik, Croatia, October 2-5, pp. 1-4, 2018.

(3) H. F. H. Mobark, J. Lukács: *HCF design curves for high strength steel welded joints,* Design of Machines and Structures, Vol. 8, No. 2, pp. 39-51, 2018.

(4) H. F. H Mobark, J. Lukács: *HCF resistance characteristics of S690QL type high strength steels and their welded joints,* PhD Doctoral Forum, Faculty of Mechanical Engineering and Informatics, István Sályi Doctoral School, University of Miskolc, November 2018.

(5) H. F. H. Mobark, J. Lukács: *Connection among the parameters of the Manson-Coffin, the Basquin and the Paris-Erdogan equations,* MultiScience - XXXIII. microCAD International Multidisciplinary Scientific Conference, University of Miskolc, 23-24 May 2019, ISBN 978-963-358-177-3.

(6) J. Lukács, H. F. H. Mobark: *Mismatch effect on fatigue crack propagation limit curves of S690QL, S960QL and S960TM type base materials and their gas metal arc welded joints,* 72nd IIW Annual Assembly and International Conference 7-12 July 2019 Conference Proceedings, Bratislava Slovakia 2019.

(7) H. F. H. Mobark, J. Lukács: *Efficient application of S690QL type high strength steel for cyclic loaded welded structures,* Solutions for Sustainable Development, Proceedings of the 1st International Conference on Engineering Solutions for Sustainable Development (ICESSD 2019), October 3-4, 2019, Klára Szita Tóthné, Károly Jármay, Katalin Voith, Miskolc, Hungary.

(8) H. F. H. Mobark, J. Lukács: *Heat input influence on fatigue crack growth characteristics of high strength steel GMAW joints,* PhD Doctoral Forum, Faculty of Mechanical Engineering and Informatics, István Sályi Doctoral School, University of Miskolc, November 2019.

(9) J Lukács, H. F. H. Mobark: *The influence of the base material - filler metal pairing on the fatigue crack propagation of 700 MPa strength category welded joints,* XII. National Conference on Materials Science OATK 2019. Under publication: IOP Conference Series: Materials Science and Engineering.

(10) H. F. H. Mobark, J. Lukács: *Mismatch effect on fatigue crack propagation limit curves of GMAW joints made of S960QL and S960TM type base materials*, Design of Machines and Structures, Vol. 10, No. 1, pp. 28-38, 2020.

IN HUNGARIAN

(11) H. F. H. Mobark, J. Lukács: *High cycle fatigue resistance characteristics of S690QL type high strength steels and their welded joints*, GépGyártás, Vol. LVIII, No. 1-2, pp. 71-75, 2019.

(12) H. F. H. Mobark, J. Lukács: *Base material - filler metal pairing influence on fatigue crack propagation resistance of high strength steels and their welded*, GépGyártás, Vol. LVIII, No. 1-2, pp. 76-80, 2019.

APPENDICES

Base material: Weldox 700 E (W700E)
Type: butt welded joint (BWJ)
Specimen location: k/1W
Mismatch condition: matching (M)
Heat input: medium (mhi)

Specimen ID	a_0	b_0	S_0	ΔF	$\Delta\sigma$	$N_{fracture}$	Remark
	mm	mm	mm^2	N	MPa	cycle	
D606-1	15.2	15.1	229.52	34470	150	1121761	–
D606-2	15.2	15.15	230.28	46080	200	253561	–
D606 3	15.2	15.3	232.56	58140	250	137972	–
D606-4	15.2	15.15	230.28	69120	300	55298	–
D606-5	15.2	15.0	228.00	28530	125	1733157	–
D606-6	15.2	15.1	229.52	22950	100	10000000	survived
D606-7	15.2	15.2	231.04	28890	125	1295778	–
D606-8	15.2	15.3	232.56	34920	150	331538	–
D607-1	15.2	15.1	229.52	68850	300	246190	–
D607-2	15.2	15.1	229.52	57420	250	204648	–
D607-3	15.2	15.15	230.28	46080	200	150119	–
D607-4	15.2	15.2	231.04	23130	100	10000000	survived
D607-5	15.2	15.1	229.52	25830	113	10000000	survived
D607-6	15.2	15.1	229.52	28710	125	10000000	survived
D607-7	15.2	15.2	231.04	31770	138	1368002	–
D607-8	15.2	15.15	230.28	28800	125	10000000	survived

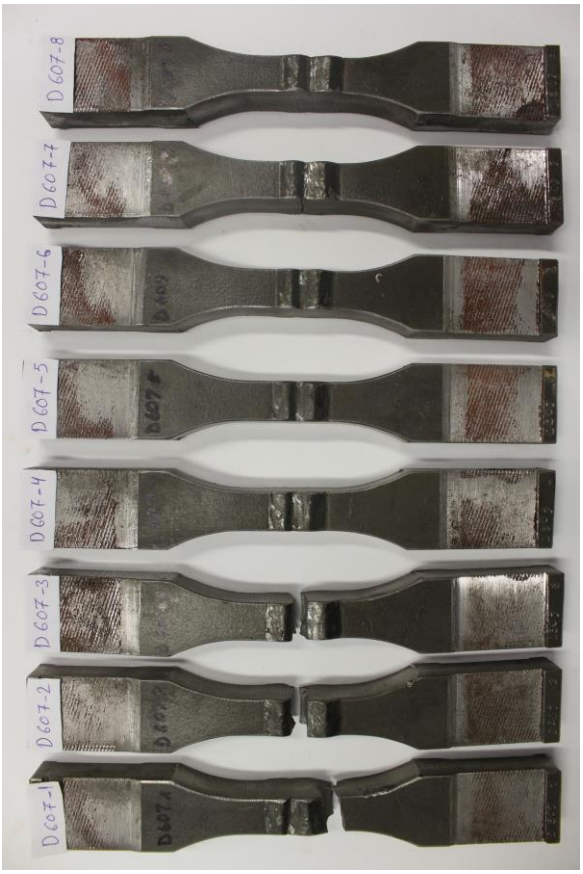

Base material: Weldox 700 E (W700E)
Type: butt welded joint (BWJ)
Specimen location: k/1W
Mismatch condition: matching / overmatching (M / OM)
Heat input: medium (mhi)

Specimen ID	a_0	b_0	S_0	ΔF	$\Delta\sigma$	$N_{fracture}$	Remark
	mm	mm	mm^2	N	MPa	cycle	
D634-1	15.2	15.3	232.56	86063	370	156165	–
D634-2	15.2	15.1	229.52	76500	333	268202	–
D634-3	15.2	15.2	231.04	67500	292	396508	–
D634-4	15.2	15.1	229.52	58500	255	570074	–
D634-5	15.2	15.1	229.52	49500	216	1093888	–
D634-6	15.2	15.2	231.04	40500	175	3952532	–
D634-7	15.2	14.7	223.44	30600	137	9773970	–

Base material: Alform 960M (A960M)
Type: butt welded joint (BWJ)
Specimen location: k/1W
Mismatch condition: matching (M)
Heat input: medium, first series (mhi1)

Specimen ID	a_0	b_0	S_0	ΔF	$\Delta\sigma$	$N_{fracture}$	Remark
	mm	mm	mm^2	N	MPa	cycle	
D906-1	14.9	15.2	226.48	22590	100	176072	–
D906-2	14.9	15.05	224.245	33660	150	128166	–
D906-3	14.9	15.2	226.48	45270	200	67967	–
D906-4	14.9	15.3	227.97	11340	50	1123881	–
D906-5	14.9	15.25	227.225	9180	40	10000000	survived
D906-6	14.9	15.2	226.48	11250	50	908066	–
D906-7	14.9	15.3	227.97	9180	40	10000000	survived
D906-8	14.9	15.3	227.97	13590	60	10000000	survived

Base material: Alform 960M (A960M)
Type: butt welded joint (BWJ)
Specimen location: k/1W
Mismatch condition: matching (M)
Heat input: medium, second series (mhi2)

Specimen ID	a_0	b_0	S_0	ΔF	$\Delta\sigma$	$N_{fracture}$	Remark
	mm	mm	mm^2	N	MPa	cycle	
D9012-1	14.9	15.4	229.46	11430	50	10000000	survived
D9012-2	14.9	15.4	229.46	22950	100	10000000	survived
D9012-3	14.9	15.3	227.97	45630	200	452029	–
D9012-4	14.9	15.3	227.97	34200	150	10000000	survived
D9012-5	14.9	15.25	227.225	39780	175	624463	–
D9012-6	14.9	15.15	225.735	39510	175	561953	–
D9012-7	14.9	15.3	227.97	56970	250	270614	–
D9012-8	14.9	15.3	227.97	56970	250	245310	–

Base material: Alform 960M (A960M)
Type: butt welded joint (BWJ)
Specimen location: k/1W
Mismatch condition: matching (M)
Heat input: high (hhi)

Specimen ID	a_0	b_0	S_0	ΔF	$\Delta\sigma$	$N_{fracture}$	Remark
	mm	mm	mm^2	N	MPa	cycle	
D909-21	14.9	15.4	229.46	68850	300	46776	–
D909-22	14.9	15.25	227.225	79425	350	36590	–
D909-23	14.9	15.25	227.225	56700	250	51953	–
D909-24	14.9	15.1	224.99	45000	200	66715	–
D909-25	14.9	15.2	226.48	34020	150	101744	–
D909-26	14.9	15.15	225.735	22680	100	187948	–
D909-27	14.9	15.2	226.48	11250	50	848956	–
D909-28	14.9	15.05	224.245	11250	50	677505	–
D908-1	14.9	15.1	224.99	9090	40	10000000	survived
D908-2	14.9	15.2	226.48	13500	60	10000000	survived
D908-3	14.9	15.2	226.48	11250	50	10000000	survived
D908-4	14.9	15.25	227.225	9090	40	10000000	survived
D908-5	14.9	15.25	227.225	15930	70	10000000	survived
D908-6	14.9	15.2	226.48	18090	80	10000000	survived
D908-7	14.9	15.2	226.48	22680	100	10000000	survived
D908-8	14.9	15.2	226.48	33930	150	859322	–

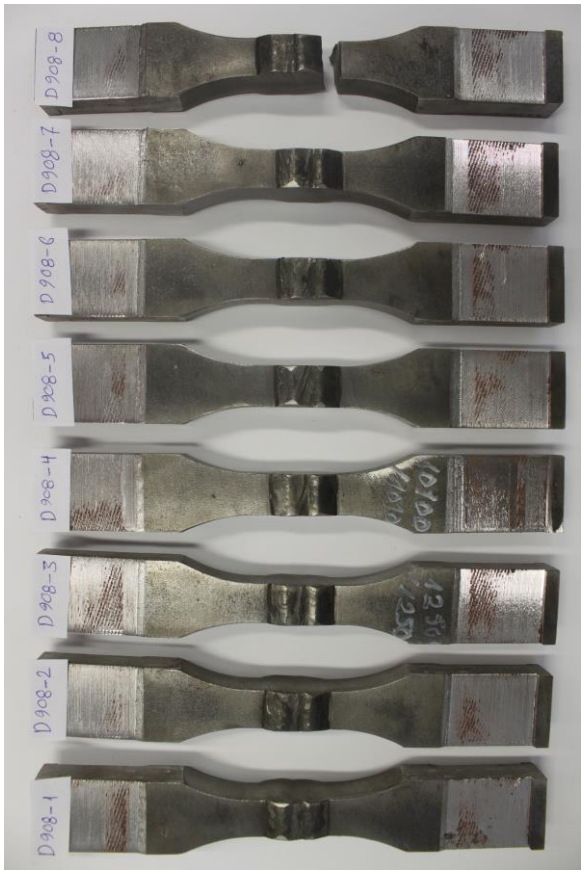

Base material: Alform 960M (A960M)
Type: butt welded joint (BWJ)
Specimen location: k/1W
Mismatch condition: undermatching (UM)
Heat input: medium (mhi)

Specimen ID	a_0	b_0	S_0	ΔF	$\Delta\sigma$	$N_{fracture}$	Remark
	mm	mm	mm^2	N	MPa	cycle	
D924-1	14.9	12.5	186.25	74520	400	44259	–
D924-2	14.9	12.5	186.25	55890	300	89447	–
D924-3	14.9	12.5	186.25	37260	200	281626	–
D924-4	14.9	12.5	186.25	18630	100	10000000	too low stress range
D924-5	14.9	12.5	186.25	27990	150	10000000	survived
D924-6	14.9	12.5	186.25	32580	175	361547	–
D924-7	14.9	12.5	186.25	27900	150	10000000	survived
D924-8	14.9	12.5	186.25	32580	175	4037515	fractured in head
D925-1	14.9	12.25	182.525	31950	175	10000000	survived
D925-2	14.9	12.3	183.27	36630	200	1129343	–
D925-3	14.9	12.2	181.78	72720	400	33930	–
D925-4	14.9	12.25	182.525	54810	300	54756	–
D925-5	14.9	12.25	182.525	31950	175	467270	–
D925-6	14.9	12.3	183.27	32040	175	223475	–
D925-7	14.9	12.3	183.27	27450	150	10000000	survived
D925-8	14.9	12.2	181.78	31770	175	10000000	survived

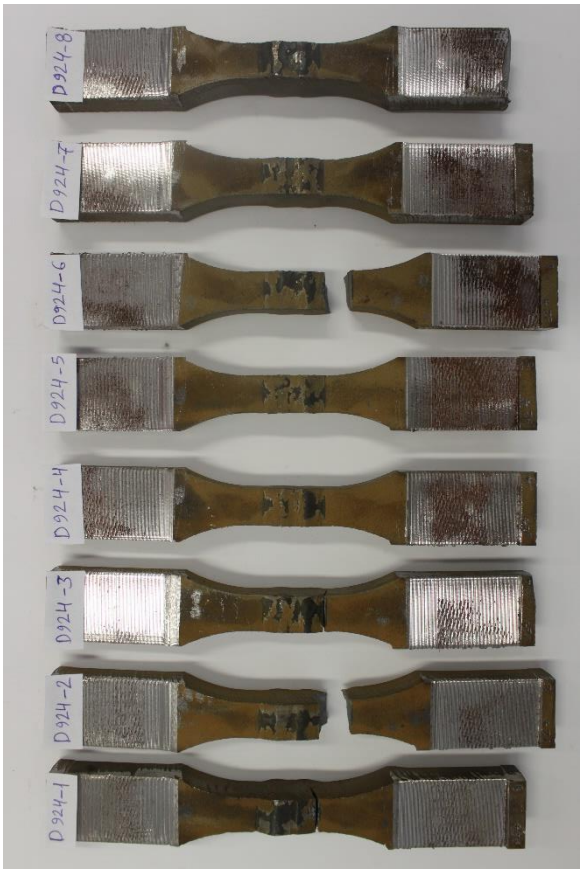

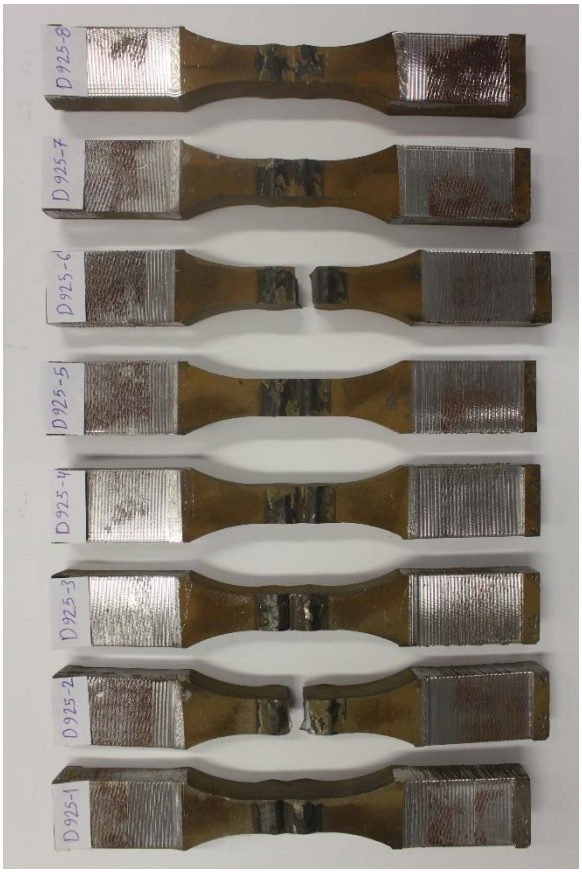

Base material: Weldox 700 E (W700E)
Type: welded joint (WJ)
Mismatch condition: matching / overmatching (M / OM)
Heat input: medium (mhi)

Specimen ID	W	B	a_0	Crack path	Nominal ΔF
	mm	mm	mm		N
Specimen location: T-S/23W					
D635-01	13.01	6.42	3.56	WM	2430
D635-02	13.00	6.43	3.50	WM	2070
D635-03	13.01	6.42	3.60	WM and HAZ	1827
D635-04	13.01	6.43	3.55	WM and HAZ	1827
D635-05	13.01	6.42	3.54	HAZ and BM	1827
D635-06	13.01	6.40	3.56	HAZ and BM	1827
Specimen location: T-L/21W					
D635-07	26.00	12.99	5.34	WM	10143
D635-08	26.00	13.00	5.33	WM	9225
D635-09	26.00	13.00	5.32	WM and HAZ	8388
D635-10	26.01	12.97	5.37	WM and HAZ	8388
D635-11	26.00	13.00	5.37	HAZ and BM	7623
D635-12	26.01	13.00	5.39	HAZ and BM	8388

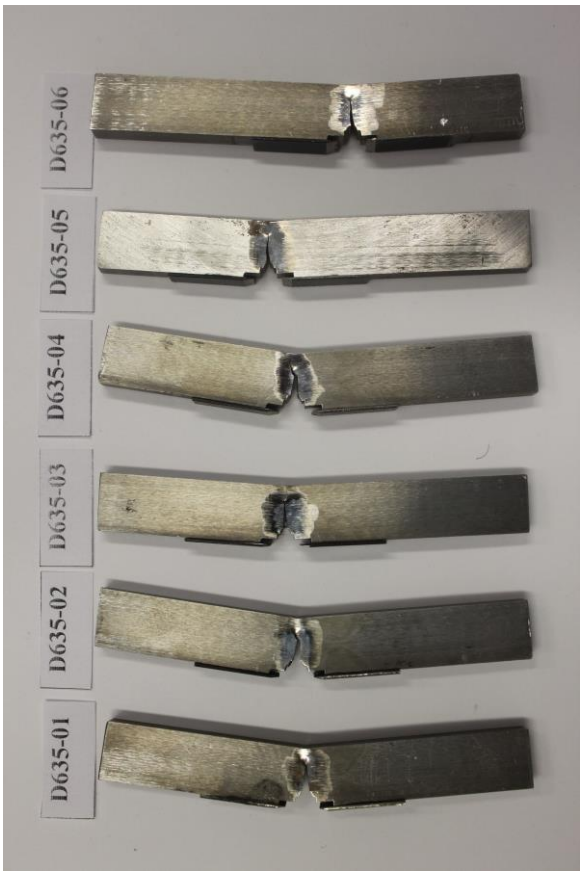

Base material: Alform 960M (A960M)
Type: welded joint (WJ)
Mismatch condition: matching (M)
Heat input: high (hhi)

Specimen ID	W	B	a_0	Crack path	Nominal ΔF
	mm	mm	mm		N
Specimen location: T-S/23W					
D9013-5s	13.00	6.48	3.24	WM	3987
D9013-6s	13.01	6.47	3.17	WM	3627
D9013-9s	13.00	6.48	3.13	WM and HAZ	2997
D9013-10s	13.00	6.48	3.29	WM and HAZ	4824
D9013-2s	13.00	6.48	3.34	HAZ and BM	3294
D9013-3s	13.01	6.48	3.35	HAZ and BM	3627
Specimen location: T-L/21W					
D9013-1	26.05	12.99	5.96	WM	8712
D9013-2	26.05	13.00	6.03	WM	8712
D9013-3	26.05	12.99	5.98	WM and HAZ	8712
D9013-4	26.05	13.01	6.00	WM and HAZ	7920
D9013-5	26.00	13.00	5.89	HAZ and BM	9261

Base material: Alform 960M (A960M)
Type: welded joint (WJ)
Mismatch condition: undermatching (UM)
Heat input: high (hhi)

Specimen ID	W	B	a_0	Crack path	Nominal ΔF
	mm	mm	mm		N
Specimen location: T-S/23W					
D926-5s	13.01	6.47	3.55	WM	2997
D926-1s	13.01	6.45	3.59	WM and HAZ	2997
D926-4s	12.99	6.47	3.45	WM and HAZ	2997
D926-7s	13.01	6.47	3.49	HAZ and BM	2997
D926-10s	13.01	6.48	3.38	HAZ and BM	2997
Specimen location: T-L/21W					
D926-1	26.00	13.01	5.61	WM	7920
D926-2	26.00	13.01	5.71	WM	8712
D926-4	26.05	13.01	5.72	WM and HAZ	9585
D926-5	26.05	12.99	5.64	WM and HAZ	8712
D926-6	26.05	12.98	5.60	HAZ and BM	9585

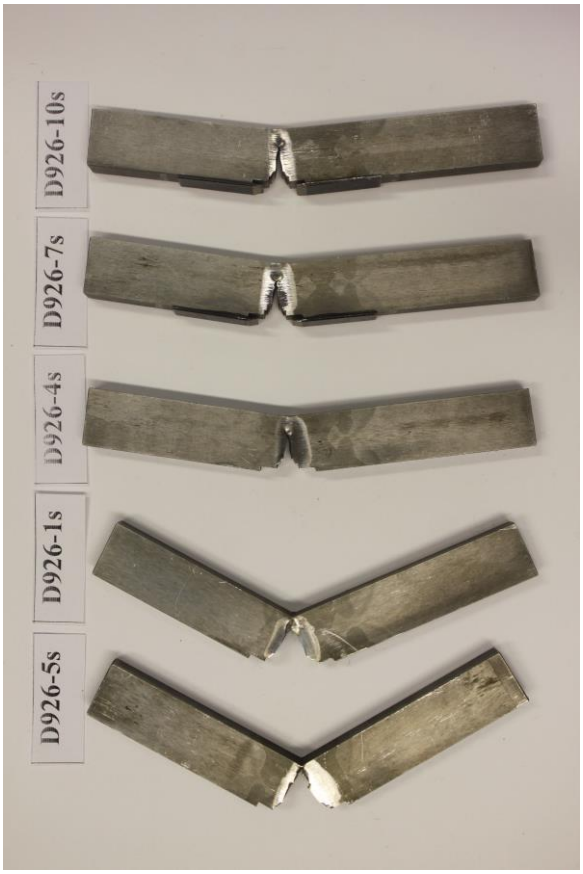

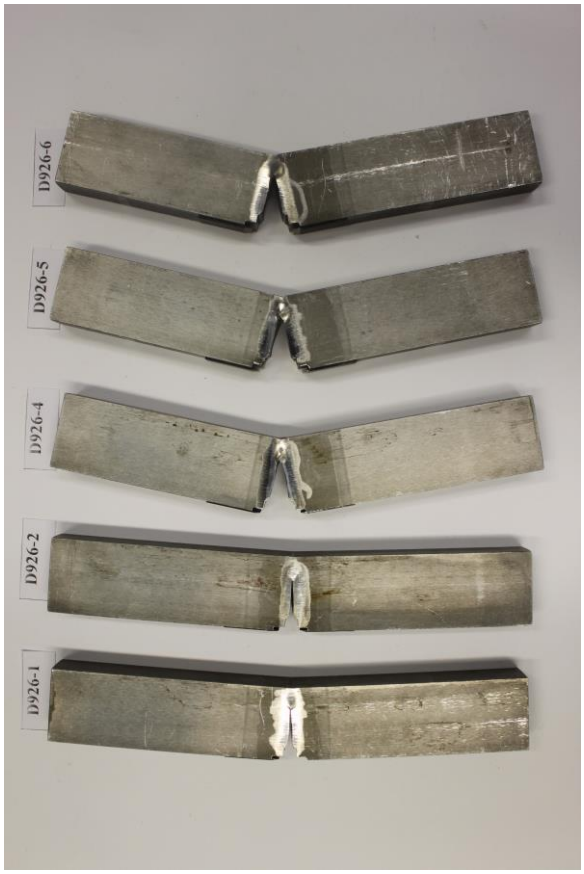

Statistical samples of Paris-Erdogan exponent values (n) and their characteristics

Base material	Mismatch type and heat input*	Orientation	Element number of sample	Average	SD	SD coefficient	Source
Optim 700QL	M	23W	5	1.81	0.468	0.2582	[14]
Weldox 700E	BM	*T-L*	*6*	*2.45*	*0.573*	*0.2337*	[9]
		L-T	*6*	*2.40*	*0.480*	*0.1999*	
		T-L and L-T	12	2.43	0.483	0.1991	
		T-S	6	2.19	0.922	0.4204	
	M	T-L/21W	6	5.10	0.600	0.1776	[9]
		T-S/23W	6	4.15	1.385	0.3334	
	OM	T-L/21W	6	3.68	1.452	0.3944	[9]
		T-S/23W	6	3.43	1.166	0.3406	
	M/OM	T-L/21W	6	3.29	0.224	0.0681	OWN
		T-S/23W	6	3.11	0.265	0.0851	
Weldox 960E	BM	*T-S*	*5*	*3.96*	*0.946*	*0.2390*	[103]
		L-S	*5*	*3.74*	*0.273*	*0.0731*	
		T-S and L-S	10	3.85	0.667	0.1734	
		T-L	5	2.44	0.615	0.2519	
	M	*T-L/21W*	*8*	*4.45*	*0.594*	*0.134*	[104]
		T-S/23W	*7*	*4.19*	*1.106*	*0.264*	
		T-L/21W and T-S/23W	15	4.32	0.847	0.196	
Alform 960M	BM	*T-L*	*6*	*2.35*	*0.396*	*0.1687*	[9]
		L-T	*5*	*2.13*	*0.292*	*0.1372*	
		T-L and L-T	11	2.25	0.355	0.1581	
		T-S	6	3.84	1.435	0.3735	
	M	T-L/21W	6	2.43	0.383	0.1580	[9]
		T-S/23W	6	2.94	0.850	0.2157	

Base material	Mismatch type and heat input*	Orientation	Element number of sample	Average	SD	SD coefficient	Source
Alform 960M	M – hhi	*T-L/21W*	*5*	*3.06*	*0.639*	*0.2089*	OWN
		T-S/23W	*6*	*3.23*	*1.017*	*0.3150*	
		T-L/21W and T-S/23W	11	3.15	0.830	0.26233	
	UM	T-L/21W	6	2.85	0.344	0.1207	[105]
		T-S/23W	7	3.23	0.911	0.2819	
	UM – hhi	*T-L/21W*	*5*	*3.67*	*0.577*	*0.1519*	OWN
		T-S/23W	*5*	*3.56*	*1.104*	*0.3102*	
		T-L/21W and T-S/23W	10	3.61	0.826	0.2287	

* Only high heat input (collective of linear energy and interpass temperature) was designated, hhi.